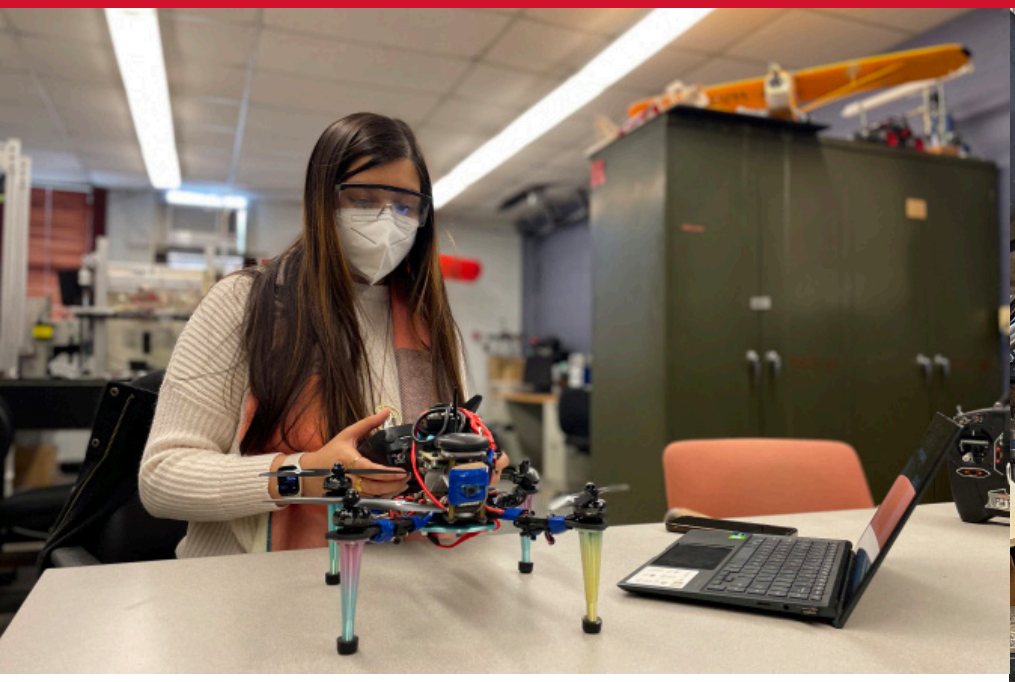

RUTGERS
School of Engineering

MAE Design and Manufacturing

Mechanical Engineering Design and Manufacturing Expo

Aerospace Engineering Aerospace Engineering Projects Expo

2021-2022 Judging Packet

RICHARD WEEKS HALL
EXPO PLAN

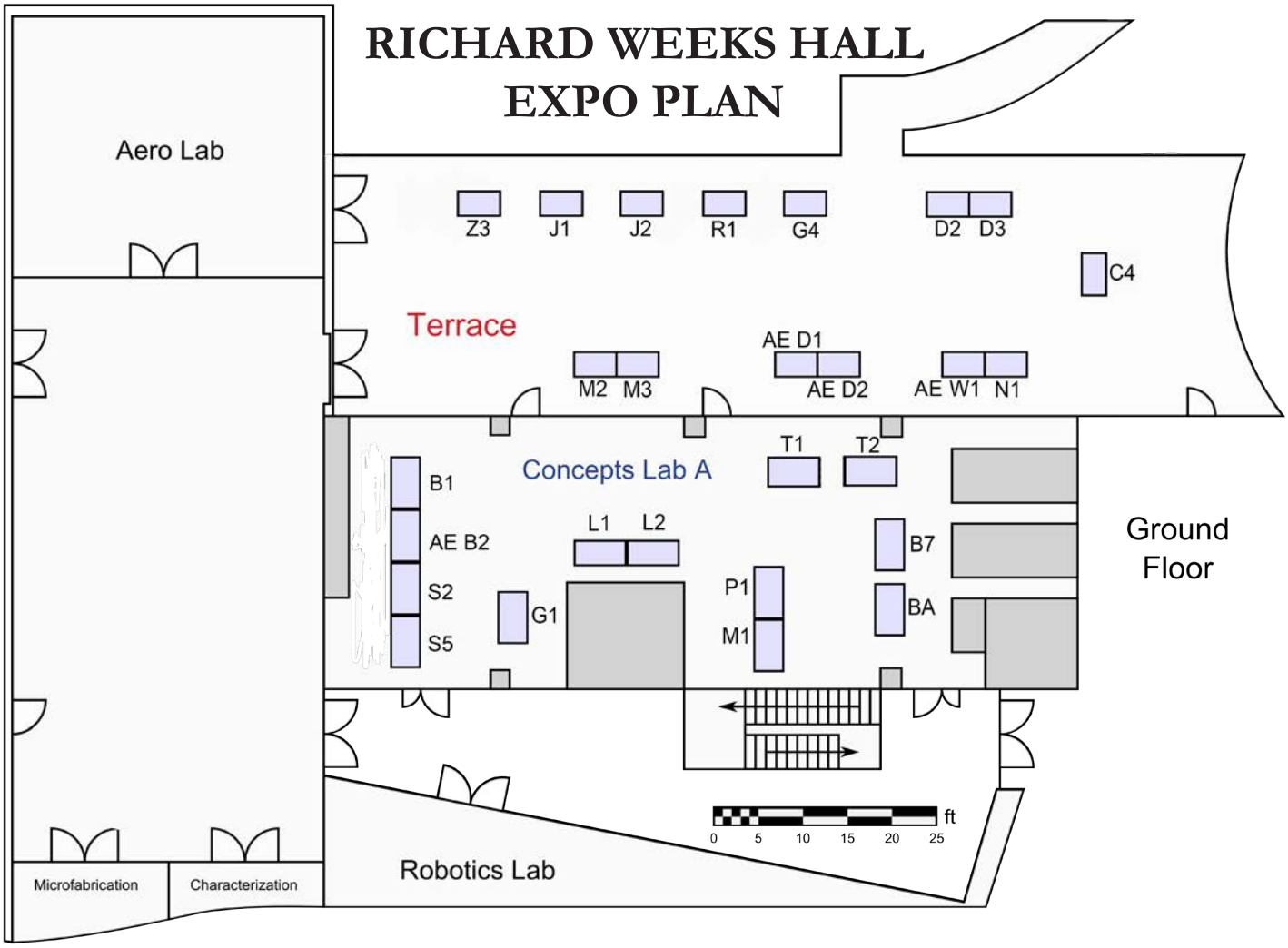

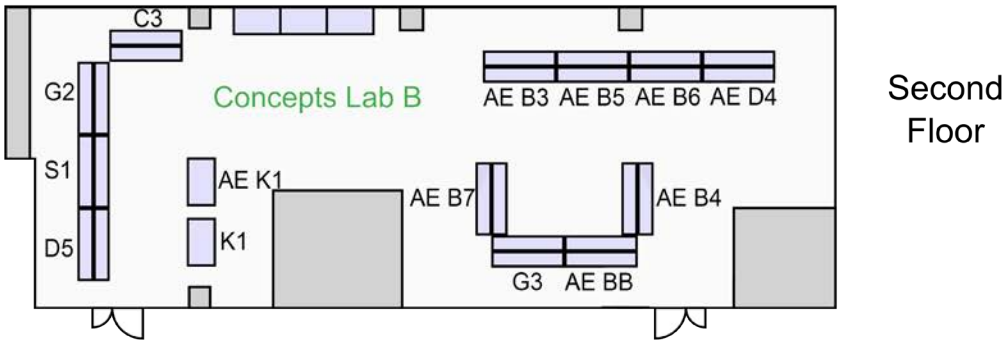

Other Points of Interest: **Judge Break Room: RWH-202**

RETURN JUDGING BOOK TO REGISTRATION TABLE

RUTGERS
School of Engineering
MAE Design and Manufacturing

Guidelines for Judging the 2021-2022 Poster Session

Welcome to the MAE Design and Manufacturing Expo!

In this packet, you will find the score sheets and posters for the 2021-2022 Mechanical and Aerospace Engineering Senior Design poster session. These sheets will be used to determine the winners of eight awards: Ingenuity Award, Prototype Development Award, Fabrication Award, Project Management Award, Analysis Award, Best Poster Presentation Award, Best Overall Mechanical Engineering Project Award, and Best Overall Aerospace Engineering Project Award. The groups you will meet today will each give you a brief poster presentation and take any questions you may have. We ask that you follow the guidelines below when judging them, as they have all followed a common course rubric that is reflected in the judging criteria.

Understanding the Criteria

Each sheet will present you with a total of 23 scoring criteria in the following format:

	Poor	Fair	Good	V. Good	Exemplary
Judging criterion is briefly described on the left-hand side.	1	2	3	4	5

For each criterion being described, please circle the appropriate score on the right-hand side. These criteria reflect the project management, fabrication and engineering skills expected of each group. As judges, you should feel free to use the entire scale, even if it seems harsh.

A box is also provided at the bottom for any comments. These could be the difference between a winner and a runner-up, so feel free to also take notes in this box during the presentation. At the end of the day, the students will receive an anonymized selection of comments for their benefit.

How to Use the Bottom of the Form

You will find a red band at the bottom of each sheet.

- Please fill in the box on the right the group number for the group that you are reviewing.
- The box on the left will be used for caculation purpose and is irrelevant to the judging process.

Primary Contact: Prof. Assimina Pelegri pelegri@soe.rutgers.edu

Department of Mechanical and Aerospace Engineering
Rutgers, The State University of New Jersey
98 Brett Road, Piscataway, NJ 08854

RUTGERS
School of Engineering
MAE Design and Manufacturing

Scoresheet for the 2021-2022 Poster Session

Project

		Poor	Fair	Good	V. Good	Exemplary
Ingenuity	The proposed solution/design...					
	...is scoped appropriately.	1	2	3	4	5
	...is innovative or clever.	1	2	3	4	5
	...is cost-effective, given the problem.	1	2	3	4	5
	...improves performance or reliability.	1	2	3	4	5
Prototype Development	The prototype...					
	...is fit for the purpose of demonstrating the design.	1	2	3	4	5
	...is optimized for manufacturing.	1	2	3	4	5
	...uses readily available materials and processes.	1	2	3	4	5
Fabrication	The fabrication process is described clearly.	1	2	3	4	5
	The end product seems well-designed and well-built.	1	2	3	4	5
Project Management	The group shows signs of good leadership and task distribution.	1	2	3	4	5
	The members of the group have equal task distribution.	1	2	3	4	5
	A project timeline was developed and was appropriate for the project tasks.	1	2	3	4	5
	The project was completed on time.	1	2	3	4	5
Analysis	Was the design analysis appropriate to meet the project goals.	1	2	3	4	5
	Method of analysis used was appropriate for the project intent.	1	2	3	4	5
	Analysis is executed well, exposes flaws, and adequately confirms that the design is fit for the intended purpose.	1	2	3	4	5

Poster/Presentation

Presentation	The group answered questions competently and professionally.	1	2	3	4	5
	The group gave a professional and organized presentation of the prototype.	1	2	3	4	5
	The poster is well organized and easy to follow.	1	2	3	4	5
	The design of the poster is visually appealing.	1	2	3	4	5
	The poster offers a good introduction to the project.	1	2	3	4	5
	The poster demonstrates results using appropriate data visualization techniques (graphs, charts, etc.).	1	2	3	4	5
	The group went the extra mile to make sure the poster draws the viewer's attention. (Points for style.)	1	2	3	4	5

Comments

Official Use Only
Ref
JID
BPA BOP

RUTGERS
School of Engineering
MAE Design and Manufacturing

Scoresheet for the 2021-2022 Poster Session

Project

		Poor	Fair	Good	V. Good	Exemplary
Ingenuity	The proposed solution/design...					
	...is scoped appropriately.	1	2	3	4	5
	...is innovative or clever.	1	2	3	4	5
	...is cost-effective, given the problem.	1	2	3	4	5
	...improves performance or reliability.	1	2	3	4	5
Prototype Development	The prototype...					
	...is fit for the purpose of demonstrating the design.	1	2	3	4	5
	...is optimized for manufacturing.	1	2	3	4	5
	...uses readily available materials and processes.	1	2	3	4	5
Fabrication	The fabrication process is described clearly.	1	2	3	4	5
	The end product seems well-designed and well-built.	1	2	3	4	5
Project Management	The group shows signs of good leadership and task distribution.	1	2	3	4	5
	The members of the group have equal task distribution.	1	2	3	4	5
	A project timeline was developed and was appropriate for the project tasks.	1	2	3	4	5
	The project was completed on time.	1	2	3	4	5
Analysis	Was the design analysis appropriate to meet the project goals.	1	2	3	4	5
	Method of analysis used was appropriate for the project intent.	1	2	3	4	5
	Analysis is executed well, exposes flaws, and adequately confirms that the design is fit for the intended purpose.	1	2	3	4	5

Poster/Presentation

Presentation	The group answered questions competently and professionally.	1	2	3	4	5
	The group gave a professional and organized presentation of the prototype.	1	2	3	4	5
	The poster is well organized and easy to follow.	1	2	3	4	5
	The design of the poster is visually appealing.	1	2	3	4	5
	The poster offers a good introduction to the project.	1	2	3	4	5
	The poster demonstrates results using appropriate data visualization techniques (graphs, charts, etc.).	1	2	3	4	5
	The group went the extra mile to make sure the poster draws the viewer's attention. (Points for style.)	1	2	3	4	5

Comments

Official Use Only
Ref
JID
BPA BOP

RUTGERS
School of Engineering
MAE Design and Manufacturing

Scoresheet for the 2021-2022 Poster Session

Project

		Poor	Fair	Good	V. Good	Exemplary
Ingenuity	The proposed solution/design...					
	...is scoped appropriately.	1	2	3	4	5
	...is innovative or clever.	1	2	3	4	5
	...is cost-effective, given the problem.	1	2	3	4	5
	...improves performance or reliability.	1	2	3	4	5
Prototype Development	The prototype...					
	...is fit for the purpose of demonstrating the design.	1	2	3	4	5
	...is optimized for manufacturing.	1	2	3	4	5
	...uses readily available materials and processes.	1	2	3	4	5
Fabrication	The fabrication process is described clearly.	1	2	3	4	5
	The end product seems well-designed and well-built.	1	2	3	4	5
Project Management	The group shows signs of good leadership and task distribution.	1	2	3	4	5
	The members of the group have equal task distribution.	1	2	3	4	5
	A project timeline was developed and was appropriate for the project tasks.	1	2	3	4	5
	The project was completed on time.	1	2	3	4	5
Analysis	Was the design analysis appropriate to meet the project goals.	1	2	3	4	5
	Method of analysis used was appropriate for the project intent.	1	2	3	4	5
	Analysis is executed well, exposes flaws, and adequately confirms that the design is fit for the intended purpose.	1	2	3	4	5

Poster/Presentation

Presentation	The group answered questions competently and professionally.	1	2	3	4	5
	The group gave a professional and organized presentation of the prototype.	1	2	3	4	5
	The poster is well organized and easy to follow.	1	2	3	4	5
	The design of the poster is visually appealing.	1	2	3	4	5
	The poster offers a good introduction to the project.	1	2	3	4	5
	The poster demonstrates results using appropriate data visualization techniques (graphs, charts, etc.).	1	2	3	4	5
	The group went the extra mile to make sure the poster draws the viewer's attention. (Points for style.)	1	2	3	4	5

Comments

Official Use Only
Ref
JID
BPA BOP

RUTGERS
School of Engineering
MAE Design and Manufacturing

Scoresheet for the 2021-2022 Poster Session

Project

		Poor	Fair	Good	V. Good	Exemplary
Ingenuity	The proposed solution/design...					
	...is scoped appropriately.	1	2	3	4	5
	...is innovative or clever.	1	2	3	4	5
	...is cost-effective, given the problem.	1	2	3	4	5
	...improves performance or reliability.	1	2	3	4	5
Prototype Development	The prototype...					
	...is fit for the purpose of demonstrating the design.	1	2	3	4	5
	...is optimized for manufacturing.	1	2	3	4	5
	...uses readily available materials and processes.	1	2	3	4	5
Fabrication	The fabrication process is described clearly.	1	2	3	4	5
	The end product seems well-designed and well-built.	1	2	3	4	5
Project Management	The group shows signs of good leadership and task distribution.	1	2	3	4	5
	The members of the group have equal task distribution.	1	2	3	4	5
	A project timeline was developed and was appropriate for the project tasks.	1	2	3	4	5
	The project was completed on time.	1	2	3	4	5
Analysis	Was the design analysis appropriate to meet the project goals.	1	2	3	4	5
	Method of analysis used was appropriate for the project intent.	1	2	3	4	5
	Analysis is executed well, exposes flaws, and adequately confirms that the design is fit for the intended purpose.	1	2	3	4	5

Poster/Presentation

Presentation	The group answered questions competently and professionally.	1	2	3	4	5
	The group gave a professional and organized presentation of the prototype.	1	2	3	4	5
	The poster is well organized and easy to follow.	1	2	3	4	5
	The design of the poster is visually appealing.	1	2	3	4	5
	The poster offers a good introduction to the project.	1	2	3	4	5
	The poster demonstrates results using appropriate data visualization techniques (graphs, charts, etc.).	1	2	3	4	5
	The group went the extra mile to make sure the poster draws the viewer's attention. (Points for style.)	1	2	3	4	5

Comments

Official Use Only
Ref
JID
BPA BOP

RUTGERS
School of Engineering
MAE Design and Manufacturing

Scoresheet for the 2021-2022 Poster Session

Project

		Poor	Fair	Good	V. Good	Exemplary
Ingenuity	The proposed solution/design...					
	...is scoped appropriately.	1	2	3	4	5
	...is innovative or clever.	1	2	3	4	5
	...is cost-effective, given the problem.	1	2	3	4	5
	...improves performance or reliability.	1	2	3	4	5
Prototype Development	The prototype...					
	...is fit for the purpose of demonstrating the design.	1	2	3	4	5
	...is optimized for manufacturing.	1	2	3	4	5
	...uses readily available materials and processes.	1	2	3	4	5
Fabrication	The fabrication process is described clearly.	1	2	3	4	5
	The end product seems well-designed and well-built.	1	2	3	4	5
Project Management	The group shows signs of good leadership and task distribution.	1	2	3	4	5
	The members of the group have equal task distribution.	1	2	3	4	5
	A project timeline was developed and was appropriate for the project tasks.	1	2	3	4	5
	The project was completed on time.	1	2	3	4	5
Analysis	Was the design analysis appropriate to meet the project goals.	1	2	3	4	5
	Method of analysis used was appropriate for the project intent.	1	2	3	4	5
	Analysis is executed well, exposes flaws, and adequately confirms that the design is fit for the intended purpose.	1	2	3	4	5

Poster/Presentation

Presentation	The group answered questions competently and professionally.	1	2	3	4	5
	The group gave a professional and organized presentation of the prototype.	1	2	3	4	5
	The poster is well organized and easy to follow.	1	2	3	4	5
	The design of the poster is visually appealing.	1	2	3	4	5
	The poster offers a good introduction to the project.	1	2	3	4	5
	The poster demonstrates results using appropriate data visualization techniques (graphs, charts, etc.).	1	2	3	4	5
	The group went the extra mile to make sure the poster draws the viewer's attention. (Points for style.)	1	2	3	4	5

Comments

Official Use Only
Ref
JID
BPA BOP

RUTGERS
School of Engineering
MAE Design and Manufacturing

Scoresheet for the 2021-2022 Poster Session

Project

		Poor	Fair	Good	V. Good	Exemplary
Ingenuity	The proposed solution/design...					
	...is scoped appropriately.	1	2	3	4	5
	...is innovative or clever.	1	2	3	4	5
	...is cost-effective, given the problem.	1	2	3	4	5
	...improves performance or reliability.	1	2	3	4	5
Prototype Development	The prototype...					
	...is fit for the purpose of demonstrating the design.	1	2	3	4	5
	...is optimized for manufacturing.	1	2	3	4	5
	...uses readily available materials and processes.	1	2	3	4	5
Fabrication	The fabrication process is described clearly.	1	2	3	4	5
	The end product seems well-designed and well-built.	1	2	3	4	5
Project Management	The group shows signs of good leadership and task distribution.	1	2	3	4	5
	The members of the group have equal task distribution.	1	2	3	4	5
	A project timeline was developed and was appropriate for the project tasks.	1	2	3	4	5
	The project was completed on time.	1	2	3	4	5
Analysis	Was the design analysis appropriate to meet the project goals.	1	2	3	4	5
	Method of analysis used was appropriate for the project intent.	1	2	3	4	5
	Analysis is executed well, exposes flaws, and adequately confirms that the design is fit for the intended purpose.	1	2	3	4	5

Poster/Presentation

Presentation	The group answered questions competently and professionally.	1	2	3	4	5
	The group gave a professional and organized presentation of the prototype.	1	2	3	4	5
	The poster is well organized and easy to follow.	1	2	3	4	5
	The design of the poster is visually appealing.	1	2	3	4	5
	The poster offers a good introduction to the project.	1	2	3	4	5
	The poster demonstrates results using appropriate data visualization techniques (graphs, charts, etc.).	1	2	3	4	5
	The group went the extra mile to make sure the poster draws the viewer's attention. (Points for style.)	1	2	3	4	5

Comments

Official Use Only
Ref
JID
BPA BOP

RUTGERS
School of Engineering
MAE Design and Manufacturing

Scoresheet for the 2021-2022 Poster Session

Project

		Poor	Fair	Good	V. Good	Exemplar
Ingenuity	The proposed solution/design...					
	...is scoped appropriately.	1	2	3	4	5
	...is innovative or clever.	1	2	3	4	5
	...is cost-effective, given the problem.	1	2	3	4	5
	...improves performance or reliability.	1	2	3	4	5
Prototype Development	The prototype...					
	...is fit for the purpose of demonstrating the design.	1	2	3	4	5
	...is optimized for manufacturing.	1	2	3	4	5
	...uses readily available materials and processes.	1	2	3	4	5
Fabrication	The fabrication process is described clearly.	1	2	3	4	5
	The end product seems well-designed and well-built.	1	2	3	4	5
Project Management	The group shows signs of good leadership and task distribution.	1	2	3	4	5
	The members of the group have equal task distribution.	1	2	3	4	5
	A project timeline was developed and was appropriate for the project tasks.	1	2	3	4	5
	The project was completed on time.	1	2	3	4	5
Analysis	Was the design analysis appropriate to meet the project goals.	1	2	3	4	5
	Method of analysis used was appropriate for the project intent.	1	2	3	4	5
	Analysis is executed well, exposes flaws, and adequately confirms that the design is fit for the intended purpose.	1	2	3	4	5

Poster/Presentation

Presentation	The group answered questions competently and professionally.	1	2	3	4	5
	The group gave a professional and organized presentation of the prototype.	1	2	3	4	5
	The poster is well organized and easy to follow.	1	2	3	4	5
	The design of the poster is visually appealing.	1	2	3	4	5
	The poster offers a good introduction to the project.	1	2	3	4	5
	The poster demonstrates results using appropriate data visualization techniques (graphs, charts, etc.).	1	2	3	4	5
	The group went the extra mile to make sure the poster draws the viewer's attention. (Points for style.)	1	2	3	4	5

Comments

Official Use Only
Ref
JID
BPA BOP

RUTGERS School of Engineering

MAE Design and Manufacturing

The ExplorFish: Mechanical Oscillatory Swimmer

Advisor: Professor Prosenjit Bagchi
Students: Sangida Akther, Jeremy Cheng,
Matthew Dembeck, Ryan Figueroa-Parsons, Sandy Truong

Problem Statement

Exploration of ocean wildlife is a difficult task due to the depths and small crevices of the ocean being unsuitable for humans. In addition, direct deployment of humans or bulky machines can disturb wildlife that are desired to be studied. A discrete, submersible device offers a critical step forward in understanding deep sea biomes.

Our Proposed Solution

Our design offers a 1.5' fish-inspired mechanism capable of thrusting itself through water and turning via the undulating and oscillating nature of its tail. It maintains neutral buoyancy and net zero internal moment in water, with ballast compartments for lead weighting. Motion is generated with an Arduino board, stepper motor, and DRV8825 driver system.

Practical Design Considerations

In addition to the analytical elements of this project, practical choices were made in order to design a waterproof body, and to eschew the need for a gear ratio in the mechanism. To achieve these ends, a unique tail geometry was employed, sealable with a neoprene sheet. A stepper motor was used in order to control tail speed without printing gears.

Iterative Electrical Design

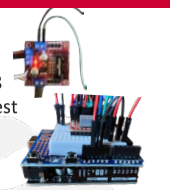

Multiple motor drivers were tested in the system, including the L298N (above, right), A4988 (below, right), and DRV8825. Best results were found with the DRV8825, while L298N drivers were damaged by overheating.

Print Modification and Electrical Work

Above are images highlighting modification of the 3D printed model necessary to complete the assembly. This included the removal of PLA support structures, sanding down components, and drilling a shaft hole in the motor bracket.

In addition to this, electrical work included the wiring of the setup shown below, as well as setting a current limit with a multimeter.

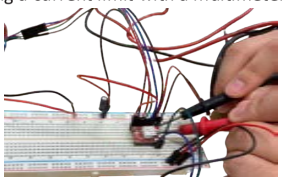

Critical Design Graphs

The following section offers a selection of the most important design graphs utilized for this project.

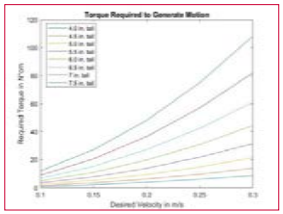

Fig 1. Necessary Torque (N*cm) vs. Desired Output Velocity (m/s)

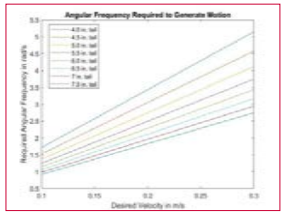

Fig 2. Necessary Angular Frequency (rad/s) vs. Desired Output Velocity (m/s)

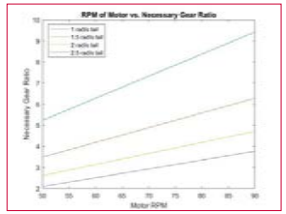

Fig 3. Necessary Gear Ratio vs. RPM of Possible Motor Choices

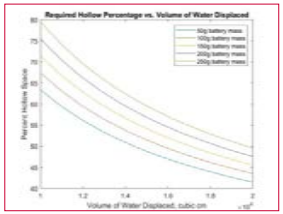

Fig 4. Percentage of Hollow Body Space vs. Volume of Water Displaced (cubic cm)

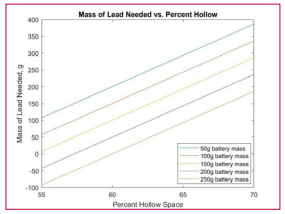

Fig 5. Necessary Mass of Lead (g) vs. Percentage of Hollow Body Space

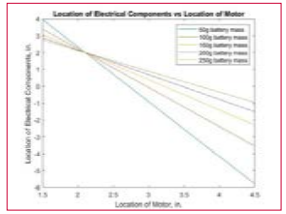

Fig 6. CoM Locations for Desired Net Zero Mass about Center of Buoyancy

Design calculations played a pivotal role in the analytical aspects of this project. These aspects included searching for proper motors with sufficient torque to move the fish's tail in water, gear ratio considerations, hollow space considerations for buoyancy, and the locations of heavy components within the body for neutral moment about the overall center of gravity. These MATLAB-designed plots assisted in making important decisions.

Finalized Design

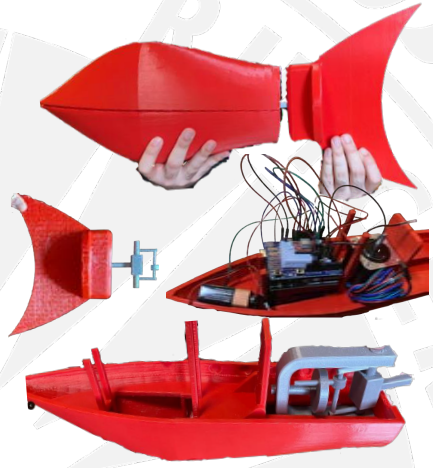

The above images offer side views of the fully-assembled printed model, the tail with mechanism attachment, and two shots of the exposed baseplate piece. Electrical components are shown in the third of these, giving an idea as to how these components fit within the model, while the fourth image offers a look at how the mechanism attaches to the motor.

Absent from these images are the neoprene sheet and silicone sealant necessary for waterproof testing.

RUTGERS
School of Engineering

MAE Design and Manufacturing

LOW PROFILE MECHANICAL ORNITHOPTER

Ruichuan Wu, Jon Dewland, Craig "CJ" Sager, Keith Lewis, Kevin Morales
Dr. Prosenjit Bagchi

Introduction

The world is an ever-changing place. The need for steadily available information on a battlefield, in a rescue environment, or in nature is greater than ever in our history.

Using the silhouette and flapping mechanism of a falcon we are creating a product that can be used to cheaply conduct reconnaissance of surveillance of any area while under a low profile.

Our product is a necessity compared to other drones.
- Bird silhouette and flapping motion blends in naturally.
- Can be launched without complicated or bulky equipment.
- Inexpensive

Aerodynamics

- **Goal: The aerodynamic structures will provide adequate lift to the structure in order to maintain flight.**
  - $Lift_{min} = Weight_{projected}$
  - Downstroke accounts for the majority of the lift created
- **Design:** The wing was modeled on thin cambered airfoils.
  - NACA 6409
  - The downstroke must provide enough lift to cover the loss in the upstroke such that, $L_{down} = mg + (mg - L_{up})$
- **Key figures**: Drive lift production
  - Flap Frequency
  - Flap amplitude

Materials

- **Wing:**
  - Foam poster board
  - Balsa wood
  - Carbon fiber rods
  - Kite fabric
- **Head:**
  - EPS Foam

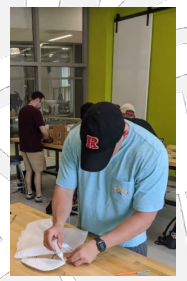

- **Tail:**
  - Foam poster board/ pvc sheet
- **Main Body:**
  - Thin birch wood
  - Carbon fiber rods
  - 3D printed gears and rod connectors
  - Battery and motor
  - Small metal hardware

Manufacturing

- ***Goal: Create a 1:1 scale of a large Peregrine Falcon***
  - *Head and Tail*
    - CAD projections cut from foam/pvc using a dremel.
  - *Wings*
    - Airfoils projected onto board via grid system.
    - Foam board and balsa wood cut using hand and power tools.
  - *Main Body*
    - Initial plan included cutting using CNC mills
    - Worksop was limited in ability to cut carbon fiber sheets
    - Material changed and cut using laser
    - 3D printer used to print connection points and gears.

Powertrain Design

- Powersource
  - 1300kV RC Motor
- Transmission
  - single reduction
  - dual rotor output
  - Laser cut gears & off-the-shelf pinion gears

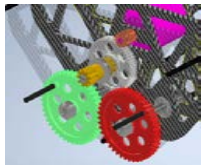

Transmission CAD Design

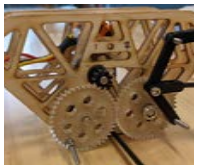

Transmission Product

- Flapping mechanism
  - Rocker-crank mechanism

CAD Flapping Mechanism Upstroke

CAD Flapping Mechanism Downstroke

End Product

The end product is a great basis for the bird to be tested and refined for any future following teams.

Functionality:
- Working transmission system
- Working flapping motion of wings
- Constructed wings to airfoil
- Electronics functioning

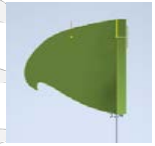

Electronics

Electronics consist of:
- Speed controller
- Hand controller
- Brushless motor
- Receiver
- Battery
- Servos

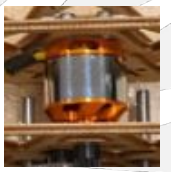

Acknowledgements

Dr. Prosenjit Bagchi: Project Advisor
Milan Simonovic: Design Consultant
Matt Rodgers: 3D Printer Technician
Rutgers Makerspace: Laser Cutting

AE B2

UAV System for CO2 Detection

RUTGERS School of Engineering
MAE Design and Manufacturing

Rahul Bhatt, Anthony Mazzilli, Kai Nissimov, Donny Putra, Gurjinder Singh, Jameson Woodell,
Dr. Xiaoli Bai

Abstract

The goal of this project is to develop a UAV system to detect carbon dioxide autonomously. The developed design would then be employed for general air quality surveillance. If optimized, this system could be integrated with Lidar technology to allow operators to design flight missions indoors, where a human examination is hazardous or inaccessible.

Background

Monitoring hazardous gases levels is dangerous to human health if done in person, and is next to impossible in high reach/remote areas. With the advancements of Unmanned Aerial Vehicles (UAVs) however, an operator can brush off all of the risks, as well as save time and resources for data collection. The group's data acquisition system is designed using an Arduino as a micro-controller and transmitted to a ground terminal to be processed with Matlab. The UAV would have two configurations, an indoor and outdoor mode. The indoor model would rely on Lidar technology to avoid obstacles along with its flight plan to its destination, while the outdoor mode would rely on GPS to fix its current position. Lidar technology takes 360° distance readings around the UAV and creates a basic map of the surroundings. This information allows the UAV to autonomously avoid objects in its vicinity. This UAV system can be expanded to monitor more than just CO2 levels, such as other types of environmental detection tasks.

Figure 1. UAV System During Flight

Data / Results

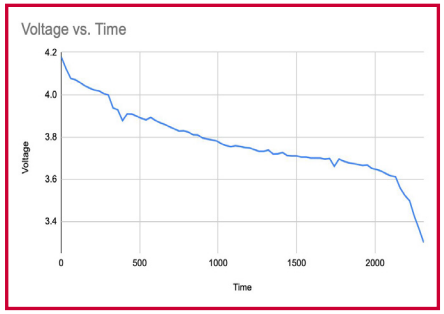

Figure 2. Battery Drainage Plot

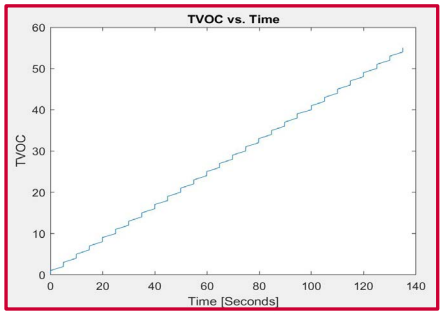

Figure 3. TVOC vs. Time Plot of Collected Data

Figure 4. LiDAR Mapping for Obstacle Avoidance

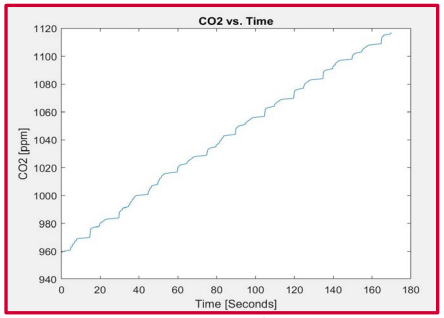

Figure 5. CO2 vs. Time Plot of Collected Data

Figure 6. Mission Planner Flight Path

Development

- Development of the UAV was done using eCalc, an online drone calculator for estimating UAV efficiency.
- From this analysis, specific components were chosen to maximize flight time and battery efficiency. After the parts were delivered, the UAV was assembled by hand.
- The motors, ESCs, and flight controllers were all soldered onto the power distribution board, and the software components were programmed using Mission Planner and a variety of Arduino freeware.
- The UAV is equipped with active obstacle avoidance using a Lidar sensor to create full autonomy. While this component was intended to be powered from the flight controller, this plan was abandoned because the necessary current was not enough. As such, a separate power adapter was connected to the main power board.
- An Adafruit CO2 sensor was employed for its simplicity and low-resolution error. Combined with an Arduino UNO, data transmission could be enabled during flight. This data would then be processed in Matlab/Simulink.

Conclusions

A UAV system for the detection of hazardous gases is a feasible solution to the issue of collecting air quality statistics in impractical locations. However, experiments have determined that any UAV that would operate inside would need to be substantially smaller than the one we have designed.

Future Work

If given a larger budget and longer time frame, the group may

- Incorporate SLAM technology to actively map the UAV, surroundings, enabling a higher level of autonomy
- Upgrade the planning algorithms to seek out larger concentrations of CO2

AE B3

RUTGERS School of Engineering

MAE Design and Manufacturing

Autonomously Deployable Inflatable Lunar Habitat

Luke Brennan, Aarya Patel, Parth Patel,
Rachael Siecinski, Sushmita Singh, Matthew Tremayne
Advisor: Professor Benaroya

GENERAL DYNAMICS Mission Systems

Gratefully acknowledged for their financial and engineering support.

April 15, 2022

Project Summary

Designing and fabricating an autonomously deploying inflatable habitat prototype. Complete proof-of-concept of a novel design that increases diameter by over 200% for reduction in volume when transported in a rocket.

Design

Fig 1. Fully deployed inflatable habitat

- Our design uses bottles of compressed CO_2 to inflate the habitat from within.
- Our microprocessor, the Feather M4 Express, is connected to an internal pressure sensor and a solenoid which releases the gas.
- The internal inflation causes a pressure buildup within the central column, causing a component at the top to be lifted, releasing the baseplates to enter the deployed state.
- Our membrane is comprised of three main features:
  - **Bottom:** made from a two large half-circle pieces of our membrane and is attached down the center.
  - **Wall:** a long piece of fabric attached in a hoop.
  - **Top:** contains unique segments connected together to give us our desired membrane geometry.
- The base is designed to utilize two different designs to create a hybrid design which would minimize any stresses applied to it.

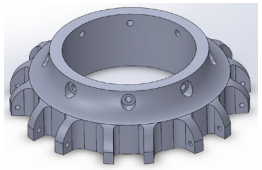

Fig 2. Base component

Manufacturing & Methodology

Manufacturing of the inflatable habitat prototype was divided into several different subsystems, evaluated separately and attached together for the final assembly.

Membrane
- Used heating sealing to connect the nylon segments at 180°C, and sewing provides reinforced strength.

Internal Inflation System
- SodaStream bottles at 3,000 PSI were used as CO_2 canisters, which were screwed to pressure reducers.

Sealing Mechanisms
- 2 worm-driven clamps joined with rubber gasket adhesives were used for the outside membrane seals.

Baseplates and Connectors
- 16 baseplates were machined using polypropylene, and 8 connectors were machined using aluminum.

Top Assembly
- The top tube, top cap and top plate components were 3D printed using a PHA filled PLA filament.

Fig 3. Heat sealed and sewed membrane connections

Fig 4. SodaStream bottle for the internal inflation system

Fig 5. Worm-driven clamp (left) and rubber gasket adhesive (right)

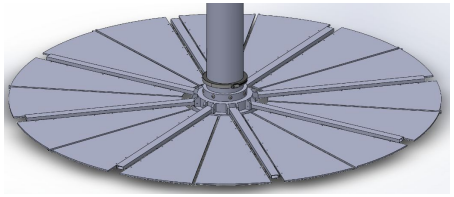

Fig 6. Deployed base assembly with connectors

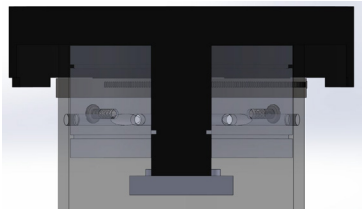

Fig 7. Top assembly

Analysis

Membrane
- A stress simulation was conducted, which proved the membrane's ability to maintain its structure from the internal pressure and external applied load.

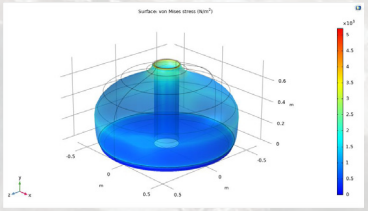

Base
- A stress simulation was conducted, which proved the base's ability to support the habitat structure with minimum deformation.

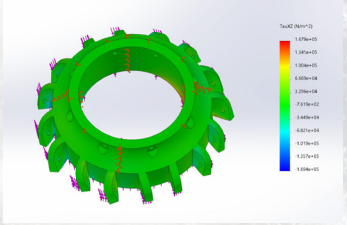

Conclusions / Results

- The design process led to a hybrid membrane structure that combines elements of both the spherical and toroidal structures.
- The habitat's individual components and subsystems proved durable enough to withstand loads during deployment, with minimum deformation.
- The pressurization system has demonstrated its ability to safely pressurize the habitat.

AE B4

RUTGERS
School of Engineering
MAE Design and Manufacturing

Zero Gravity Drone

Allison Scarinci, Tiffany Kensah, Prutha Patel, Aditya Anikode, Ali Hamza, Brenda Noriega
Dr. Onur Bilgen

Introduction

Analyses of zero-gravity environments have established a foundation from which one may predict its effects on equipment and personnel in space. These efforts are however restricted by physical expenses, environmental issues, time restrictions, and limited accessibility. The goal of this project is to design, analyze, fabricate, and test a small unmanned aerial vehicle to act as a platform to conduct zero gravity experiments. This solution presents a portable and cost-effective alternative to existing tests. During a three-phase flight, the drone will engage maximum thrust as it rapidly accelerates up. Upon entering the zero-gravity phase, the vehicle will briefly hover before going into a freefall. In this interim period, the drone will experience microgravity.

Multi-Rotor Unmanned Aerial Vehicles

Figure 1. Hexacopter Drone

Figure 2. Test Vehicle

Experimental Platform

- Includes pendulum, test platform, accelerometer, and electronics such as the camera, ESC telemetry, and wires
- Replaces GoPro camera in gimbal and is securely inserted to control rotational acceleration applied to body

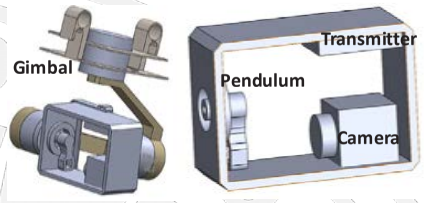

Figure 3. Gimbal and Experimental Platform

Flight Profile

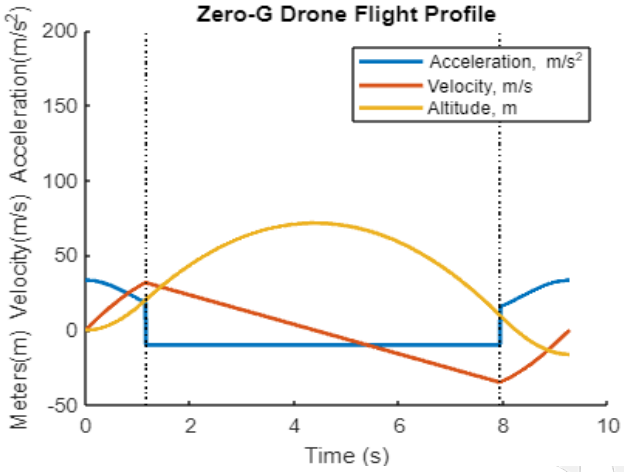

Figure 4. Zero-G Drone Flight Profile: Acceleration, Velocity, Altitude vs Time(s)

Systems Organization

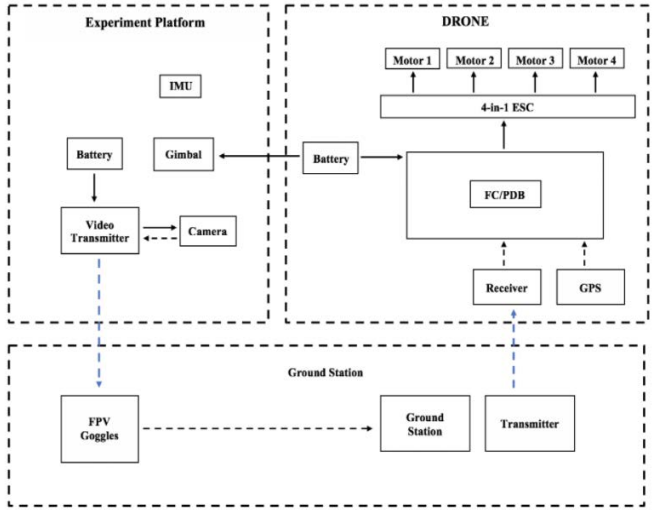

Figure 5. System Diagram for Experimental Platform, Ground System, and Drone

Finite Element Analysis Results

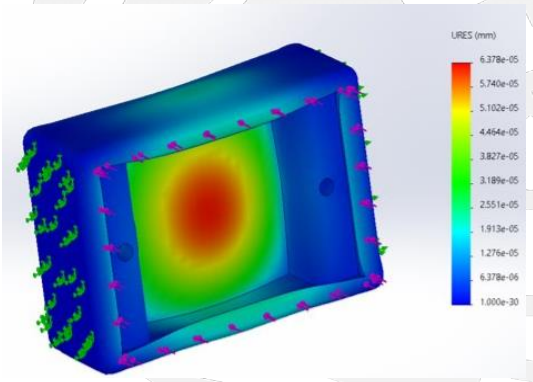

Figure 6. Stress Analysis on Inertial Measurement Unit Adapter

- Resistance to clamping load evaluated on each face under load of 10N
- Low deflection observed
- Induced stresses are below yield strength

AE B5

RUTGERS School of Engineering

MAE Design and Manufacturing

Multi-Mode Hybrid Drone Delivery System

Jessica Carvalho, Aditya Dabas, Dov Frommer, Renée Ghosh,
Pooja Gupta, Brijesh Mangrolia, Anusha Nagar
Advisor: Dr. Onur Bilgen

Background

The MMHDDS is a multi-UAV delivery system that combines a quadcopter with a fixed-wing airplane, capable of both long-range and vertical flight. This project will result in faster, cheaper, and more reliable delivery, and cut down on costs associated with fuel and labor.

Conceptual Delivery Procedure

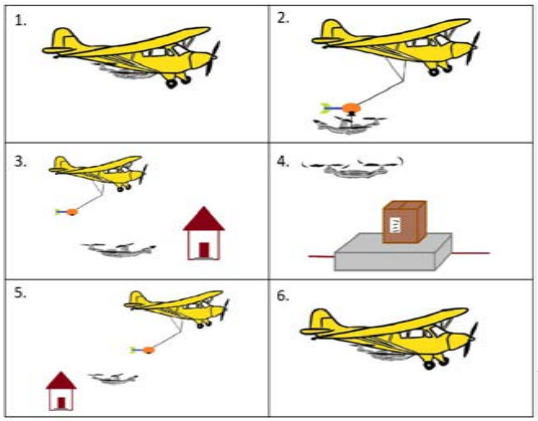

Timeline

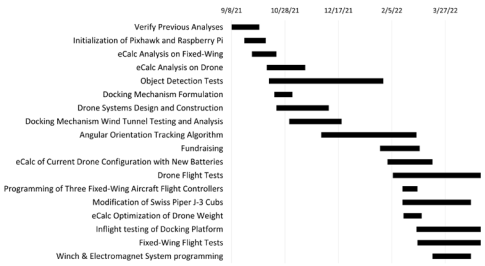

Conclusion

This year, we:

- Built and modified a commercial RC fixed-wing plane
- Completed wind-tunnel tests and flight tests for docking platform
- Completed the drone's computer vision tracking script

Future work:

- Update the drone's tracking script to switch between GPS and computer vision tracking
- Continue flight tests and integrate all systems

Acknowledgements: Dr. Bilgen, Muhammet Gungor, Subash Kungumaraj, and NASA USRC program

Fixed Wing Electrical Components

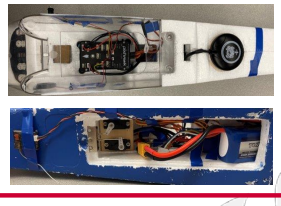

Battery Drain Test

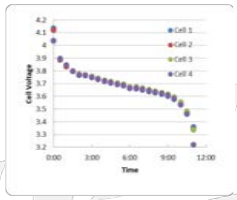

Winch CAD Model

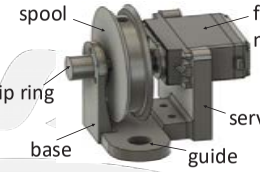

Winch Prototype

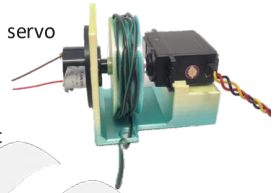

Fixed Wing CAD Model

Fixed Wing Power Breakdown

Component	Model/Type	QTY	Voltage, V	I_MAX(mA)	P_MAX(mW)
Servos		3	5	733.5	11002.5
Rudder Servo		1	5	1102.4	5512
Winch		1	5	2000	10000
Electromagnet		1	10	320.5128205	3205.128205
ESC		-1	5	5000	-25000
Flight Controller		1	5	0	0
				DEFICIT	4719.628205

Docking Platform

Wind Tunnel Test

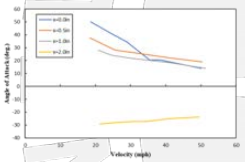

Wind Tunnel Results

Flight Test

Quadcopter CAD Model

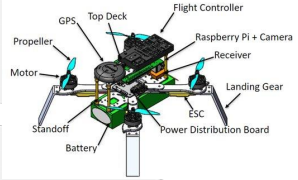

Quadcopter E-calc Optimization

eCalc Output \ Battery	4S-3400 mAh
Battery Weight (g)	348
Hover Flight Time (minutes)	15.8
Thrust to Weight Ratio	2.8
Specific Thrust (g/W)	5.85

Battery Drain Test

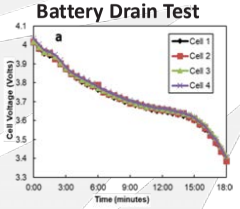

Computer Vision

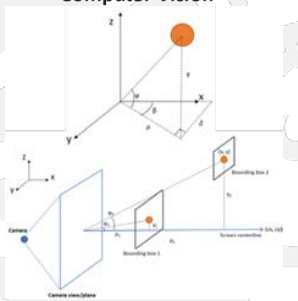

A) Object in drone's reference frame

A) Raw video frame B) Masked video frame

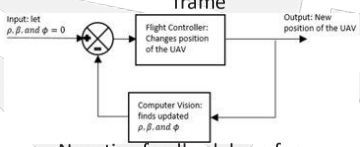

Negative feedback loop for Computer Vision Control System

AE B6

RUTGERS School of Engineering

MAE Design and Manufacturing

Aircraft Stability and Control Derivatives

Anthony Autera, Jeffrey Bandara, Matthew Mariner, Michael Philip, Dr. Haim Baruh

Problem Statement

Modern aircraft contain autopilot systems to maintain in-flight stability. These systems require information on the aircraft's response to various motions and control surface inputs. Obtaining these values require expensive and extensive testing methods. Our project aims to reduce and expedite the process of obtaining aircraft stability derivatives for early stages in aircraft design.

Constraints

Our solution adheres to the following constraints:

- Budget constraint of $650.00
- System is versatile and can be used in multiple airframes
- System weight and location do not impact the airworthiness of the airframe

Design

Our design utilizes RC model aircraft with additional electronics onboard. The electronics system consists of an Arduino Nano, MPU 6050 6-axis Gyroscope/Accelerometer, and an SD card reader. The electronics are installed within the aircraft and are positioned in a fashion to maintain the original center of gravity.

Target Audience

- University aerospace clubs
- New startup aerospace companies
- OEM manufacturers with new type designs in early concept stages

Methodology

Data must be collected to allow for stability derivative determination.

Data Collection Flight Procedure

- Aircraft enters steady, level flight path
- Single control surface deflected (aileron, elevator, or rudder)
- MPU measures changes in flight path
- Arduino stores data from MPU on SD card
- Procedure is repeated for each control surface

The collected data is then uploaded to MATLAB. The recorded data from the gyroscope will reveal the angular velocities for the X, Y, and Z directions. Our MATLAB code will compute the associated derivatives from these values.

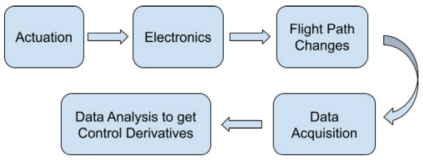

Figure 1: System Flowchart

Results and Analysis

- **Figure 2** offers an example of the raw data acquired from the MPU6050 gyroscope
- **Table 1** reports the acquired stability derivatives and their respective partial derivative expressions
- Subscripts **m**, **l**, and **n** correspond to the pitch, roll, and yaw moments respectively
- Delta subscripts **e, a,** and **r** correspond to elevator, aileron, and rudder respectively
- The derivatives acquired are consistent with theory in terms of sign but are smaller than expected
- Derivatives will need to be verified with more testing

```
Pitch = 0.00,  Roll = 0.00,  Yaw = 0.00
Pitch = 0.00,  Roll = 0.00,  Yaw = 0.00
Pitch = 0.00,  Roll = 0.00,  Yaw = -14.84
Pitch = 39.24,  Roll = 0.00,  Yaw = -8.74
Pitch = 44.31,  Roll = 34.96,  Yaw = 0.00
Pitch = 0.00,  Roll = 38.26,  Yaw = 0.00
Pitch = -21.00,  Roll = 0.00,  Yaw = 0.00
Pitch = -60.75,  Roll = -41.93,  Yaw = 0.00
Pitch = -30.45,  Roll = -47.11,  Yaw = 7.54
Pitch = 15.95,  Roll = 0.00,  Yaw = 0.00
Pitch = 0.00,  Roll = 39.35,  Yaw = -8.01
Pitch = 44.06,  Roll = 43.93,  Yaw = -8.68
Pitch = 70.46,  Roll = 0.00,  Yaw = 0.00
Pitch = 0.00,  Roll = -44.98,  Yaw = 0.00
Pitch = -58.50,  Roll = 0.00,  Yaw = 0.00
Pitch = -55.39,  Roll = 0.00,  Yaw = 0.00
```

Figure 2: Raw Data from MPU6050

$$C_{m_{\delta_e}} = \frac{\partial C_m}{\partial \delta_e} \quad C_{l_{\delta_a}} = \frac{\partial C_l}{\partial \delta_a} \quad C_{l_{\delta_r}} = \frac{\partial C_l}{\partial \delta_r}$$

$$C_{n_{\delta_a}} = \frac{\partial C_n}{\partial \delta_a} \quad C_{n_{\delta_r}} = \frac{\partial C_n}{\partial \delta_r}$$

$C_{m_{\delta_e}}$	-1.2394e-06
$C_{l_{\delta_a}}$	3.7121e-06
$C_{l_{\delta_r}}$	2.2272e-05
$C_{n_{\delta_a}}$	-6.6199e-06
$C_{n_{\delta_r}}$	-3.9719e-05

Table 1: Acquired Stability Derivatives

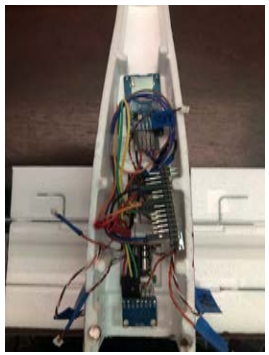

Figure 3: Electronics Integration

Future Work

- Measure different stability derivatives (sideslip, incidence angle)
- Measuring the same derivatives with changes in the plane geometry such as adding more aerodynamic features
- Move system to new airframe and measure new derivatives
- Scale real aircraft down to RC scale and determine stability derivatives

Figure 4: RC Plane

AE B7

RUTGERS
School of Engineering
MAE Design and Manufacturing

Solar Powered Terrain Walker

Trevor Shin, Isaac Berroa, Ase Awari, Adam Columbia, Matthew Nugent, David Stein
Professor William Bottega

Objective & Background

Our goal was to create a walking robot that could traverse a multitude of different terrains using only solar power as an energy source. Our stakeholders prescribed several limitations:

- It could not use wheels.
- It had to have a solar panel connected to its main body.
- It had to be less than a foot tall.
- Carry a 8oz payload

Current robot walker designs are based on a typical four-legged design. Our research and development have found that more legs better handle rough and sharp terrain. Not only are more legs important, but the stride and step they provide are just as significant. A footpath with a high step and long stride is considered an "ideal" footpath for unknown terrain.

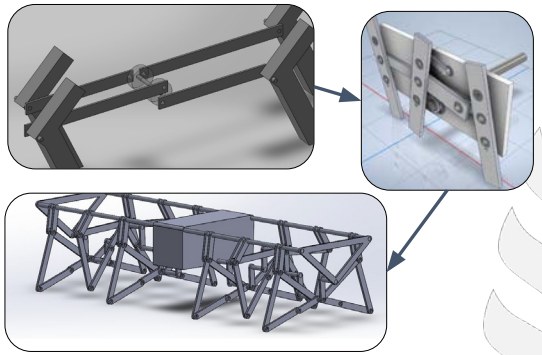

Design

We went through multiple design choices. We wanted to see if we could simplify the four-legged dog design using the possibility of two motors. The method we saw was to use a push-pull system with one motor controlling a single side. Another design we considered was turning rotational motion into linear motion. Similar to the slider-crank mechanism, the linear motion in this design. The design we picked used the engineering mechanisms of linkages, specifically, using the four-bar linkage.

Motion Analysis and Simulations

As we were limited in energy, we could not expend extra energy on the vertical motion of our walking cycle. We predicted the wobble in the robot's gait with a tracepoint in a dynamic simulation in Autodesk Inventor. We achieved a height change over one complete cycle of just 0.518 in. by optimizing the link sizes. We calculated an energy loss of 2.819 Joules per cycle using the mass of our robot's frame and components.

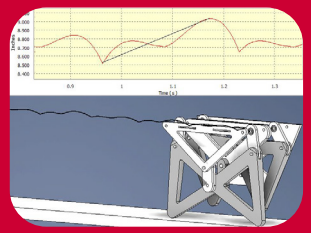

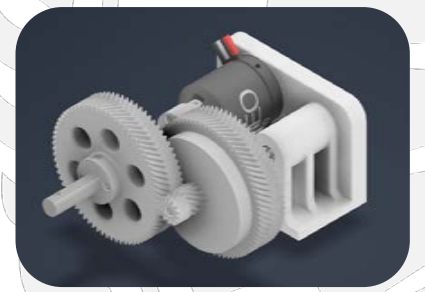

Electronic and Motor System

The gears are arranged to provide us with a 1:29.47 speed reduction. With an applied RPM of 120 on the rotating bars, we can determine the vehicle's speed to be 11.36 inches per second. Each cycle pushes the vehicle approximately 11.07 inches forward over 0.9746 seconds. The central brain of the system is the transmitter and receiver. The receiver then activates the motors by sending a signal to the ESC, whose job is to modulate each motor's speed, power, and direction depending on the input command on the transmitter.

Manufacturing and Challenges

The robot is primarily constructed from 3D printed parts. The plastic parts were an optimal replacement for metal, given the size of the robot and the goal to reduce weight and increase speed.

The design process had inevitable difficulties. The robot had to withstand the weight of its solar panel, so there was a need to make the robot structure lightweight and strong. The motors were another problem. There were concerns that a single motor could not power a traditional legged design. That was solved by installing one motor for each side and making the locomotive appendages four-bar linkages.

Engineering Analysis

PLA plastic is generally not very strong. The deformation is minimal, but as the legs degrade at different rates, it may compromise the overall robot's balance. The upside to using using PLA plastic is how cheap it is, and the pieces are easy to produce. So, during our testing and final production, if we find a leg deforming beyond use, we can easily swap it out for a brand new one. This easy re-creation of broken parts is also why we planned to produce more than the eight legs that the robot uses.

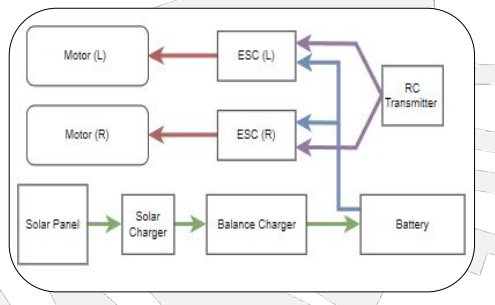

B7

Solar Powered Terrain Walker

RUTGERS School of Engineering
MAE Design and Manufacturing

Advisor: Dr. William Bottega

Group ME_BA: Luke Cicala, Folarin Davies, Zachary Ford, Ankit Kumar, William Landre, Jordan Naumovski

Abstract

The purpose of this project is to create a walking robot that is capable of traversing various terrain. Our final objective is to race our walker against another team's walker at the end of the semester.

In a new age of automation, many tasks that have previously been dictated by people are now achievable using robots. Our project follows in this endeavor as we aim to create a solar-powered robot that can walk on various terrain while carrying a 8 oz payload.

In Order, Our design optimizes:

- Stability
- All-Terrain Capabilities
- Speed

Design Objectives & Constraints

Objectives:
1. Walk 20 ft.
2. Carry an 8 oz Payload
3. Navigate Uneven Ground

Constraints:
1. Solar-Powered
2. Uses Legs
3. < 1 Foot Tall

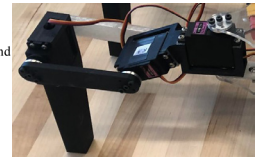

Mechanical System

Body
- Chassis - Acrylic
  - Houses Electronics
  - Payload Compartment
  - Legs Mounted on a Pivot Point
  - Center of Mass - 86 to 100 mm above the ground
- 6 Legs
  - 3D Printed - PLA Plastic
  - 3 Servo Motors per Leg: Abductor, Hip, and Shin
  - Steel Bearings, Screws, Bolts, and Washers
- Solar Panel
  - Mounted using Clips atop Chassis

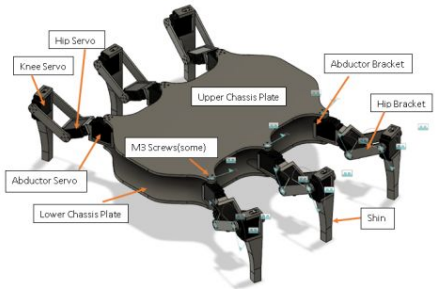

Manufacturing Process and Results

Figure 1. 3D Printing Parts

Figures 2-4. Leg Design Features

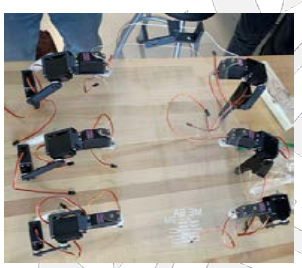

Figure 5. Legs on Hollow Body

Figure 6. Servo Driver

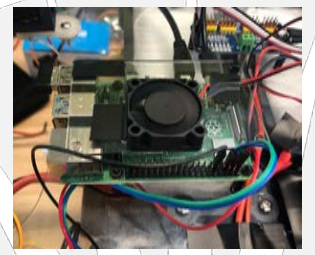

Figure 7. Fan Cooling Raspberry Pi

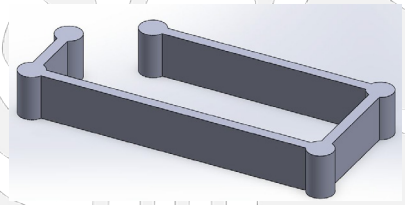

Figure 8. LiPo Battery Container

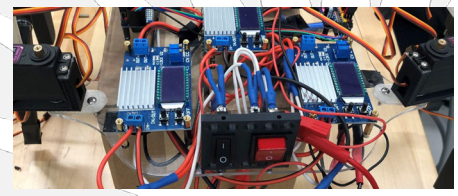

Figure 9. Different Switches for Legs and Pi

Timeline

Electrical System

Electrical System
- Objective - Power all 18 servos to drive legs
- Sun's energy -> Solar Panel -> Battery Charger -> Lipo Batteries
- Buck Converters step down voltage to be suitable for other electronics
  - Three main converters to 6V for servos and smaller one to 5V for Raspberry Pi and Gyro
- Raspberry Pi connected to servo drivers to control angles and speed of servos

Control System
- Control loop done by Raspberry Pi
  - Coded in Python 3.0
- Wireless controller used to control walking motion
- Inverse kinematics calculated using gyroscope data

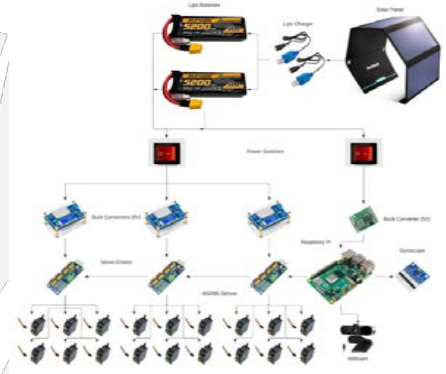

Conclusion

We successfully designed, analyzed, and fabricated a Solar-Powered Terrain Walker capable of overcoming an array of different landscapes. Its mechanical components were designed to maintain stability and its walking gait was programmed in Python to maximize speed. Tests were conducted to assess different gaits and the optimal one was chosen based on our objectives.

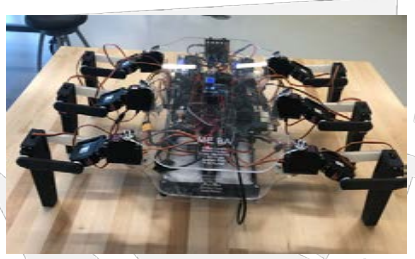

BA

Development of a 3-DoF Satellite Test Bench for Sloshing Control Research

Connie Liou, Ryan Chen, Lisa Vu, Samantha Carey, Dr. Laurent Burlion

Mechanical and Aerospace Engineering, Rutgers University, Piscataway, New Jersey 08854

SATELLITE PROPELLANT SLOSH

Non-linear Sloshing Problem

- Spacecraft liquid propellant undergoes complex motions during orbital maneuvers or attitude corrections
- Oscillatory modes and forces are imparted on spacecraft
- Spacecraft stability is affected with difficult-to-reject torques

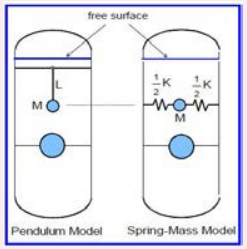

Active Control Algorithms

- Equivalent Mechanical models
  - Pendulum and spring-mass models of sloshing fluids
- Vary control parameters depending on state of system
- Safe Mode (Robust PID Controls)
- Fusion of control methods for optimal performance

Test-Bench Experiment

- Minimize time to stability
- Various satellite-like maneuvers
  - Bang-bang
  - Bang-stop-bang

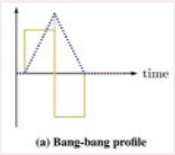

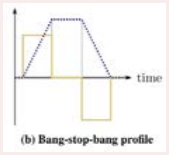

DESIGN & METHODS

Payload

- Sloshing fluid tank
- Propellant management device (PMD)
- VICON/OptiTrack/Encoders

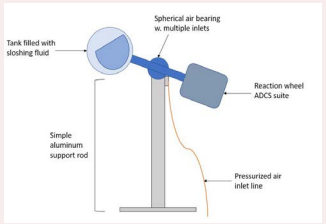

Attitude Controls and Sensors

- 3.5 in steel flywheel to generate inertia
- Maxon EC-45 brushless DC motors
- Spherical air bearing
- Arduino microcontroller
- Inertial measurement unit
- Aluminum support structure

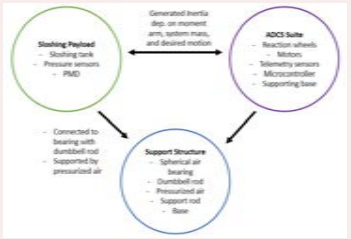

Support Structure

- Dumbbell rod
- Pressurized air and air bearing socket

THEORY

Governing Equation

- Input torques are determined to keep the angular acceleration and velocity of the system at zero
- Net input torque generated by wheel to stabilize the system
- Sloshing torques predicted with Equivalent Mechanical Models

Control Algorithms

- Output Feedback Adaptive controller
  - Adaptively update PID controller to obtain desired wheel torque
- Machine Learning Controller
  - Predict satellite control torques using a “black box” approach
- Reference Governor Controller
  - Used to ensure control outputs remain within safe constraint

$$I_{sys}\frac{d^2\theta_{sys}}{dt^2} = T_{wheel} + T_{sloshing}$$

$$I_{sys}\frac{d\theta_{sys}}{dt} = I_{wheel/sys}\frac{d\theta_{wheel}}{dt} + L_{sloshing}$$

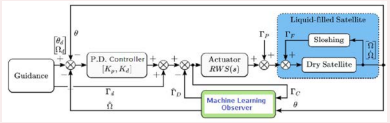

RESULTS & FUTURE DIRECTIONS

Results

- Initial software and configurations completed
- Assembled and demonstrated initial configuration performance

Future Directions

- Bring this setup to a Zero-G flight to test functionality in microgravity environment
- Explore PMD device designs and effects on sloshing dynamics and controls

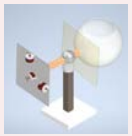

REFERENCES

[1] A. Bourdelle, J-M. Biannic, H. Evain, C. Pittet, S. Moreno and L. Burlion, "Modeling and control of propellant slosh dynamics in observation spacecraft", in Proc. of the 8th European Conference for Aeronautics and Space Sciences, (EUCASS 2019), Madrid, Spain, (Best Student Paper Award in Flight Dynamics, GNC and Avionics).
[2] Cho, Sangbum & Mcclamroch, N.H. & Reyhanoglu, M.. (2000). Dynamics of multibody vehicles and their formulation as nonlinear control systems. Proceedings of the American Control Conference. 6. 3908 - 3912 vol.6. 10.1109/ACC.2000.876955.
[3] Dodge, Franklin. (2000). The New "Dynamic Behavior of Liquids in Moving Containers".
[4] Reyhanoglu, M. & Rubio-Hervas, Jaime. (2011). Nonlinear control of a spacecraft with multiple fuel slosh modes. Proceedings of the IEEE Conference on Decision and Control. 6192-6197. 10.1109/CDC.2011.6160660.

AE BB

RUTGERS
School of Engineering
MAE Design and Manufacturing

Design of a Biomechanical Hand

Emma Nichols, James Randolph, Yaxin Mo, Jack Goodall, Prof. Kimberly Cook-Chennault

Abstract

Soft robotics is a subfield of robotics that utilizes compliant materials such as silicone in the fabrication process. In this project we used soft robotics principles to design and manufacture a biomechanical hand that can be used as a prosthetic. Each finger is driven by a silicone actuator that expands linearly when inflated with air. A 3D-printed exoskeleton converts this expansion into the bending motion of a finger.

Background

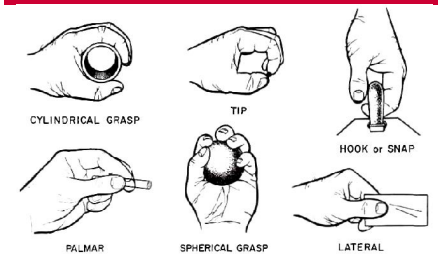

Figure 1: Common Grasps of the Human Hand

- In this approach, we are utilizing soft robotics principles to take advantage of cheap, flexible material in order to keep the costs low and our hand pliable
  - ➢ This will combat the high cost and limited functionality of current prosthetics.
- This hand drives motion in response to compressed air, and is adaptable to different movements to give the user a better feeling prosthetic.
- The most common types of grasps are displayed in Figure 1, which assisted the group when creating different movements that the hand makes.

Timeline

Figure 2: ME_C3 Project Gantt Chart

This Gantt Chart explains the timeline of the project, including manufacturing, prototyping, and assembly time.

Design

Figure 3: Finger Design with Actuation

The linear expansion of the actuator is converted into a bending motion by the geometry of the exoskeleton (red). The actuator expands linearly when it is inflated with air, and it is prevented from ballooning outwards by a tightly wrapped reinforcement thread.

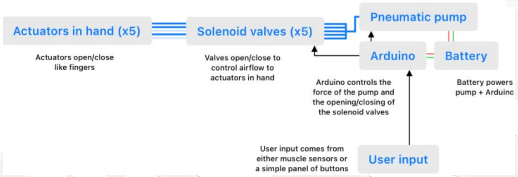

Figure 5: Apparatus Flow Diagram

Figure 4: Integral Hand Design

The actuators are inflated by a pneumatic pump controlled by an Arduino. Solenoid valves determine which fingers are supplied with air, and therefore which fingers bend. The diagram of the entire system is shown on the left.

Manufacturing Process

Figure 6: Actuator Curing in Mold

Figure 7: Mold Opened to Reveal Actuator

Figure 8: Completed Actuator with Threading

Manufacturing (cont.)

Prototyping for this project began with constructing a working finger prior to an entire model in the hopes of saving material and conserving resources. This allowed the group to focus on the conceptual and technical details of the design before working with large-scale parts.

- The perfected finger design was tweaked to assure proper bending motion is achieved when pressure is applied
- Difficulties included: Air bubbles in actuators, actuator molds not of the right size, thread alignment not tight enough, exoskeleton material too fragile
- A simulation of an individual finger is shown in Figure 6 below

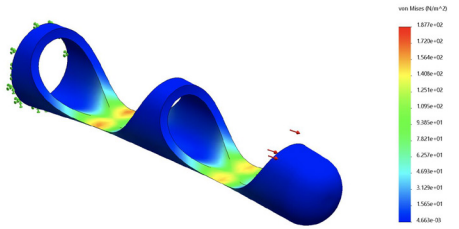

Figure 9: Solidworks Simulation Showing von Mises Stress when Pressure is Applied Internally

Results

In result of this project, we delivered a hand that has the capabilities of achieving different grasping motions. Our hand allows the amputee to be able to grasp spherical objects, cylindrical objects, complete a hook and grasp to pick up objects, and flex each finger. This will allow the user to complete actions like a fisting motion, grabbing door knobs, and picking up a variety of objects such as water bottles, phones, etc.

Our project allows the user to have access to more affordable hands with a wider range of motion. Because of the flexible material, the overall feel of the hand is softer, more adaptable, and similar to human skin. This allows grip around an object that is only dependent on pressure. Access to prosthetics such as these grants the amputee more independence and quality of life, and allows them to be more self-reliant.

C3

RUTGERS
School of Engineering
MAE Design and Manufacturing

Desktop-Size Non-Destructive Material Identification Device

Michael Peck, Mohammad Khan, Kyle Kuhl, Jonathan Williams, Ethan Hurilla, Boyan Lazarov
Dr. Alberto Cuitino (Advisor)

Project Summary

This project is to create a desktop materials testing device that measures the Young's Modulus and displays the result. The device is also capable of determining the material placed in the device based off of the young's modulus.

Equations

- Using Eulers Critical Buckling Equation to calculate the Youngs Modulus.
- E is the Young's Modulus
- I is the moment of inertia of the sample
- L is the length of the sample
- Pcr is the force applied to the sample

$$\frac{P_{cr}L^2}{\pi^2 I} = E$$

Eq 1. Eulers Critical Buckling Equation

Conceptual Designs

- Two major concepts were created
- Both of them were different ways to apply the load and measure the force
- The one method we didn't select uses a level to apply the force onto a specimen.
- It was not selected due to the extra space that would be taken up by the lever

Manufacturability

- Uses 8020 Alluminum Standoffs as the main support of the system
- Three, ½" Aluminum 6011 Plates separate the layers of the structure
- The first layer is the base, which houses the gears, motor, Ardino and display.
- The second layer is where the force is applied and measured and the displacement is measured
- Top layer holds the ACME screws in line with the second layer.
- The sample holder is also made of the same aluminum with a milled channel for the sample to rest.

Description

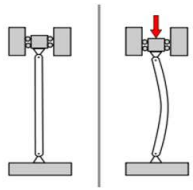

Fig 1. Model explaining the general setup

Goal is to produce a device that can conduct material testing on a sample with only the push of a button. The size of the device is small enough that it would fit on the corner of a persons desk, while being able to measure any material known to man. Below is the process for how the Young's Modulus is found.

- A sample is loaded into the machine, it is slotted into a notch that allows rotation
- The force is applied at the top of the sample
- This causes the specimen to buckle
- The displacement is measured in the vertical and horizontal
- When yielding is determined, the force measured on a load cell is staved.
- Using the measured force to calculate the Young's Modulus
- All of this is controlled by an ardino and motor
- The results are then displaced on a panel on the front of the device

Final Design

Below are the images of the final design assembly in Solidworks CAD

Of the three potential design concepts, we decided to go with the screw mechanism pictured below. We chose this design because of its structural integrity, and compact form factor.

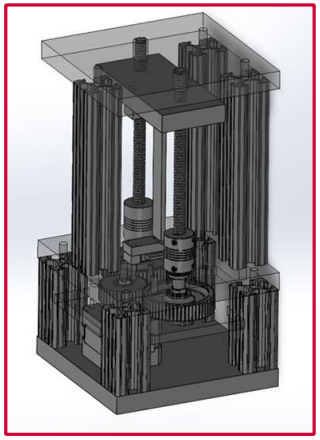

Fig 3. Full assembly with transparencies for detail

The idea is to use a ball and screw mechanism to generate a downward force on the specimen causing it to buckle. Our initial inspiration for this design came from the tensile test machine used in the materials properties lab. It uses the ball and screw method to apply force to the specimen using tension. We took this design and created a sketch that involves the use of a motor to move the mechanism.

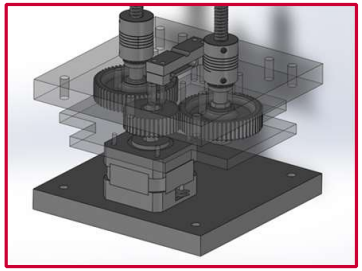

Fig 4. Lower mechanism detail. Structural components hidden for clarity

These rods are driven by gears that are connected to a stepper motor. The way we are automating the machine is by using an Arduino board to program the necessary inputs we need to compress the material. The arduino board, gears, and stepper motor are enclosed in the main base enclosure.

All simulations that have been run worked as expected and did not change the status or progress of our report. Our design has been finalized and is currently in the manufacturing process. We are working on the code and the wiring of the arduino board.

Conclusion

- The original goals of this project are to create a desktop sized materials testing device that is
  - Can test any material
  - Fully Automated
  - <100$ in cost to manufacture
  - Precision of .1MPA per run on the sample
- We did not complete the last two goals with
  - The cost of the device being around $650
  - The load cell used varying by more than .1MPA per run
- The device was fully automated from the press of a button.
- The design is proven to work with standard materials such as steel and aluminum.
- While we have not tested for more exotic materials, it is likely that it would work with much more rigid materials.

Overall, the design accomplishes the major goals set out before it, while missing secondary goals. If we were to turn this into a project a lot of effort would be spent on finding a more accurate load cell, and optimizing the design for cheaper manufacturing.

C4

Synthetic Jet Actuator For Active Flow Control

RUTGERS School of Engineering
MAE Design and Manufacturing

Artur P. Kurdusiewicz, Jose Jimenez, Deep Patel, Michael Wallin, Said Koubane,
Dr. Edward P DeMauro

Motivation

Aircraft experience boundary layer separation at high angles of attacks which causes the lift of an aircraft to decrease despite increasing the angle of attack. Active flow control can prevent this separation and return the aircraft to normal operating conditions.

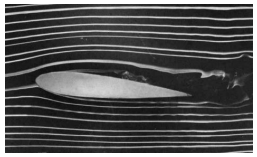

Picture from "An Album of Fluid Motion" by Van Dyke

Objective

With synthetic jet actuators, momentum is injected into the boundary layer preventing separation at high angles of attack.

- Create a synthetic jet actuator to prevent boundary layer separation.
- Use piezoelectric discs to create an zero net mass flux across an orifice.
- Simulate the designed system in a wind tunnel
- Visualize results using smoke machine to view streamlines of the flow.
- Incorporate results to an actual aircraft.

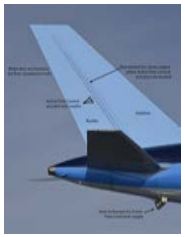

Picture from NASA/Boeing showing an example application of synthetic jets.

Parameters

Voltage: 60 V

Frequency: 1kHz

Wave Shape: Sine

Orifice shape and aspect ratio: rectangle 1:15

Design

The design consists of two main subassemblies:

1. MAIN BODY

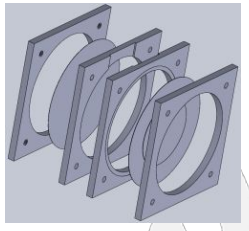

The main body is composed of 4 aluminum machined square plates (45.7mm x 45.7mm x 2.54mm) that are screwed together.

The square plates are machined to include concentric cut outs to place the piezo discs. Between the two inner plates there is a cavity of air.

2. MOUNT

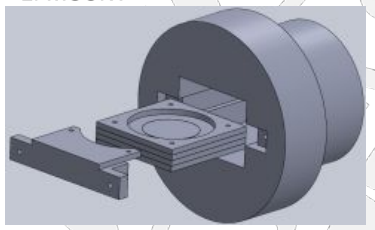

Our design is conceptually based on a zero net mass flux system. By applying a voltage to piezos discs we can cause a displacement of air and push it out through an orifice creating a jet. A 3D mount with a locking mechanism is used to attach the jet to the wind tunnel at the rutgers laboratory.
The mount is comprised of the head body and the locking mechanism. The body has two circular extrusions of diameters 3.5 and 2.5 inches. The center of the mount has rectangular cuts which allows room for wiring of the piezoelectric discs.

Results

Results from our experiments are presented below:

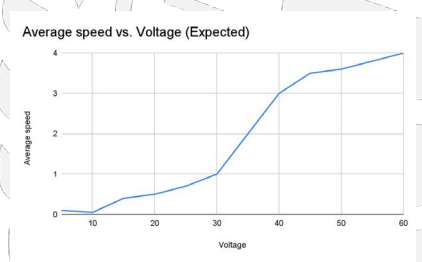

Average Velocity of the synthetic Jet as a Function of the Voltage applied.

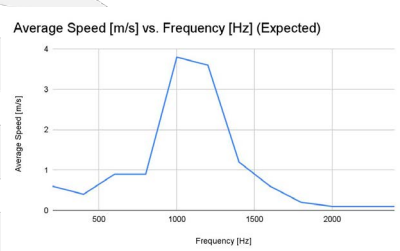

Average Velocity of the synthetic Jet as a Function of the frequency of the signal.

We expect the maximum velocity to be around the resonance frequency of 1kHz.

Testing

The synthetic jet is inserted into the wind tunnel using a specially designed mount. The piezo discs are then connected to the function generator and amplifier. The amplifier is used to increase the voltage of the function generator to the 60V range.

The wind tunnel is run with the smoke seeded into the flow to represent the streamlines and qualitative data is collected.

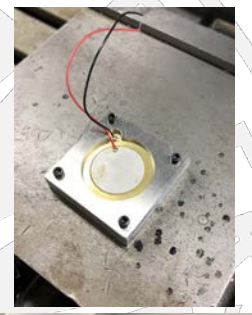

The quantitative tests are performed using a hotwire where the synthetic jet actuator is run with different settings and then the output speed is measured and data is collected.

Acknowledgement

We would like to thank our advisor professor DeMauro for his guidance and patience. Furthermore we would like to extend a gratitude towards, Mr. Simonovic, Dr. Basily.

Sources: https://www.nasa.gov/press-release/nasa-wraps-up-first-green-aviation-tests-on-boeing-ecodemonstrator

AE D1

Sustainable Transport Research Aircraft For Test Operation (STRATO)

RUTGERS School of Engineering
DEPARTMENT OF MECHANICAL AND AEROSPACE ENGINEERING

Daulton James, Bertrand Smith, Michael Ferrell, Roy Monge Hidalgo, Frederick Diaz, Connor Magee, Jean Alvarez, Professor Edward DeMauro

NASA Partner

Abstract

Our system, STRATO, integrates a synthetic jet and a driver system to a model wing. The driver system is designed around the Texas Instruments DRV2667 piezo driver. As part of our objective to support research endeavors, the design process is thoroughly documented and openly available. Subsonic wind tunnel testing on the model wing is used to provide a framework for integration onto other airframes. Important design parameters were initial jet array placement, choice of non-dimensional frequency (F+), and momentum coefficient (Cm) for separation control.

Introduction

Aircraft maneuver by deflecting parts of the wing known as control surfaces. However, control surfaces are constrained by their maximum deflection angle. Integrating arrays of small, energy efficient jets into control surfaces can re-energize the flow of air to increase the maximum deflection angle.

- Aircraft maneuver by applying control surface
- Actuator jets increase deflection angle
- Improve performance and decrease fuel consumption

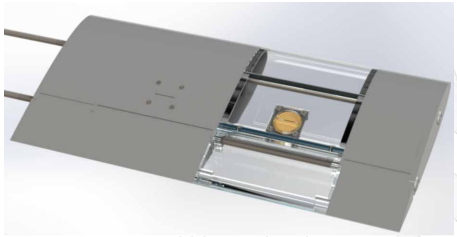

Figure 1: Wing model design with synthetic jet

Objective

Our objective is to bridge the gap between lab research and commercialization by providing engineers with an adaptable, open-source solution for researching how synthetic jets operate on real aircraft. We hope to catalyze research on the obstacles barring the adaptation of synthetic jets by aircraft manufacturers.

- Create a solution for synthetic jet research
- Modular and inexpensive wing model for testing
- Integrate system into an RC plane

Model Wing Design

- NACA 0018 with flap at 30% chord from trailing edge
- Designed to be modular and easily swappable
- Different configurations available if desired
- Flap deflections set at 30° and 60°, 90° is possible
- Pressure taps installed on flap

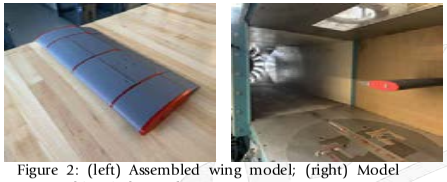

Figure 2: (left) Assembled wing model; (right) Model mounted in wind tunnel

Experimental Results

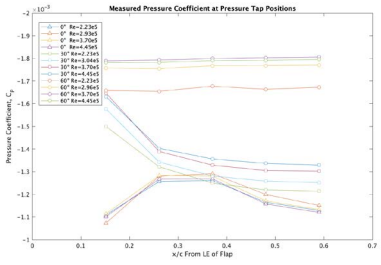

Figure 5: Baseline wind tunnel results

- Static pressures recorded along flap
- Reynolds number ranging from $2.2x10^5$ to $4.45x10^5$
- Flap Deflections of 0°, 30°, 60°
- Processed in MATLAB for baseline testing

Electrical Systems

- Arduino is used as a signal generator
- Sine wave is sent to an amplifier (DRV2667)
- Piezoelectric actuators run at 60 Vpp

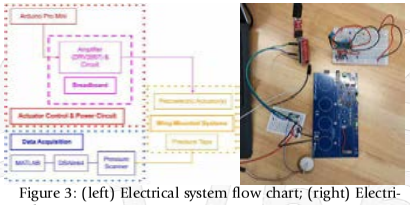

Figure 3: (left) Electrical system flow chart; (right) Electrical setup

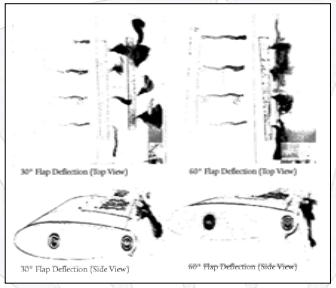

Figure 6: Baseline Tufts flow visualization

- Tufts flow visualization preformed
- Video recorded and processed in MATLAB to present mean string position over 4 seconds
- Baseline testing correlates to what is expected, flow separates with high angle of attack flaps

Project Timeline

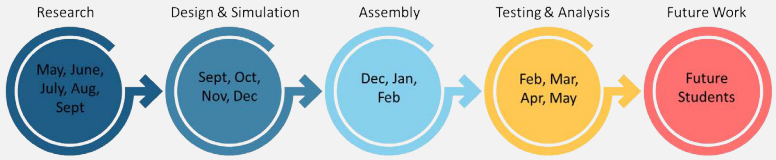

Simulations

COMSOL Simulations

- Varied flap deflection and Reynolds number
- 2D and 3D simulations
- Turbulent and Laminar Models
- Produced simple model for a synthetic jet

ANSYS Simulations

- 2D Turbulent Flow
- Varied flap angle and freestream velocity
- Predicted flow separation
- For flap angle >20 deg at 5-50 m/s

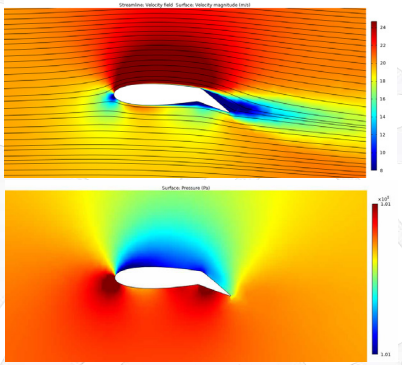

Figure 4: (top) COMSOL velocity field; (bottom) pressure distribution

Conclusions

- Baseline tests confirm flow separation over flaps
- Overall structure of the wing is ridged and robust
- Driving circuit can be compact
- Future work is necessary

NASA Crowdfunding

As part of the NASA USRC cost sharing requirement, we are crowd funding for our project. Scan the QR code to the right for more information.

STRATO

AE D2

RUTGERS School of Engineering

MAE Design and Manufacturing

ME-D2: Flapping, Bio-Inspired Wind Energy Harvester

Advisor: Professor Mitch Denda
Ashwin Baskaran, Vaibhav Gupta, Neil Patel, James Mehrtens, Justin Holgado, Kaif Mahajan

Introduction

•The problem proposed for this project is to create a more efficient way to harvest energy from the wind.
•flapping motion of bird wings and fish fins is far more efficient than man made turbine at utilizing fluid flow energy
•Why not utilize this biological flapping motion to generate energy from fluid flow?

Analysis

- Length of rod is very important when trying to generate more power, chose around 0.2m to maximize power gains while keeping weight relatively low (Figure 6)
- Diameter of rod has little influence on power gen., cheapest diameter chosen (Figure 5)
- Delrin plastic holds up well in stress test, should stand up to all of our design's needs (Figure 4)

Design

- Three airfoils to be connected via hinge joints and taper off in size (Figure 2)
- Smallest size airfoil attached to horizontal rod.
- The horizontal rod to be connected to base tower and rotate with an influx of fluid flow onto the airfoils
- The main energy generation for this design is rotational energy through two generators connected via a gear system below the main shaft
- Piezoelectric disks for secondary energy generation
- Discs would accumulate energy from the continuous vibrations of the flapping airfoil.

Design Flow Chart

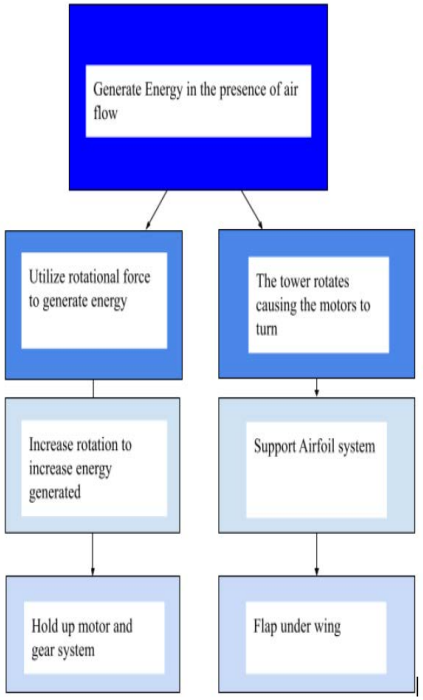

Figure 1: Design Flow Chart

Data/Figures

Figure 2. 3-D Printed Wing Apparatus

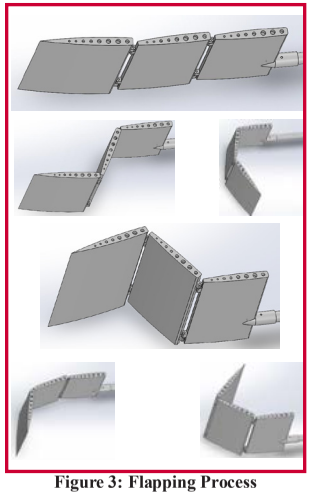

Figure 3: Flapping Process

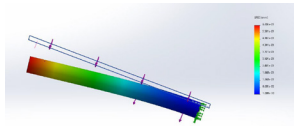

Figure 4. Stress Analysis of Rod

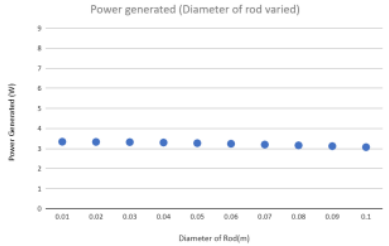

Figure 5. Power Generation vs. Diameter of Rod

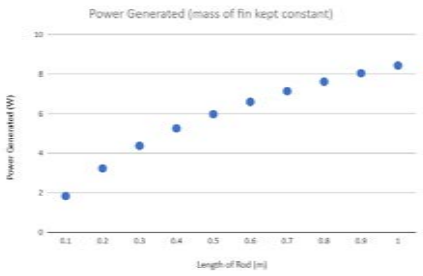

Figure 6. Power Generation vs. Length of Rod

Flapping Process

- Articulated wing design to help with fish-fin like flapping motion. (Figure 2)
- Flapping motion meant to generate further vibration which should add to the rotational motion of the design. (Figure 3)

Conclusions

- The finalized design for this project entails an articulated wing motion approach to energy generation
- fluid flow acts on the vertebra-like wing structure which in turn imparts a moment towards the center rod and causes rotation about its axis (Figure 1)
- Design will generate energy by using generators and piezoelectric discs to harness rotational and vibrational energy
- Design will have tabletop form factor, allowing for portability
- The goal that this project seeks to accomplish is to power a 1-Watt LED light bulb
- This design is meant to be manufactured using PLA plastic as it is meant to be lightweight and durable.
- Delrin plastic was used to fabricate the tower and horizontal rod
- Future plans include scaling the design in order to generate for more heavy power usages

D2

RUTGERS School of Engineering

MAE Design and Manufacturing

Bio-inspired Flapping Wing Energy Harvester

Vevikanand Deonarine, Donald Grabinsky, David Tran, Cole Woloszyn
Advisor: Dr. Denda

Motivation

Most of the world's energy is produced by the burning of fossil fuels that release toxic and harmful gases that pollute the atmosphere. Greenhouse gases are an example of the products produced from the burning of fossil fuels. These fumes have been proven to contribute to climate change which have negative effects on the environment. There are forms of clean energy production: solar power and wind turbines. However, these are not without their drawbacks: solar power depends heavily on the position of the sun and weather conditions. Traditional wind turbines are massive, require complex and costly manufacturing techniques, and can only be built on sites where there is minimal harm to wildlife and people.

Critical Design Challenges and Manufacturability

Harvesting energy from the wind using a flapping motion was the critical design challenge of this project. The current design allows for a smooth transition of motion that harvests equal amounts of energy in both directions. The design limits the flapping motion of the airfoil via direct connection to a flywheel. This allows for a predictable flapping motion under steady wind conditions.

The largest challenge faced during this project was fighting the frictional effects of the components. To combat this, all parts were designed to be efficiently weighted. They were light enough to not cause too much friction but were heavy enough that enough moment of inertia was there to keep the system in motion.

Aside from being lightweight the components were also designed to be simple, and easy to manufacture. With a limited budget and manufacturing capabilities the design process was focused of ease of manufacturability. All of the components are possible to be manufactured in a typical machine shop. This prototype proves the design has potential to harvest energy from the wind.

How the Harvester works

Wind Energy
The wind energy is captured by a symmetrical airfoil. A symmetrical airfoil was chosen so that lift would be generated at both of the opposite extremes of the wing pitch.

Linear Motion
The airfoil sits on top of a low friction linear rail. The energy captured from the wind gets transferred to the linear rail as the airfoil oscillates back and forth.

Rotational Motion
The energy from the linear motion gets transferred to rotational motion via a link that connects the airfoil to the flywheel. As the flywheel rotates the wing pitches.

Generator
Finally, the energy in the flywheel drives a generator that can produce energy through a speed increasing gearbox.

Physical Design

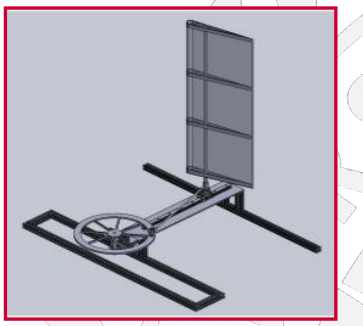

Figure 1: CAD Model of the harvester

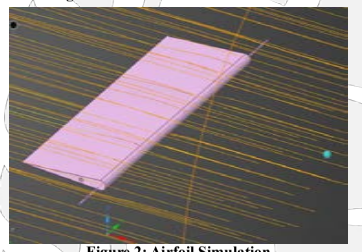

Figure 2: Airfoil Simulation

Figure 3: Manufactured Design

Important Dimensions
Airfoil: 11 inch chord length, 30 inch height
Flywheel: 12 inch OD , 11 inch crank diameter
Linear Rail and Carrier : 11 inch travel

Testing and Results

Testing at wind speeds of 33 mph (14.75 m/s) saw the project oscillating at about 111 rpm. The ac motor acting as the generator has a KV rating of 330 which means for each volt applied the motor spins 330 rpm.

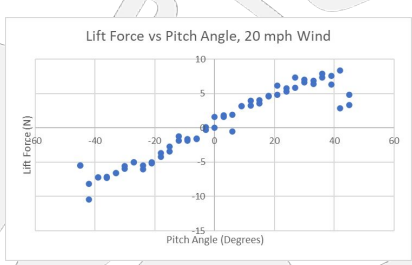

Figure 4: Lift Force vs Pitch Angle Plot

This process works in reverse when the motor is spun backwards it generates voltage. Through testing efficiency was estimated to be about 80 percent. The gear ratio from the transmission is set to 1:12. Giving us 1320 rpm to the generator. Therefore about 3 volts are produced at a current of 0.34 amps giving a power generation of 1.02 watts.

$$V = \frac{\varepsilon^{*}\omega_{rpm}}{K_v} \quad P = V * I$$

Equation One

Project Timeline

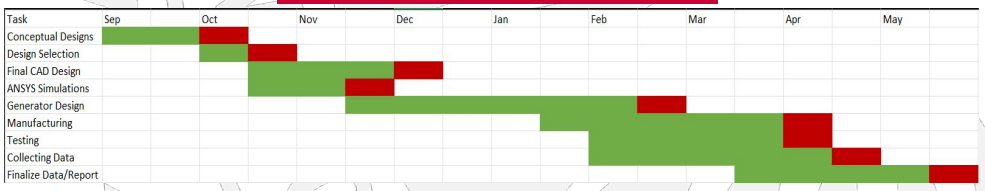

Future Design Changes

- Rotating base than can adjust to varying wind direction in real world applications
- Multiple rail designs that are interchangeable based on application's environment and conditions
- Source lower friction bearings and components to increase efficiency further
- Dynamic airfoil to eliminate no-lift zones

D3

DRONE CAPABLE OF DELIVERING MEDICAL SUPPLIES

RUTGERS School of Engineering
MAE Design and Manufacturing

Rohit Rajeev, Mangesh Nadkarni, Nicolo Spinelli, Nelson Ngai, Andy Yang, Sebastian Toledo, Thomas D'Auria, Prof. Francisco Diez Garias

Abstract

A mechanical claw is attached to a Hobbypower F550 Hexacopter:

- Frame weight: 3.63 lb
- Claw Weight: 0.63 lb
- Package Capability: 1.40 lb
- Flight Time: 10 minutes

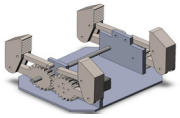

Fig. 1. CAD model of claw mechanism

Fig. 2. Testing claw with 1lb package

Background

An estimated 2 billion people don't have direct access to medical supplies. Current technologies for drone delivery in the public health industry are mainly used for emergency purpose supply airdrops. This drone has the ability to both securely pick up and drop off supplies to people in need. General purpose items that fit in small standard size packages can be delivered in addition to delicate items like vaccines, blood bags, or IV drips. The ability of the claw system to pick things off the ground without requiring a specialized loading system is another advantage of the design that many drone delivery systems in the industry require. The claw can be scaled to attach to any drone and is easy to repair in situ during emergency situations.

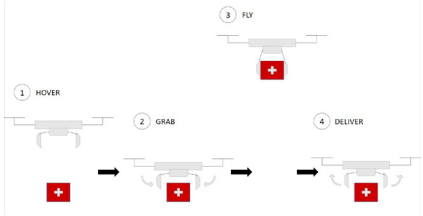

Fig. 3. A diagram for the planned operation of the drone

Final Design

The final CAD assembly can be seen in Figure 4 below. The final claw design can be seen in Figure 5. The hexacopter layout was chosen to maximize thrust/weight ratio in order to carry the highest payload. The claw design was chosen after much testing of previous design iterations.

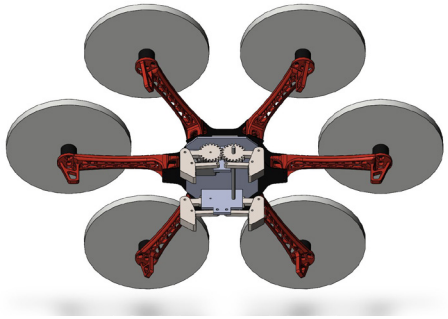

Fig. 4. Final CAD Assembly with landing gear removed

Fig. 5. Finalized claw design prototype

For a thrust/weight ratio of 2 and assuming the claw mechanism weighs 0.63 lb, the drone can lift a maximum package weight of 1.4 lb. Testing determined the claw mechanism itself can provide enough force to hold 2 lb (See Table 1).

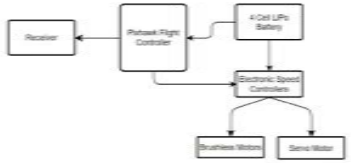

Fig. 6. Power flow diagram of claw and drone system

Analysis

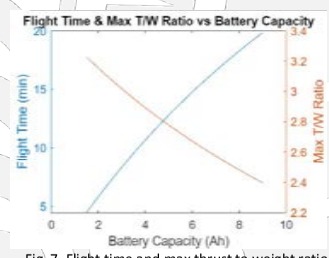

Fig. 7. Flight time and max thrust to weight ratio vs battery capacity for a 4 cell LiPo

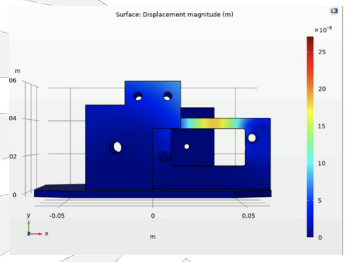

Fig. 8. FEA analysis of baseboard for claw

Flight Time and Thrust to Weight Ratio due to 4S battery capacity (left). FEA analysis performed for the motor compartment on baseboard when motor applies torque (right) for component design optimizations of claw

Analysis (Continued)

Table 1. Max Claw Payload Weight for Gripper Surfaces of the Claw.

Claw grip	Max Weight (lb)
PLA only	0.25
PLA with adhesive	1.25
PLA with rubber	2

Fig. 9. (left) Single motor thrust test vs applied throttle. Thrust at 50% was 0.83 lb, thrust at 100% was 2.1 lb.

Project Management

The SCRUM/agile methodology of work was used for this project. The group had both one-week and two-week sprints. The one-week sprint provided deliverables to the advisor, while the two-week sprint provided deliverables to both the advisor and the TA. Larger tasks (called epics in Jira) will be broken into issues. A Kanban board is also used to visualize the progress of the group, and a list of to-do issues, in-progress issues, and completed issues.

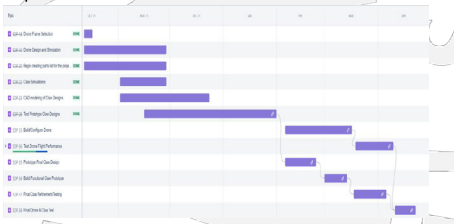

Fig. 10. Gantt Chart

Acknowledgements

The team would like to thank advisor Professor Diez for his guidance. The team would also like to thank the Rutgers Mechanical and Aerospace Engineering Department.

AE D4

RUTGERS
School of Engineering
MAE Design and Manufacturing

Virtual Reality Cycling for Patient Rehabilitation

Timothy Tchou, Melanie Alpert, Charm Nicholas, Connor Devosa, Kelsey McLennan, Michael Guzman, Dr. German Drazer

Statement of Purpose

Oftentimes, a stroke patient will have asymmetry, or one-sided weakness, which can lead to poor coordination. An exercise bike is often used in physical therapy to improve muscle coordination and gait. By providing a kit of pedals fitted with load cells, practitioners will be able to collect data to monitor patient progress.

Project Description

The project consists of two main parts: a pedal and a virtual reality (VR) program. The bike pedal is sandwiched in between 2 aluminum plates and load cells beneath the contraption. The purpose of the modified pedal is to measure the amount of force the patient can produce and the rate at which they do it at that moment in time, and it has the ability to pinpoint if the patient is generating more force on one side. The pedal will assist the practitioner in taking these measurements, and every time the patient uses the kit, ideally they should be better at generating force and be much better coordinated. The purpose of the VR program is to provide a visual background to the patient because more often than not, cycling patients get bored staring at nothing. The VR program is a more enjoyable way for the patient to cycle because the program can be set up in a way much like a game.

Design Methods

- The pedal consists of four load cells which are placed directly within the pedal. Using nuts, they are secured in place by aluminum plates above and below the pedal
- The four load cell signals are combined and directed to a wheatstone bridge of an Openscale board to amplify the voltage difference.
- The electronics components of our product are housed in a 3D printed basket placed below the pedal. This allows for easy replacement of the LiPo battery.

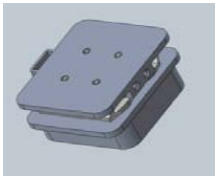

Fig 1. CAD model for the pedal.

- The Unity software was used to create a virtual reality environment. The track consists of a circular road and a grassy terrain (Figure 4a). As a person pedals, the software would have the person "move" as if they were biking along the road.

Results

Fig 2. Pedal prototype.

Fig 3. Bluetooth results from varying applied forces

Fig 4. Pedal Calibration and Accuracy Testing

a)

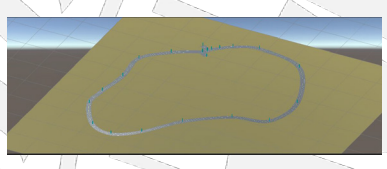

b)

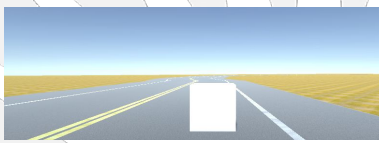

Fig 5a. Track developed in Unity
Fig 5b. Patient's 3rd person view on the track.

Future Work

- We want to focus on getting the load cells in the pedal to communicate with the VR environment in real time so that the patient would have a fully interactive experience
  - Requires writing a new C# script

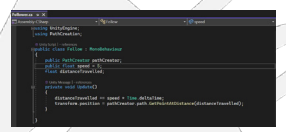

Fig 6. C# script of the cube moving around the path at constant speed

- To measure the upward force applied while pedaling, we would like to add a strap on top of the pedal
- After successful integration with the Bluetooth data with the VR environment, we would like to acquire patient data and analyze the data of a cycling pattern

Discussion

- The VR environment is able to move a cube representing a patient's 3rd person perspective along a predetermined path at a constant speed
- The pedal can currently provide real-time force data to be analyzed (Figure 3) using the load cells
- We have been unsuccessful in integrating the pedal's force readings from the Bluetooth to the VR environment in real time

Conclusion

The current design is lightweight, compact, and easy to change out parts if needed. The load cells are able to obtain accurate force readings. Future groups will have to ensure compatibility of the VR-data system.

D5

RUTGERS School of Engineering

MAE Design and Manufacturing

Tabletop Automated Gantry for Fragile Objects

Rutvik Parikh, Juan Jaramillo Barnuevo, Manav Vaghasiya, Dhruv Chawla, Sahith Nagireddy

Background

When innovation occurs, the objectives of the design are to increase efficiency and decrease costs. Processes used at Amazon, FedEx, UPS transport a high volume of different shaped products at a high rate everyday. Our motivation is to create a

- Unique handling process that reduces damage to materials such as glass or clay
- Is transportable and lightweight
- Is additive to various processes

Fig 1. Multi-Axis Automated Gantry

Project Overview

An automated gantry is an automated industrial robot that moves in a linear direction that can support and carry a load. Our automated gantry is designed to:

- Reduce speed of transport based on item fragility
- Create a system that is additive to manufacturing processes
- Can be manipulated for different purposes depending on manufacturing processes

Our goal was to create a simple and creative process for product transport. The whole system should weigh less than 10 lbs., the object weight is less than 3 lbs., and the overall system should cost less than $350. Additionally, the velocity of the gripper must vary according to a parameter (we chose color).

Fig 2. 6-Axis Robotic Arm

Design

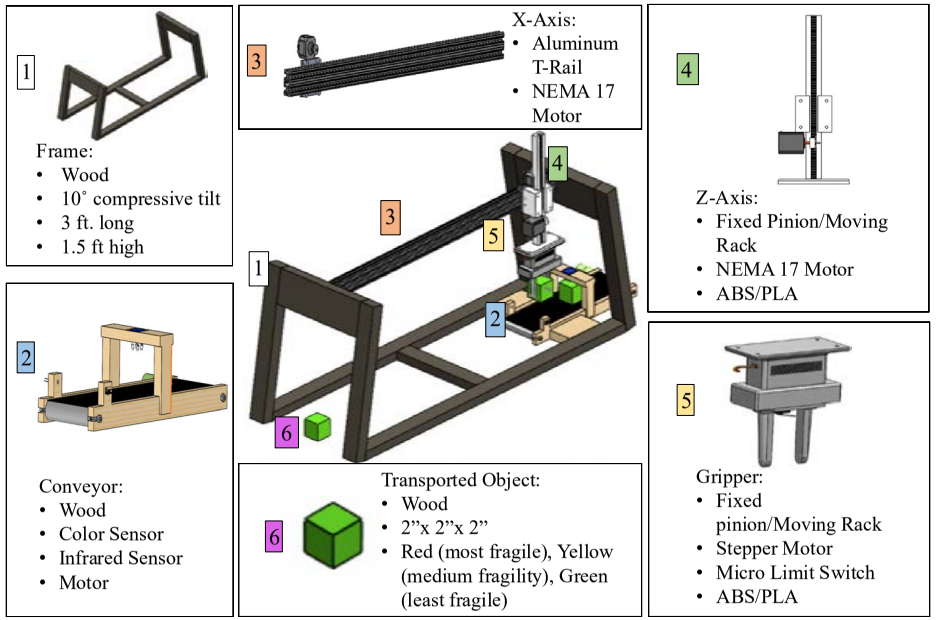

Fig 3. Assembly Breakdown of Components

Results

Our frame and gripper was simulated for stress distribution and displacement as those components carry the largest loads. The magnitude of stress is low and does not spread to other components as much in both components. There is very little displacement in the frame and gripper.

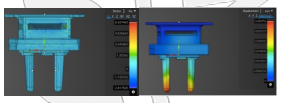

Fig 4. Gripper Stress (left) & Displacement (right) analysis

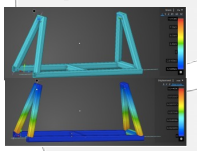

Fig 5. Frame Stress (top) & Displacement (bottom) analysis

From our previous conceptual designs, we aimed to fix a few flaws:

- Swinging caused by overextended Z-axis
- Vibrations
- Gripper Velocity
- Simplicity
- Uniqueness

Our solutions to these flaws (respectively) were:

- Bearing support along moving rack
- Stable frame structure
- Color Scanner to adjust number of rotations of the motor
- Mechanical and electrical approach, little cost
- Focused on a problem in manufacturing processes and aimed to solve/reduce the effects of it

Functional Decomposition

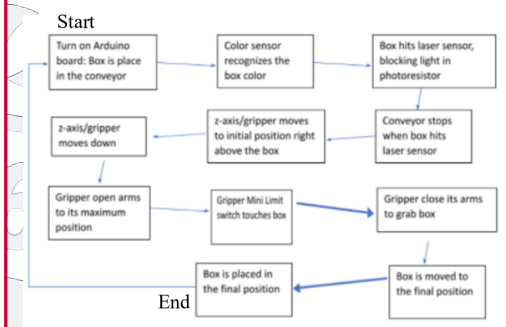

Fig 6. System Functional Decomposition

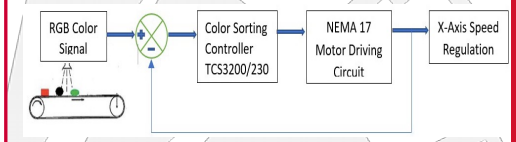

Fig 7. Control System Feedback Loop

Conclusion

Based on our design, we were able to meet our criteria and deliver our product.

- Cost <$350
- Weight <10 lbs.
- Length = 3 ft.

Our understanding of robotics and the design process has helped us achieve our goals and build a product that is reliable and versatile.

Acknowledgements

This project was successful with the support of many others: Professor Xi Gu, Professor Assimina Pelegri, our teaching assistant Hang Zhang, the Rutgers MAE Faculty and Staff and, our parents

RUTGERS
School of Engineering
MAE Design and Manufacturing

Hybrid Manufacturing of a Customized Knee Implant

Parker Scott, Jonathan Perino, Riley Meskill, Ryan Andrews, and Cristian Contreras
Advisor: Dr. Yuebin Guo

Problem Statement

- Each year over 600,000 Americans undergo a knee replacement surgery otherwise known as arthroplasty
  - Aimed to cure patients of a variety of debilitating knee illnesses namely osteo, rheumatoid, and psoriatic arthritis
  - This is done through replacement of the knee joint components with a new prosthetic one
- The modern knee replacement:
  - Lifespan of roughly 20 years
  - Range of motion of roughly 75 degrees
  - Can withstand three times the patient's body weight in force before failure.
- Our project aims to generate a 3D model of a customized knee implant, specifically it aims to design, manufacture, and run extensive analysis on a model that is newly generated and customizable.
- Our model improves lifespan, range of motion, and durability through the incorporation of additive strength along with an internal lattice structure.

Conceptual Design

Initial design goals were to meet the standards of modern total knee replacement systems. These include the following:

1. Full load bearing capabilities up to 2200 N (500 lbs)
2. 75 Degree Range of Motion

With these goals in mind, point cloud data from a patient's CT scan were imported to Solidworks to derive the rotational outline of both the Femoral Head and the Meniscus. These profiles as well as other dimensions of the knee were combined to form the design for the rotational contact surfaces, comprising the bulk of Prototype 1.

Once proper range of motion was achieved Prototype 2 was developed to include the Tibial Component as well as the mechanical linking geometry, designed to bind the Meniscus and Tibial component together. This involved a keyed plus shape, preventing improper installation of the Meniscus and limiting translational motion across the top of the Tibial Head under load. The second prototype was also used for initial simulations, demonstrating it exceeded the range of motion goal reaching 82 degrees, and met the load goal.

Upon completion of these prototypes, the geometry was further optimized to take advantage of additive manufacturing. This involved incorporating internal lattice geometries which would provide two benefits.

1. Overall lightening of the geometry.
2. Creating voids within the geometry which would allow the femur to regrow around the implant..

The process of refining this geometry is discussed in the "Simulations" section as well as the methodology to determine the optimum lattice design.

Materials Selection

Materials Used in Manufacturing and Properties:

Component	Material Used	Tensile Strength	Young's Modulus	Ultimate Strength	Bio-Compatibility
Femoral	Stainless Steel 316	480 MPa	190 GPa	700 MPa	No
Meniscus & Tibial	Nylon 12	50 MPa	2.7 GPa	82 MPa	Yes

- Materials were selected for accessibility & cost considerations
- Traditional surgical implants use Cobalt Chromium for the femoral and tibial components and high density polyethylene (HDPE) for the meniscus
- Limited by constraints (cost, printing capability, and machining)
- Simulations run in real world and manufactured materials for better analysis

Manufacturing

Our project is consisted of 3 components: femoral head, tibial head, and meniscus spacer. These parts were 3D printed in PLA for the prototypes and Nylon-12 and Stainless Steel 316 for the final. They then needed to be machined in order to reduce surface roughness for rotation. Due to the degrees of freedom in the parts the manufacturing included machining the smaller features such as the contact surface of the femoral head with the meniscus spacer for optimal knee flexion. The files for these programs have been run through multiple softwares to ensure that it converts well for our printing. Our final product consists of a femoral head printed in SS316, tibial and meniscus components ordered in Nylon 12 from an outside vendor. These materials were chosen in regards to cost and availability constraints as they are not all biocompatible.

Designs, Prototypes, and Final 3D Prints

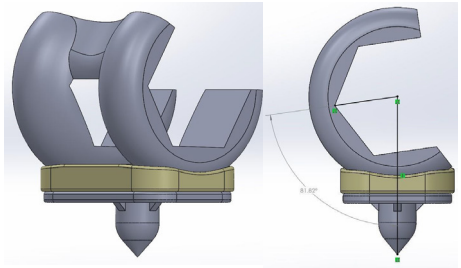

Figure 1. (a) Solid Prototype Isometric and (b) Side View

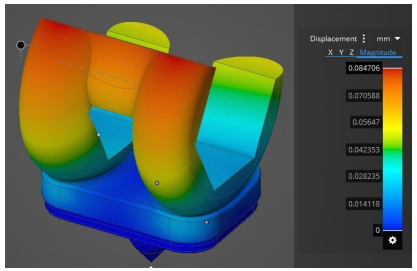

Figure 2. Deformation of Solid Prototype

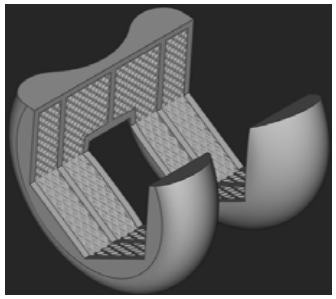

Figure 3. Latticed Femoral Component–Isometric View

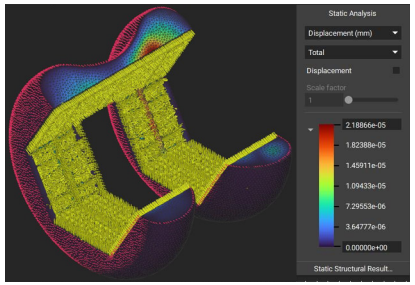

Figure 4. Deformation of Lattice Structured Femoral

These Figures are representative of the standard knee replacement. As shown through the simulation, whether it is the solid prototype or the lattice structured femoral head it proves that it follows the working functions of the knee as far as rotation, and ability to withstand intended load, the materials were selected to ensure the longevity.

Simulations

This project relied heavily on finite element analysis as there was limited potential for physical testing of these components. Preliminary analyses began with deformation studies of the solid versions of the prototype. The results of these studies are shown in Figure 2. Revised simulations were performed within nTopology to optimize the shape and size of the lattice structure. The results of these simulations are tabulated below.

Cube Edge

Orientation	Lattice Type	Edge Length	Diameter	Load	Mass	Max Deformation CE	Deformation/Gram CE
Vertical	CE	1	0.05	2200	2047.69	Error	Error
Vertical	CE	1.5	0.375	2200	2249.92	25.88	0.011524917
Vertical	CE	2	0.5	2200	2302.62	30.91	0.013360928
Vertical	CE	2.5	0.625	2200	2277.99	16.05	0.007075458
Vertical	CE	3	0.75	2200	2302.69	Error	Error
Vertical	CE	3.5	0.875	2200	2301.61	280.4	0.121.865276
Vertical	CE	4	1	2200	2313.56	129.5	0.055990173
Vertical	CE	4.5	1.125	2200	2302.42	129.3	0.056134592
Vertical	CE	5	1.25	2200	2301.86	25.83	0.01211104

Cube Edge–Vertex Centroid Face

Orientation	Lattice Type	Edge Length	Diameter	Load	Mass	Max Deformation VCF	Deformation/Gram VCF
Vertical	CE-VCF	1	0.05	2200	428.09	Error	Error
Vertical	CE-VCF	1.5	0.375	2200	423.25	6.05	0.014294405
Vertical	CE-VCF	2	0.5	2200	417.85	12.33	0.029509125
Vertical	CE-VCF	2.5	0.625	2200	375.29	6.43	0.017133234
Vertical	CE-VCF	3	0.75	2200	375.71	Error	Error
Vertical	CE-VCF	3.5	0.875	2200	374.29	7.5	0.020039363
Vertical	CE-VCF	4	1	2200	374.69	8.53	0.022726952
Vertical	CE-VCF	4.5	1.125	2200	374.79	6.13	0.016451104
Vertical	CE-VCF	5	1.25	2200	375.43	6.5	0.017319766

Cube Edge–Central Axis Edge Face

Orientation	Lattice Type	Edge Length	Diameter	Load	Mass	Max Deformation CAEF	Deformation/Gram CAEF
Vertical	CE-CAEF	1	0.05	2200	338.09	Error	Error
Vertical	CE-CAEF	1.5	0.375	2200	340.98	8.34	0.024.46987
Vertical	CE-CAEF	2	0.5	2200	337.9	8.32	0.024.61396
Vertical	CE-CAEF	2.5	0.625	2200	336.18	4.23	0.012.67054
Vertical	CE-CAEF	3	0.75	2200	336.08	Error	Error
Vertical	CE-CAEF	3.5	0.875	2200	336.53	10.43	0.0311.59713
Vertical	CE-CAEF	4	1	2200	337.03	21.01	0.062350921
Vertical	CE-CAEF	4.5	1.125	2200	338.09	5.91	0.017478962
Vertical	CE-CAEF	5	1.25	2200	338.86	9.73	0.028697206

The optimal solution is highlighted in green. It was chosen this was the minimum of both maximum deformation and deformation/gram. The overall scatterplot of all results is shown below with the minimum solution highlighted in green. Note, those data points whose solutions are "Error" in the table are excluded from the scatter plot.

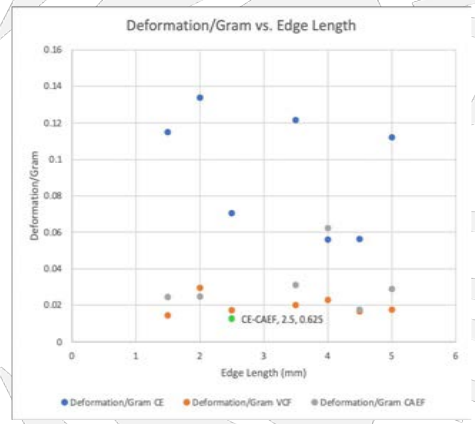

Figure 5. This graph combines the deformation/gram data for each lattice stype. This optimum geometry is highlighted in green.

G2

SOLAR POWERED PLANE FOR INDEFINITE FLIGHTS

RUTGERS School of Engineering
MAE Design and Manufacturing

Austin Lampitt, Aamir Mansuri, Oluwaloba Jacob, Waleed Faizi
Advisor: Dr. Guo

Overview

The purpose of this project is to design and build a solar powered UAV prototype that is suitable for indefinite endurance flights. This project aims to enhance flight duration by means of renewable energy. High performance flexible solar panels are utilized to maximize power generation per unit of area of wing space.

Such aircraft / drones could prove useful in military recon and film applications if high degree of robustness can be achieved.

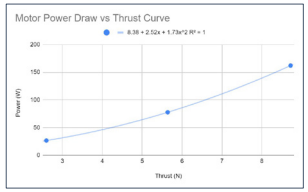

Figure 1: Motor power vs thrust produced

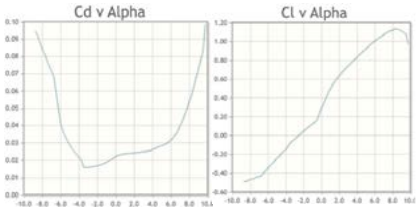

Figure 2: Coefficient of Lift and Drags for AG36

Airfoil and Propulsion Design

The most important component in this project is the airfoil. The ideal airfoil needs to have low drag and high lift at low flight speeds. Further, airfoil performance at high angle of attack is not critical in a more glider focused design as high maneuverability is not a focus. The ag36 airfoil was selected from airfoiltools.com. Referring to figure 2, one can see that the coefficient of drag in the angle of attack range (alpha) that we will be operating in is quite low. Conversely, the lift is high in the same range when compared to other profiles in its class.

The motor and airfoil selection process is tied closely to one another due to the motor and prop needing to overcome the drag produced by the wings while consuming relatively low power relative to the amount of panels that can be fit on the wing. One can increase power generation capacity, but would also increase drag and weight as a consequence of extra span. See figure 2.

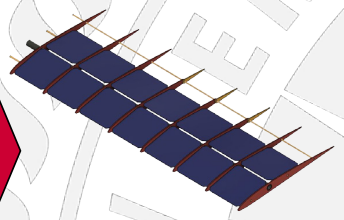

Figure 3: AG36 solar wing assembly

Electronics System

The electronics on the aircraft consists of the flexible high efficiency solar panels, the novel charging circuit, and the normal flight systems (controls servos and motor). The solar panels are in 2 sets of 14 (additional cells on fuselage). Each set is on each wing and wired in series to increase the voltage to a maximum of 8.4 volts. Each set from each wing is then wired in parallel for redundancy in the case of a failure in one of the sets. The power is monitored by an arduino microcontroller and passed into the battery charge controller. This controller has a minimum voltage threshold to function, and given certain circumstances, the solar output could drop below it. As such, the microcontroller monitors voltage output and flips a relay to a boost converter in order to re-engage the charge controller at lower output conditions.

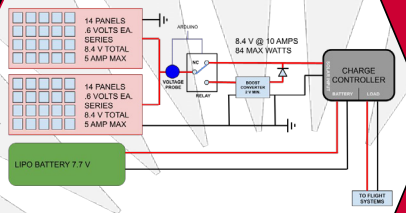

Figure 4: Solar panel charging circuit

Manufacturing

Multiple types of machine were used to manufacture solar airplane parts. The ag36 airfoil, fuselage and flight control surfaces needed to be CNC cut, thus a universal laser system PLS6.75 was used to manufacture the airfoil. 3D printed brackets were used to connect the wing and elevator sections to the fuselage. A saw cutter was used to cut carbon fiber tube to 1 m for the wing spars. Airfoils were slid over the carbon fiber tube and glued together. The carbon fiber tubes had to be electrically insulated to prevent the solar panels resting on top of them from shorting out. The solar panels were soldered together in packs of 2 between each airfoil section. Each section would produce 1.2 volts in optimal conditions.

Figure 5: CAD rendering of final assembly

Project Management

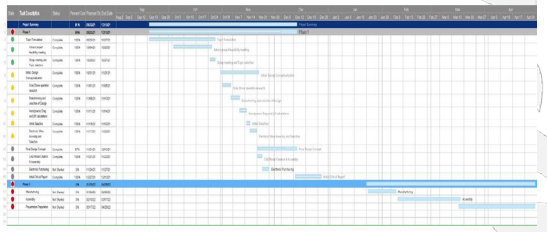

Figure 6: Development plan Gannt chart

Data Analysis

Motor power would increase exponentially as angle of attack is increased due to the drag forces. Additionally, the share on the vertical component of lift that is parallel to gravity decreases as angle of attack increases, despite an overall increase in lift generated. This contributes to the increase in power requirement.

It should be noted that this is all in ideal flight conditions. Windy days or overcast will greatly increase power consumption or decrease power generation capabilities respectively.

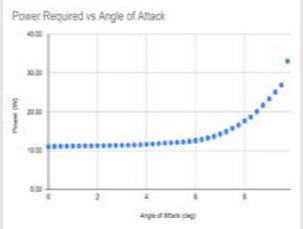

Figure 7: Power requirements vs angle of attack

Conclusion

The solar powered aircraft was able to achieve meaningful extended range in ideal flight conditions, though indefinite flight was not achieved. The reduction in performance of the solar panels from the film covering was greater than anticipated. Additionally, the panels would heat in prolonged ideal flight conditions, thus reducing solar panel effectiveness. Future work would be to use the solar panel itself as the aerodynamic skin which would eliminate light obstruction and cool the panels.

G3

RUTGERS School of Engineering

MAE Design and Manufacturing

SOLAR DESALINATION COOLER DEVICE: Desal Camper

Chelsea Cheng, Alice Krauze, Ryan Halloran, Christine Vu, Stepan Zybin
Advisor: Dr. Zhixiong Guo

OVERVIEW

- Clean water is a necessary, but scarce resource for impoverished countries
- In disaster zones or coastal safehouses, the Desal Camper would be invaluable resource
- Uses low cost and lightweight materials and utilizes a parabolic dish and concave dome to focus solar energy to a focal point
- Water is evaporated and then condensates on the dome wall before continuing into a clean water reservoir

MOTIVATION

- ¼ of the world's population does not have access to clean, drinkable water
- Less than 1% of the world's water is drinkable
- It is recommended that the average person drinks half a gallon of water per day

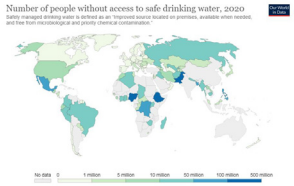

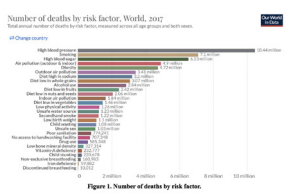

Figure 1. Number of deaths by risk factor.

ENERGY GENERATION

We were also able to identify the required amount of heat and funnel placement via these equations:

U2-U1 +1/2mv^2+ mgh = E = Q - W

Which yielded the 37.65 J that needed to heat the water.

Focal length = r^2/4d

The thermodynamic equations that drove our design are:

Q = mCΔT (Heat required for evaporation and condensation); Constants: 4.18 J/g °C

Focal Point of the parabolic disk 4.9 inches, focal point of the clear dome is 1.25 inches

DESAL CAMPER

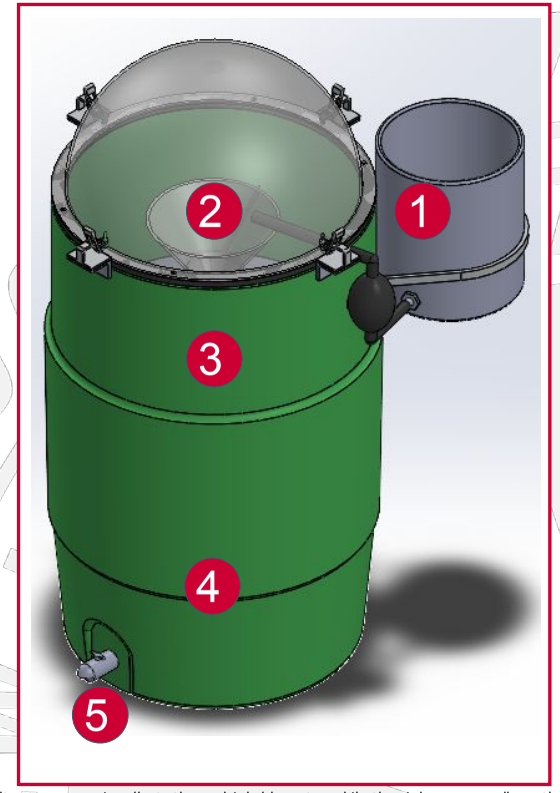

1. The saltwater reservoir collects the undrinkable water while the siphon pump allows the user to pump the saltwater into the heating chamber
2. The heating chamber will need to heat up to 100 °C in order for evaporation to occur. The parabolic reflector should collect a value of 37.65 J, while the dome needs to collect a heat of 30.3 J. The glass being filled with the saltwater has a rate of heat transfer of 23.4 J.
3. The condensation chamber will allow the evaporated water to rise to the top of the dome and slide down the dome walls into the clean water reservoir chamber. In order for this to be. A temperature drop of below 100 deg C exists for condensation to occur..
4. The clean water reservoir will collect all the clean drinkable water ready for use.
5. The valve will dispense clean drinkable water for the user to access anytime anywhere.

RESULTS

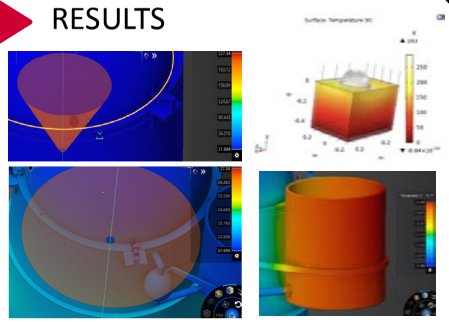

Fig 2. ANSYS and COMSOL heat generation simulations

PROJECT MANAGEMENT

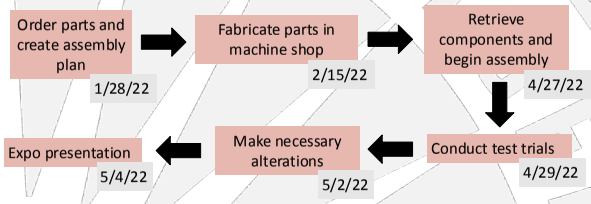

CONCLUSION

- The parabolic dome creates a focal point for the irradiation solar energy incident upon it
- The parabolic reflector is then coupled together to capture the radiation transmitted through and reflects this energy back to the focal point
- Lightweight, cheap materials, and lack of an electrical heat source provides rugged design without the need for repairs or replacement parts
- Intended for a single person to operate
- All materials used are FDA Article-21 GRAS (generally recognized as safe) for human consumption

G4

Hybrid Wind & Solar Energy Generation System

RUTGERS School of Engineering
MAE Design and Manufacturing

Saifeldeen Khalil, Gabriel DeMarco, Panayiotis Kousoulas, Evan Williams, Srinath Menon, Wai-Jian Chia
Advisor: Yogesh Jaluria

Project Background

- **Renewable power generation** is a rapidly growing field of innovation, and one that is necessary for transitioning our power demands to sources not reliant on limited resources.
- **Wind power and solar power** are typically considered separate means of energy generation, totally standalone in functionality.
- **Solar panels lose efficiency** as they heat up.
- Methods of cooling solar panels and other devices have been developed, but among the most efficient is that of **water-cooling**, a perfect medium of cooperation for a wind turbine's mechanical nature.

Objectives

- **Design and Fabrication of System**
  Manufacture and test prototype system with budget of $650 (USD) for design validation
- **Hybrid Electrical Generation/Storage**
  Simultaneous use of wind and solar energy for charging batteries in a ½ hour test period
- **Improved Panel Efficiency**
  Custom-built heat exchanger for reducing PV panel operating temperatures
- **Heat Capture**
  Gather heat energy from PV panel through water cooling and store in a reservoir for use

Design Features

- **Arduino-based Control System**
  Automation of system functionality, applied monitoring conditions, data collection capability
- **Manual Emergency Brake**
  Encoded warning system to signal operator intervention in high wind speeds
- **Direct Mechanical Power Transfer**
  Mechanically powered pump by turbine through gear transmission system
- **Energy Preservation** with pump disengagement based on temperature readings for the system, taking load off of the wind turbine when not needed.
- **Functional frame** constructed out of pine timber with metal caster wheels for added mobility
- **Maximum efficiency** using a copper heat exchanger brazed to aluminum heat transfer plates attached to back of PV panel.

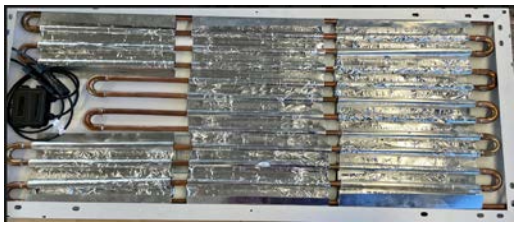

Fig. 1: Copper heat exchanger inside PV panel

System Components

1. **Wind Turbine**
   Three 18 inch blades, 3-phase generator with AC-DC power converter, fixed nose direction
2. **Transmission**
   3D printed (PLA) gears, 1:3 speed ratio, ¼ inch steel shaft, automatic gear engaging/disengaging
3. **Centrifugal Pump**
   3D printed (PLA) pump, 1 inch inlet, ½ inch outlet, submerged, 20 inch head pressure at 400 RPM
4. **Water Reservoir**
   Insulated PVC 5 gallon bucket fitted with a pump stabilization system
5. **Photovoltaic (PV) Panel**
   20 inch x 42 inch, 100 W, 10 A charge controller
6. **Heat Exchanger**
   37 feet copper tubing, aluminum heat transfer plates (not shown), fully insulated, water as coolant
7. **Frame**
   Heavy-duty repurposed pine timber construction, mobile wheelbase (not shown)

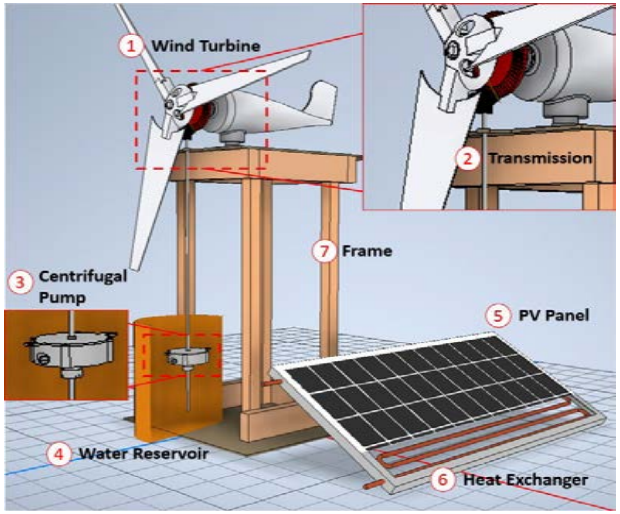

Fig. 2: Prototype system model.

Timeline

System Test Methods

- **Outdoor Testing**
  - Sunlight: 1/2 hour test periods, monitored conditions (panel temperature, electrical output)
    - **Case 1: no water cooling**
    - **Case 2: with water cooling**
  - Wind: 1 hour test periods, monitored conditions (RPM, wind speed, electrical output)
    - **Case 1: no pumping**
    - **Case 2: with pumping**
- **Indoor Testing**
  - Sunlight: simulated with heat lamp
  - Wind: simulated with fan, 10 m/s free-stream velocity

System Performance Statistics

- **PV panel Average Power with water** - 22W
- **PV panel with Exchanger no water Average power** - 21W
- **Turbine** - Peak voltage of 13V average RPM of 322 with a max of 470.

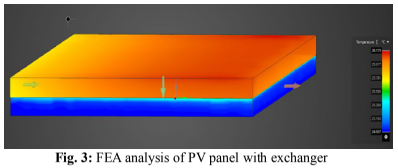

Fig. 3: FEA analysis of PV panel with exchanger

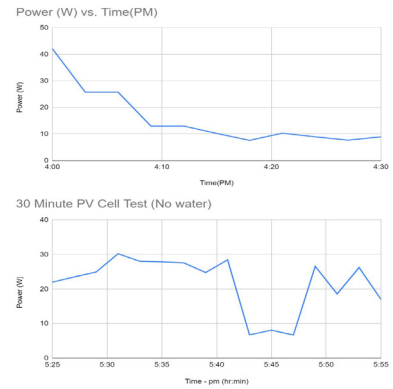

Fig. 4: (Top) water through exchanger. (Bottom) no water through exchanger.

RUTGERS

J1

RUTGERS
School of Engineering
MAE Design and Manufacturing

Wind and Solar Powered Filtration and Heating System

Nicole Zelaya, Ahmad Nadeem, Christopher Gorka, John Wiech, Mariam Refai
Dr. Yogesh Jaluria

Background

In the past decade, there has been a push to replace traditional gas powered water heaters with electric heaters. However with much of the world still dependent on fossil fuels for their electric needs, a carbon neutral solution still eludes us.

With the limitations of the electric grid, it is important to keep any system independent from it. The advantage of said system makes it highly modular and portable, along with being intuitive and easy to use.

Proposed Solution

Our solution involves using a wind turbine to power a centrifugal pump to take water from a lake and pass it through a filtration system. The filters main purpose is to remove dirt and other contaminants from the water. From the filtration system, the water will dump into a thermally insulated reservoir, where the water will circulate from there to a thermal collector to heat it up to 80°C to store as energy and kill any bacteria in the water. Once done, the water will stay heated in the filtration system for 8 hours.

We designed the system to be highly modular. That way if anything breaks, it is easily replaceable. The system is to operate on very little human input.

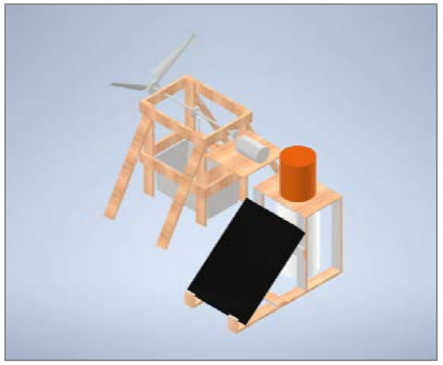

Figure 1: Completed Design

Wind Subsystem

- Function: Mechanically pump water into the filtration system and generate electricity for control system
- Wind Turbine Blades
  - Builder's foam cut with CNC machine
  - Fitted with Shaft Collar and Attached to Driving Shaft
  - Blades drive generator and pump
- Pump
  - Simple Hand drill Pump
  - Attached to 40:1 Worm Gear Box w/ pulleys for enough torque
  - Fitted with 5/16'' ID plastic Tubing
  - Pumps water up by 3 feet to reach filtration bucket
- Generator
  - Driven by a 3D printed 2:1 gear attached at the end of the driving shaft
  - 1.5 A Magnetic Generator
  - Generates 12V and stored in battery

Figure 2: Initial Wind Turbine Design

Figure 3: Assembled Wind Subsystem

Solar Subsystem

- Function: Takes filtered water and circulates the water to heat the water and retain heat for a minimum of eight hours
- Thermally Insulated Reservoir
  - 15-Gallon Food Safe Container
  - Filtered water enters from the top along with a temperature sensor
  - Connected to inlet and outlet copper pipes attached to thermal reservoir
  - Insulated with Fiberglass to reduce heat loss
- Pump
  - Electric Pump
  - Circulates water through the thermal reservoir
  - Powered by the battery
  - Controlled by an Arduino so that it turns off when water reaches 80°C
- Thermal Collector
  - 2 ft x 3 ft Aluminum Framing
  - Copper piping painted black to absorb the most heat
  - Glass Panel to trap in heat

Figure 4: Initial Thermal Collector Design

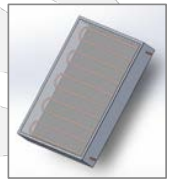

Figure 5: Assembled Solar Subsystem

Control System

- The wind turbine powers the battery
- The battery powers the pump
- Arduino collects succinct data from wind and solar system
  - Voltage from generator
  - Temperature Reading from circulating water in solar collector
  - The control system will turn off the electric pump when the water reaches 80°C
- A kill switch is integrated with the pump

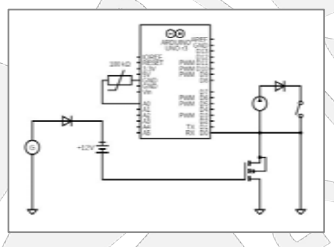

Figure 6: Circuit Diagram

Miscellaneous Design Components

- Ceramic Filter
  - 4 symmetrically placed dome-shaped ceramic filters inside a 5-Gallon Bucket
  - Removes contaminants in water and empties into insulated reservoir
- Wood Frame
  - SPF wood support system cut on band saw
  - Intuitive Box Framing
- Valves
  - Ball Valves: Used to isolate water into insulated reservoir after heating
  - Exit Valve: Valve to empty reservoir for usage

Figure 7: Wood Frames

Figure 8: Filtration System

Acknowledgements

We would like to show appreciation across the MAE department. We would like to thank our advisor, Dr. Yogesh Jaluria for his support and guidance throughout the project. We would also like to thank Hang Zhang for his constant updates. We appreciate the machining support and advice from Dr. Basily and Milan Simonovic. They kindly explained machining practices and engineer standards. We'd like to shout out our fellow team under Jaluria's advising, J1. For helping construct the electrical system, we would like to thank Dave Stewart and Anthony Remo from OPT, and Kevin Wine from the Rutgers ECE department. Special thanks to Dr. Bertuccio and Maricely Ramirez Hernandez for 3D printer access.

J2

RUTGERS School of Engineering

MAE Design and Manufacturing

TABLETOP SUBSONIC WIND TUNNEL

Asjad Shaikh, Owen Kunzle, Daniel Pursell, Leonard Rowley, Cody Conroy
Dr. Doyle Knight, Dr. Assimina Pelegri, Dr. Xi Gu, Hang Zhang

Executive Summary

The project aims to create an affordable solution to the accessibility and cost constraints that large-scale wind tunnels pose. By creating a collapsible model that can be disassembled, the standard functions of a wind tunnel can be performed anywhere at a fraction of the cost.

Timeline

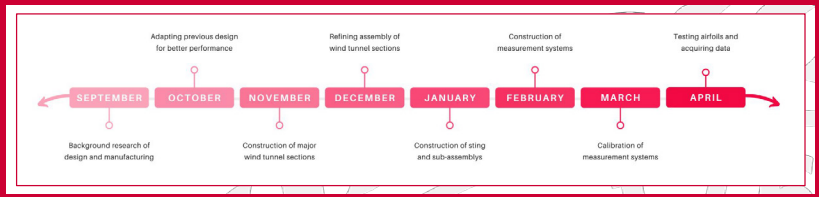

Equations

$$L = F_N \cos(\alpha) - F_A \sin(\alpha) \quad [1]$$

$$D = F_A \cos(\alpha) + F_N \sin(\alpha) \quad [2]$$

$$\varepsilon = \frac{M}{ZE} = \frac{32WL}{\pi d^3 E} \quad [3]$$

Conceptual Design

The design of the wind tunnel was planned in order to recreate the capabilities of a full-sized wind tunnel but on a tabletop scale, through the use of modular components. The major sub-assemblies for the wind tunnel are the intake, test section, diffuser, and fan mount.

Intake
- Accelerates incoming airflow
- Reduces in cross-sectional area

Test Section
- Houses sting and airfoil models
- Removable lid for ease of access
- Acrylic box for visual clarity

Diffuser
- Decelerates outgoing airflow
- Increases in cross-sectional area
- Attaches to fan mount for stability

Fan Mount / Legs
- Houses computer-controlled motor
- Pulls air through the wind tunnel
- Increase tunnel stability and support

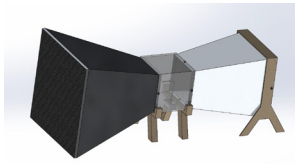

Fig 1. Model Design of Wind Tunnel

Project Status

During the 2021 fall semester, a working prototype (Fig. 2) of the wind tunnel was completed with all sub-assemblies and a functional LabVIEW interface. The original model drafted by the previous year's team was updated (Fig. 1) in order to ease manufacturing complexities and to provide a more aesthetic and functional design. The spring semester was spent refining unforeseen issues such as vibration and motor speed control, as well as calibrating the electrical and measurement systems.

Fig 2. Final Wind Tunnel Assembly

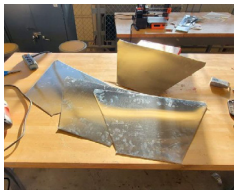

Fig 3. Intake Manufacturing

Fig 4. Laser-Cutting Fan Mount

The intake and diffuser (Fig. 3) were manufactured using automatic metal shears, a metal brake, J-B Weld epoxy, and rivets. The fan mount (Fig. 4) along with the leg supports were manufactured out of laser-cut plywood. The test section was made from laser-cut acrylic and epoxy with a cross-sectional area of 10"x10".

The sting in the test section was manufactured from nylon rod which is flexible enough to give readable strain measurements for the purpose of force measurement. The nylon is also stiff enough to not deform to the point of changing the angle of attack of the test specimen. The sting is attached to a gearbox and stepper motor to allow the user to change the angle of attack from -12° degrees to positive +12°.

The test specimen for data collection was a NACA-0012 airfoil. LabVIEW calculates in real-time the lift and drag (in newtons) from the input angle of attack and force measurements from the strain gauge mounted on the sting (Fig. 5-6).

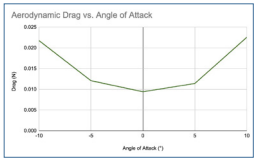

Fig 5. Drag Versus Angle of Attack

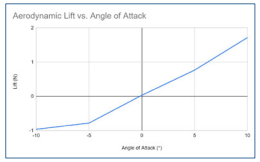

Fig 6. Lift Versus Angle of Attack

Measurement

The wind tunnel measures the airflow velocity as well as lift and drag forces on mounted objects.

A hot-wire anemometer measured voltage changes observed by cooling wires in an airflow. These readings, in combination with the dynamic pressure measured by a pitot-static tube, were converted to velocity via Bernoulli's equation.

Calculation of lift and drag was performed via a strain gauge attached to the horizontal portion of the sting. Deadweight tests were conducted to convert the output voltage of the strain gauge into a known normal force, and then into strain (Equation 3). A calibration curve was developed to determine strain values directly from output voltage.

Axial force was calculated by converting stress into strain and multiplying by the cross-sectional area. The lift and drag were found using the axial and normal forces (Equations 1 & 2).

Acknowledgements

To Professor Doyle Knight, for his guidance and assistance throughout the project

To Dr. Milan Simonovic, for his expertise and advice in regards to manufacturing

To Group AE_K1 (2020-2021), for their initial research and design of the system

AE K1

Tabletop Subsonic Wind Tunnel

RUTGERS School of Engineering
MAE Design and Manufacturing

Christian Martin, Catherine Biava, Kevin Lin, Vraj Mantora, Justin Liu, Ronan Laaouina,
Professor Doyle D. Knight

Mechanical and Aerospace Engineering, Rutgers, The State University of New Jersey

Introduction

A wind tunnel is a structure that has a controlled flow of air. Tunnels that measure flow with a Mach number between 1.2 and 5 are referred to as supersonic, and subsonic if the Mach number is less than 0.8. They can be used to model an aircraft flying through air. Wind tunnels can be an excellent resource to study aerodynamics forces; however several factors prevent it from being accessible to students. The tabletop subsonic wind tunnel will allow students to study aerodynamics with an easy to use interface at an affordable price.

Background

The creation of the wind tunnel is thought to have been towards the end of the 19th century. It wasn't until the Wright brothers began their testing that the wind tunnel would be put to good use. In their efforts to create a flying machine they had quickly found that they needed a method of examining the aerodynamic forces that would be in play. The Wright brothers created one of the first wind tunnels, which can be seen in figure 1, in 1901 to study forces from wind at different angle of attacks.

Fig 1. Wind Tunnel Created by the Wright Brothers

The team was tasked with taking a wind tunnel design from the previous year and fabricating it. The team was given a final report and computer aided design drawings and needed to make adjustments to make the project feasible.

Objectives

The requirements and objectives of the tabletop subsonic include being:

- Affordable
- Easily disassembled and stored to fit inside a 2x2x2 foot locker
- Capable of measuring wind speeds up to 15 meters per second
- Easy to use LabVIEW interface equipped with air speed measurements, fan speed controller, and lift and drag measurements
- A servo motor to change the angle of attack of the sting

Project Status

As of the Spring 2022 semester, the physical construction of the wind tunnel has been completed, shown in figures 2 and 9. Changes were made from the original design to allow for a feasible construction plan. The three subassemblies were machined from aluminum sheet metal and acrylic. Figure 3 shows the diffuser sub-assembly and figure 4 shows the intake sub-assembly. The tools used to create the sub-assemblies include electric shears for cutting, and JBWeld adhesive and rivets for connecting the pieces of aluminum.

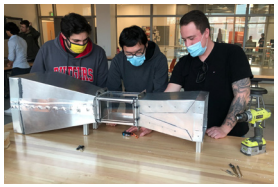

Fig 2. Physical Wind Tunnel Assembled

Fig 3 . Diffuser Sub-assembly

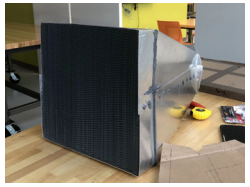

Fig 4. Intake Sub-assembly

After construction of the wind tunnel sub-assemblies, the measurement system assembly began. Wiring diagrams were made to plan how the electronic systems would connect. Figures 5 and 6 depict the wiring diagrams for the air speed sensor and motor respectively and figure 7 shows the setup for the lift and drag measurement systems. These wiring diagrams were used to set up the measurement system which then needed to be connected to the LabVIEW interface. The LabView interface allows for control of the fan speed, angle of attack controlled by the servo motor, and data collection of lift and drag measurements. After implementing each electronic system into LabView, the air speed sensor and strain gauges needed to be calibrated. Calibration of the air speed sensor was done using a manometer connected to a pitot tube, and the strain gauges were calibrated by applying a known force to them.

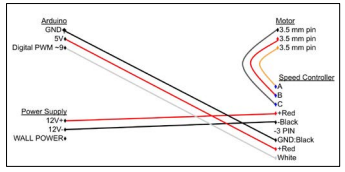

Fig 6 . Motor Wiring Diagram

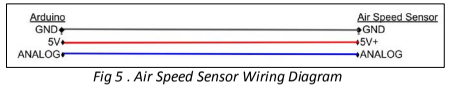

Fig 5 . Air Speed Sensor Wiring Diagram

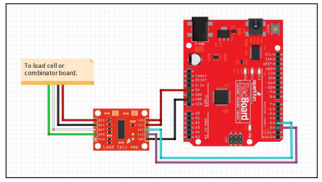

Fig 7. Strain Gauge Wiring Diagram. Note that an Arduino Uno will be used in place of RedBoard

Design

The wind tunnel is divided into 3 sub-assemblies: intake, test section, and diffuser. The structure is made of 20 gauge aluminum for rigidity. The initial CAD assembly is shown in figure 8.

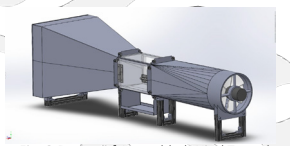

Fig. 8 Design of Assembled Wind Tunnel

Equations and Measurement

Lift and drag force can be calculated with the equation: $F=(½)\ \rho v^2 CA$, with C being the coefficient of lift or drag. From this it was calculated that the lowest force that would need to be measured was 0.00889N and the highest force was 2.13N. Using these values a strain of 2.927×10^{-6} to 5.009×10^{-4} can be expected. The measurement system consists of two cantilever beams, with mounted strain gauges to measure lift and drag forces. The strain of a cantilever beam can be defined as: $\varepsilon=M/ZE$, where M is bending moment, Z is section modulus, and E is Young's Modulus. The voltage reading that the strain gauges can be used to find strain by using the equation: $\varepsilon = 4E_0/E*k$. This value can then be used with the equation above to find the forces of lift and drag.

Acknowledgements

This project is a continuation of the work done by the previous group ME_K2. The designs and research that they had completed was invaluable to the completion of the wind tunnel. Our team would also like to thank Professor Knight, Milan Simonovic, and the MAE Department for their support throughout this project.

Fig. 9 Full Wind Tunnel Assembly

K1

PHYSICAL INFORMATION PROCESSOR [PIP]

RUTGERS School of Engineering
MAE Design and Manufacturing

Gleb Orlov, Seth A. Seely, Joseph Erreich, Evan Krause, Dr. Hao Lin

Inspiration

Industry sorters are often large and bulky. Developing a PIP system defies the usual drawbacks while also tackling multiple object characteristics to decrease the already large costs of such systems.

Description

As a prototype, the PIP aims to sort objects by color. It does so via two subsystems: the Vibratory Bowl Feeder (VBF) and the Sorter. The VBF was chosen for its ability to sort objects by shape and size with only minor adjustments. The Sorter design was chosen due to gravitational potential energy being its main driver.

Optimization

- Approximated natural frequency to be 22Hz from Okabe and Yokoyama (1981):

$$f_{n1} = \frac{1}{2\pi}\sqrt{\frac{nEbh^3\left\{1+\frac{1}{12}\left(\frac{b}{h}\right)^2\left(\frac{l}{r}\right)^2 \sin\sin(2\gamma)\left(3\kappa^2-3\kappa+1\right)\right\}}{l^3\left(M\cos^2(\gamma)+\frac{J\sin^2(\gamma)}{r^2}\right)}}$$

- Performed iterative testing to acquire RGB values depicted in Table 1

VBF Design

The VBF linearizes a randomly assorted mass of objects by:

- Reaching resonance of 45° leaf springs
- Powering a 4500 RPM rumble motor
- Inducing vibrations to oscillate the bowl
- VIbrating objects up a 30mm pitch helical ramp

Engineering Process

1. Researching:
   - Reviewing current industrial sorters
   - Sept 16th - Sept 20th
2. Concepts:
   - Develop Feeder and Sorter system ideas
   - Sept 20th - Sept 30th
3. Design/Optimization:
   - Decide on design and begin drafting
   - Further research into chosen systems
   - Oct 1st - Dec 4th
4. Manufacturing
   - Gather and create required material and parts
   - Nov 1st - March 10th
5. Prototyping
   - Make subsystems as proof of concept
   - Feb 15th - March 20th
6. Testing
   - Make subsystems function together
   - March 15th - April 30th

Data and Pictures

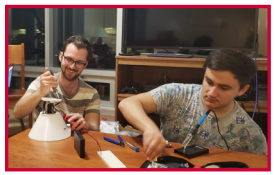

Figure 1: Initial VBF Tests

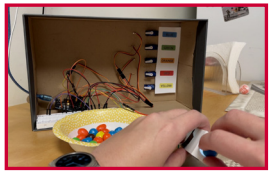

Figure 2: Initial Sorter Tests

Figure 3: Prototype Printing

		R	G	B
Blue	MAX	188	249	253
	AVERAGE	137.36	227.52	239.64
	MIN	50	177	213
Green	MAX	140	252	241
	AVERAGE	113.56	245.8	224.26
	MIN	89	243	204
Orange	MAX	253	198	155
	AVERAGE	244.68	151.76	113.88
	MIN	236	125	88
Red	MAX	250	247	207
	AVERAGE	248.4	188.96	159.76
	MIN	241	147	130
Yellow	MAX	250	252	192
	AVERAGE	238.68	242.08	181.96
	MIN	227	230	167

Table 1: Sorter RGB Data

Figure 4: VBF - CAD->Render->Prototype

Figure 5: Sorter - CAD->Render->Prototype

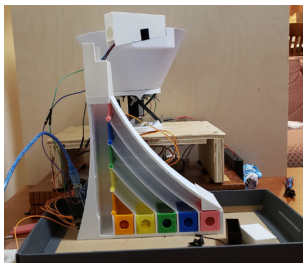

Figure 6-8: Full System Assembly

Sorter Design

The sorter is designed to receive the linearized objects from the VBF by:

- Detecting objects using a color sensor
- Utilizing a tunnel to remove ambient light
- Processing sensed color through an Arduino
- Actuating a servo motor opening a gate corresponding to the color

Total System Flow

The total system is modular but interconnected through its process:

Figure 9: Blendr Rendering of Entire System

- Test Method B–Resonance Search Using Random Vibration was utilized from ASTM D3580-95(2015)
- Resonance was achieved by coupling VBF with the damping properties of the wooden base compartment
- Sorting was tested independently of the VBF before total system assembly
- Modularity allows for combining with any compatible feeding mechanism

L1

RUTGERS
School of Engineering
MAE Design and Manufacturing

Tabletop Color Based Sorter
ME_L2

Niyati Patel, Daniel Conforti, Joseph Breslin, Soham Shah, Siddarth Kanoongo
Advisor: Professor Hao Lin

Introduction

The purpose of this project is to design and build a color-based sorter that uses a color sensor to identify objects by their color and sort them into their appropriate receptacles. Our project tackles the issue of accurately sorting several multi-colored objects at a greater rate. We want to build a system that can streamline manufacturing processes and increase the efficiency of sorting processes.

Our design consists of 3 main subsystems: a feeder subsystem, a dispensing and detection subsystem, and a sorter subsystem.

- The feeder system consists of a funnel with an agitator that feeds the objects into a vertical slotted wheel
- This vertical wheel is part of the dispensing subsystem that drops the objects onto a ramp.
- The ramp guides are controlled by servos that direct the objects into the appropriate receptacles, and this makes up the sorting subsystem.

Circuitry

- We are using an Arduino Mega 2560 Rev3 to control the electronics for our project.
- The color sensor, TCS3200, is directly connected to the Arduino and powered by the 5 V output from the microcontroller. The sorter consists of 4 micro servos that will guide the sorted objects to their appropriate receptacles.
- Two additional servos, Bilda Dual Mode Servo and Parallax Feedback 360, utilized in our design to control the vertical wheel and the agitator.

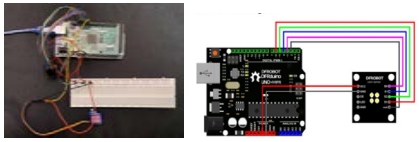

Figure 1: Wiring of Color Sensor and 1 Micro Servo

Coding

The code we wrote is written so that the standard and continuous servo rotate constantly without any stop. At the same time, the color sensor detects what color has passed through it and the according servo rotates to guide the object into the receptacle. Each servo is associated with a separate color, so when the detection occurs, only one servo moves to sort the correct color.

	RED	BLUE	GREEN	YELLOW
R Value	50-80	40-75	40-55	15-35
G Value	25-50	95-125	20-40	15-35
B Value	13-35	70-100	30-55	30-70

Figure 2: RGB ranges for all 4 colors

Timeline

Subsystem Breakdown and CAD Models

- Throughout the course of this project, a fully detailed CAD assembly has been maintained with the current status of the design concept.
- In the conceptual phase, this assembly consisted of the key components for each subsystem which were mated in the correct positions to display overall functionality.
- As the project progressed into the manufacturing stage, the assembly evolved to include imported models of any purchased parts such as the servo motors, shaft, coupler, and mounting hardware.
- The feeder subsystem consists of a funnel and an agitator mechanism. We 3D Printed the funnel and the agitator's head.
  - A large tolerance was added to the agitator's head which accounted for any print error and ensured a proper fit with the motor axis rod.
- The Dispensing subsystem consists of a vertical slotted wheel which is rotated by a continuous servo.
  - The speed is controlled via Arduino and is set to a certain speed in our code. The slotted wheel was also 3D printed because it was made specifically for the project, and printing it allowed us to make modifications to it.
  - The component that the wheel's servo rests on is also 3D printed and allows the servo to remain stationary and in place.
- The Sorting system consists of a ramp with a color detection chamber and slots for actuators to push a marble into its respective bin.
  - The ramp was sectioned in 2 parts due to its size and printed separately and then joined together.

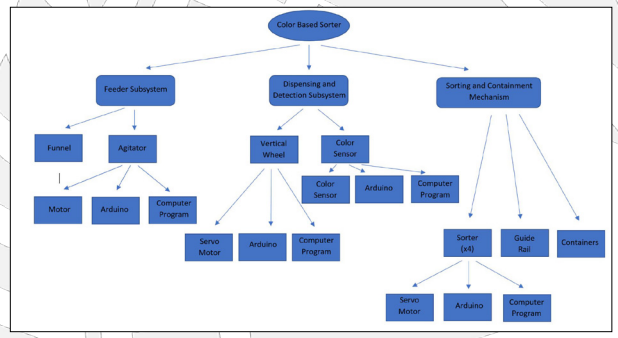

Figure 3: Flow Chart

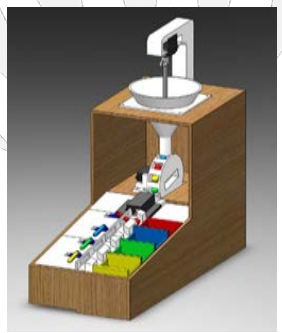

Figure 4: Full Assembly

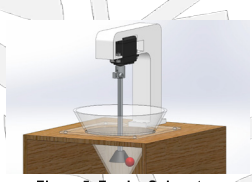

Figure 5: Feeder Subsystem

Figure 6: Dispensing and Detection Subsystem

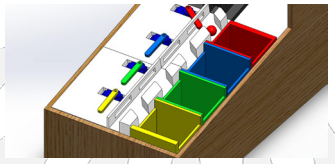

Figure 7: Sorting Subsystem

Manufacturing Process

Our group used additive manufacturing (AM) technology such as 3D Printing to manufacture a significant portion of our system.

- Benefits associated with 3D Printing utilization
  - 3D Printing excels at generating parts with complex geometry, which traditional manufacturing techniques such as woodworking struggle with.
  - A significant amount of time was saved by using simple tools such as Fusion, SolidWorks, and Cura to create, mesh, and print our designs.
  - The quick turnaround time and low-cost nature of 3D Printing with PLA enabled rapid prototyping, which allowed us to quickly correct design errors and test new ideas.
- Common issues encountered using 3D Printing and our applied solutions
  - Our group routinely tested the Ender 3 Pro for dimensional accuracy and updated CAD models accordingly with a print error tolerance.
  - Performed routine maintenance on the printer, such as tightening belts along the x and y-axis to increase dimensional accuracy by reducing the "jerk" experience by the print nozzle when changing directions.
  - Tested multiple support structure infill percentages and patterns to find the combination that produced the easiest to remove support structures. This reduced post-print damage to components.
- Print material selection
  - Polylactic Acid (PLA) was selected as the ideal print material due to its low cost, durability, and compatibility with the printer.
  - Our group performed stress analysis on several system components in COMSOL to ensure that no element manufactured using PLA would experience loads that exceed the component's load-bearing capacity.
- Conventional woodworking was used to manufacture the enclosure for the entire system

Conclusions

We found that compared to industrial and other color sorters, ours is a very simple model yet still succeeds in meeting the design requirements set forth by the client. The design incorporated 3 subsystems into a single system. The system was constructed to limit the possible points of failure and the energy consumption while meeting the customer's sorting accuracy and speed requirements. Our feeder design supports batch feeding and consists of an agitator to prevent jamming. The sorting speed is dictated by the rate at which the dispensing wheel drops the objects onto the ramp. Extensive experimental testing was performed on the system to calibrate the color sensor, agitator mounting position, wheel placement with regards to the ramp, and the sorting performed by the micro servos. The system is up to compliance with industry standards in the sensor, additive manufacturing, woodworking, quality management and tolerancing disciplines.

3D Printer for Thermoplastic Materials and Compatible Materials

RUTGERS School of Engineering
MAE Design and Manufacturing

Badder Hussein, Dhairy Patel, Yash Patel, Ishan Shah
Advisor: Dr. Rajiv Malhotra

Abstract

Thermosetting plastic materials are everywhere, from cookware to tiffin boxes and aircraft noses to machinery components. The problem is, conventional injection mold techniques are unsustainable, they consume too much energy and there is a lot of material waste. The research for this senior design project focuses on trying to solve this problem using materials that can frontally polymerize, causing chain reaction so that it requires less heat energy to harden. These kind of materials are good to be used as ink for 3D printing.
The project was divided into two main aspects: Material Research and Manufacturing of the 3D printer.

Scope

The primary goal of the project is to create a functioning 3D printer that includes 3 systems below working in in tandem .
System 1: Extruder setup
Houses Mixing Chamber and Extrusion Point
System 2: Arduino Synced Syringe Pumps
Controls Output and Ratio of Materials
System 3: Rail Gantry System to put up the Nozzles.
Controls Positioning of Extruder

Mechanical Design

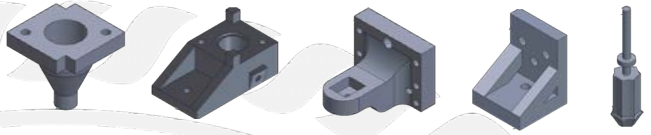

Fig 1. Extruder Nozzle 3D CAD Models Created in SOLIDWORKS

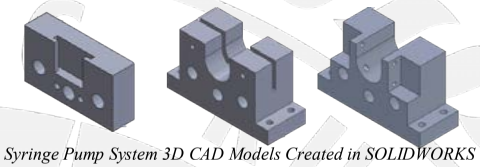

Fig 2. Syringe Pump System 3D CAD Models Created in SOLIDWORKS

Analysis

For the analysis of this project, COMSOL and ANSYS softwares were used. The mechanical design was analyzed as well as the testing phase. The mechanical components such as the mixing paddle and the extruder were used to perform the analysis. The extruder had a viscosity fluid analysis done on it, whereas the mixing paddle had a stress/strain analysis performed. The images below showcase the results. These analyses helped the team understand the boundary conditions of our project and take certain parameters into account before the manufacturing phase.

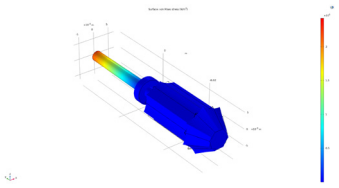

Plot 1. Stress Analysis of the Mixing Paddle

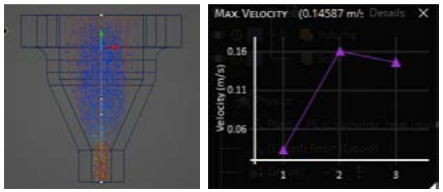

Plot 2. Fluid Flow Analysis - Extruder

Inside the Lab

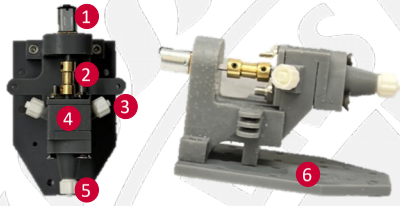

Fig 3. Extruder Nozzle Assembly (Front and Right View)

Legend for *Fig 3*:
1. Gear Motor
2. Connector between motor and mixing paddle
3. Resin Inlet
4. Mixing Chamber
5. Extrusion Tip
6. Base Support for fixing to Gantry system

Fig 4. Syringe Pump Assembly

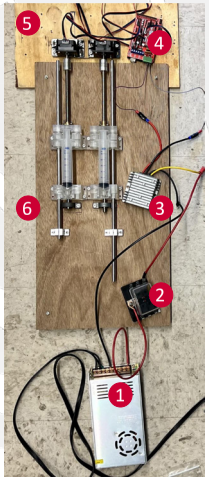

Legend for *Fig 4*:
1. Power Supply
2. Fuse
3. Stabilizer
4. Arduino Board
5. Stepper Motors
6. Syringe pump design using screw rod system

During the manufacturing phase of the project the team used multiple sources to bring the design to life. For the extruder design as seen above, Makerspace Labs at Rutgers University were used to 3D print the parts. Amazon was also used to order parts for assembly of the systems. The systems include the following:

- Syringe Pump - arduinos, motors, power supply, pusher, base plate
- Extruder - extruder housing, base plates, motor,

These systems were assembled by the team using the tools and space provided in Dr. Malhotra's lab

Conclusion

Creating a 3D printing extruders that have the capability to successfully print thermoset and thermoplastic materials benefiting the industry in many ways. For instance, creating these materials takes a lot of energy due to the nature of the large autoclave systems in the aerospace industry. This project tackles the issues of high energy high-cost manufacturing and offers a more sustainable solution while being environmentally friendly. During the testing phase of the project, the team was able to successfully print the materials in different shapes and sizes. This project helps Dr. Malhotra's research to move forward

Acknowledgements/References

1. Fast, low-energy additive manufacturing of isotropic parts via reactive extrusion, Oliver Uitz, Pratik Koirala, Mehran Tehrani, Carolyn Conner Seepersad, Received 10 September 2020, Revised 27 January 2021, Accepted 15 February 2021, Available online 1 March 2021. https://doi.org/10.1016/j.addma.2021.101919
2. https://www.osborneindustries.com/news/how-thermoset-plastics-are-manufactured/

Appendix & Further Information

For further information and Appendix please scan the following QR Code:

M1

Propulsion Unit for Surfboards

RUTGERS School of Engineering
MAE Design and Manufacturing

Max Kuhlman, Samieh Abdul-Raziq, Thomas Bruckman, Jiapeng Ding, Gennaro Gencarelli, Allen Lim
Prof. Aaron Mazzeo
Mechanical and Aerospace Engineering, Rutgers, The State University of New Jersey

Intro / Background

Surfing is one of the most time consuming and physically demanding sports. With significant paddling required to catch a wave, many new or disabled people may not have the ability to learn the sport. However, we believe surfing is an experience everyone should be able to participate in regardless of physical limitations.

To solve this problem we have designed a surfboard implemented with a water jet thruster. The thruster is located at the tail of the board and uses an impeller, which is safely enclosed from the user. The thruster will allow the board to reach up to 2 m/s for a given interval. Overall, this will greatly alleviate the strain that the paddling process requires when catching a wave. With this design we hope to make surfing a more accessible sport for all.

Conceptual Design

Our design is comprised of three subsystems: Electronics, Propulsion, and Board.

Electronics:

- 6s 6000mAH Li-Po battery, 150A electronic speed controller, Arduino
- Momentary push button controls the motor speed and thruster output.

Propulsion:

- 2000Kv - 1800 Watt Brushless Motor coupled with a Water Jet Impeller.
- Will Provide at least 1170 Watts of power to the thruster. This will achieve 175N of thrust at 30% efficiency.

Board / Waterproofing:

- 8 ft foam Wavestorm surfboard.
- Housing components: (Figure 3)
  - ½ inch acrylic sheets bound with high strength acrylic cement and bolted to board.
  - Housing is sealed with epoxy and water tight lid.

Manufacturing

Figure 1: Power Module and Thruster Assembly

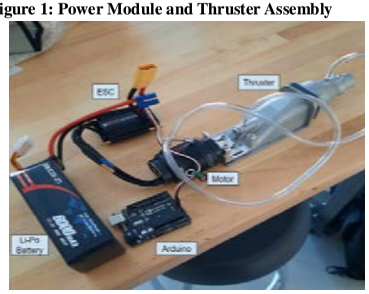

Power delivery is regulated from a button connected to a microcontroller (Arduino), this allows the user to have full control of the system.

Figure 2: Waterproof Housing with Components Enclosed Inside

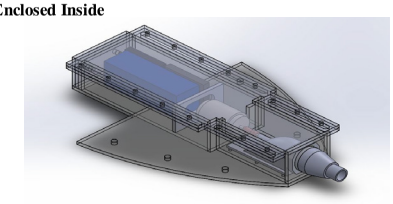

The acrylic box is secured to the board using bolts that connect the base of the box to the surrounding foam. The acrylic box then has a lid, along with a gasket that will bolt down to create a waterproof seal.

Figure 3: Surfboard and Housing CAD Model

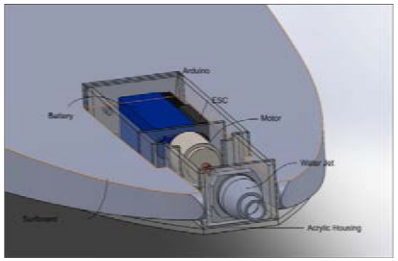

In order to maintain structural integrity and buoyancy, a minimal amount of foam was removed to fit the housing.

Figure 4: Final Assembly

Test Results

Figure 5: Power Output of Thruster

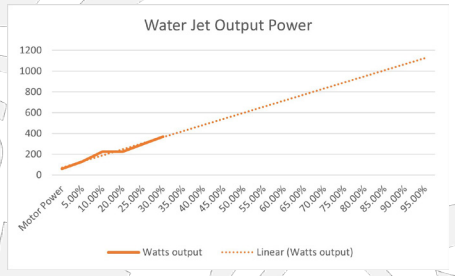

Test results show that the water jet thruster will be able to pull 1200 Watts at 95% of throttle power; this matches our target power output.

Future Model

If more resources were available throughout the year, our design would have the following changes :

Desired future parts:

- Custom surfboard would be designed for the sole purpose of fitting our unique housing.
- Marine grade stainless steel would be used for all bolts and metal connections.
- A fully waterproof brushless motor would be implemented.

Additional Testing:

- In depth thrust calculations for different types of brushless motors.
- Test jet thrusters of varying shaft/propeller size.
- Long term waterproofing analysis.

Project Timeline

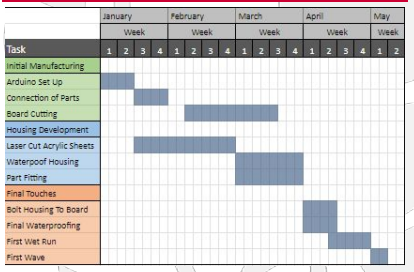

Acknowledgement

Special thanks to our advisor's, TA's, and professors.

- Prof. Aaron Mazzeo
- Prof. Gu and Prof. Pelegri
- TA Hang Zang
- Prof. Simonovic and Basily

M2

RUTGERS School of Engineering

MAE Design and Manufacturing

Retractable Surfboard Propulsion Unit

Max Chmigelski, James Branagan, Salman Haider, Eric Knauss, Elijah Somrah, Michael Zacieracha, Bharat Gianchandani, Roy Brown, Professor Mazzeo

Motivation

- Every year there are about 2 to 3 million new surfers around the world. With so many emerging, we believe that our project will be a great business opportunity in the surfing media.
- Surfing is physically demanding and even veterans of the sport get winded during long periods of paddling.
- The goal of our project is to create a self propelled surfboard with enough power and speed to get the surfboard far out into the ocean.
- This way, surfers can spend more of their energy actually surfing instead of struggling to paddle.

Project Outline & Components

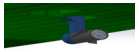

Fig 1. Side view of the earliest model of the board with the deployment mechanism

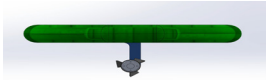

Fig 2. Back view of The earliest model of the board with the deployment mechanism

Fig 3. The earliest model of the board with a stowed deployment mechanism

This project has both mechanical and electrical elements that work together to propel the board in a controlled manner. All of these components are housed underneath the board in a custom cut cavity. The propulsion system can be controlled with a Bluetooth remote attached to the surfer's wrist, or via an optional external monitoring system on a computer.

- Mechanical Components
  - Deployment Motor
    - 5V servo capable of delivering 20kg of force
  - Propulsion Motor
    - 22.2V
  - Machined 6061 Aluminum Structural Arm
  - Waterproofed Wooden Frame
- Electrical Components
  - Battery
    - 6000 mAh LiPo
    - Powers motors
  - ESC
  - Bluetooth communicator

Conceptual Design

- Our design requires a motor to be attached to the bottom of a surfboard.
- Taking into consideration the center of mass of the components embedded in the board, the main challenge is to overcome the drag induced by the assembly in the water.
- To solve this problem, the motor can be retracted with the help of a servo motor, ensuring it remains deployed only when in use.

Safety

Our design puts machinery in close contact with a surfer, which could pose a danger.

- The electronics and the water are kept apart by a sturdy fishing box attached to the craft's underside and good sealant.
- The motor blades are isolated from the surfer's extremities and other foreign objects with a 3D printed sheath, which ensures the design remains both hydrodynamic and safe.

Project Management

Engineering standards:

- To help inform decisions about our use of electronics (IEEE 802.15.1)
- Use of sealant to keep water away from those electronics (IEC 60529).
- Proper organization of an engineering group (ISO 9001).

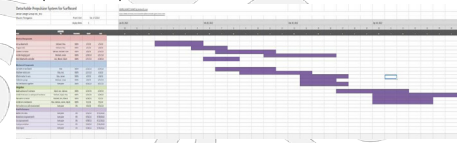

Fig 8. The Gantt Chart used to organize tasks.

Schematics

A view of various design iterations and mathematical models.

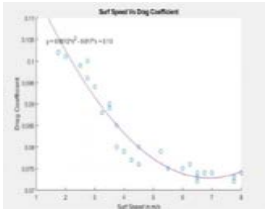

Fig 4. (a) A chart showing the drag coefficient as a function (f) surfboard speed (b) Drag and power calculations.

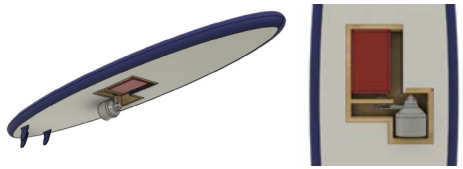

Fig 5. (a) A final model of the deployment mechanism on the bottom of the board (b) A close view of the final deployment mechanism.

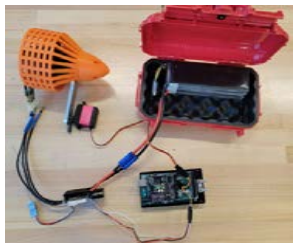

Fig 6. Electronic components including the main motor with sheath controlled by servo motor connected to an arduino and an ESC with the battery placed in the waterproof box cover.

Fig 7. Model of the sheath used to keep objects from coming into contact with the motor.

The project and its design have undergone a number of iterations.

- The mechanisms for deploying the propulsion motor have been changed in order to streamline and eliminate a convoluted spring mechanism.
- The new mechanism uses a servo that allows for positioning of the motor and prevents its unintended deployment.
- The original plan called for an electronics container that was twice as large as the container we ended up using. By reducing the size of this container, it protruded into the water less and decreased induced drag.

Results/Conclusion

The current design has a number of significant issues that make it unwieldy to ride and inconvenience the surfer. We believe that future iterations of this design can maximize its efficiency and improve the user experience. Our implementation is merely a proof of concept that does not fully embrace what this board could be.

- Current Issues
  - Modification induce lots of drag
  - Board is unbalanced
  - Battery needs to be removed for charging
  - Requires permanent and extensive modifications to the board
- Further Plans
  - Wrist mounted controller
  - Mass production plans

Despite these issues, we believe our current design can serve as a great board for introducing beginners to surfing, as well as helping experienced surfers spend less time and energy on paddling and more time catching waves. The board remains sturdy even though significant portions of it were cut out and the design prioritizes the safety of the surfer. Furthermore, the controls are simple, and the motor provides a significant and helpful boost.

M3

Dynamic Vibration Absorber

RUTGERS School of Engineering
MAE Design and Manufacturing

Russell Soto, Azhar Safa, Javier Ramirez, Gafar Tajudeen
Dr. Andrew Norris
Mechanical and Aerospace Engineering, Rutgers, The State University of New Jersey

Background Information

When force is acting on a mass in an undamped mass-spring system, it enters natural frequency if the frequency force is equal to the natural frequency of the main mass. Natural frequency creates resonance, which causes vibrations to the system and can cause failure.

Project Overview

- The goal is to create a Dynamic Vibration Absorber (DVA) that diminishes the vibration of a dynamic system.
  - Our DVA features a rail and carriage which is connected to a larger mass being held by a spring and a smaller mass attached via a spring. (spring-mass system)
- The smaller, absorber mass, on a spring is added to the initial spring-mass system at the same natural frequency.
- A small potentiometer sensor is added to show any residual vibration.

Real-World Applications

- Intended for use in areas that experience high seismic activity. Applicable to skyscrapers in order to absorb excess vibrations caused by high wind pressure.
- Applied in industrial machines with various moving parts that vibrate and throw off efficiency when the structure is not stabilized with counteractive mass.
- Mass dampeners are also utilized in vehicle components to provide a smoother and safer ride.

Initial Design

- A guide rail with a lubricated carriage oscillates the motor base so friction can now be neglected in calculations.
- Utilizes vertical springs and a double shaft motor.
- A secondary, hanging mass is featured.

Figure 1. The CAD model of the initial design with both eccentric masses and guide-rail included

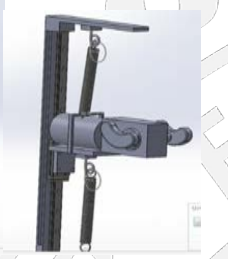

Figure 2. Close up of the primary mass system created for the initial design

Final Design

- Features a metal plate that connects the carriage to the motor.
- Machine screws connect the top and bottom spring of the design to the motor.
- Rotated the guide rail so that our springs would have more space in the vertical direction without the mass hitting the base.

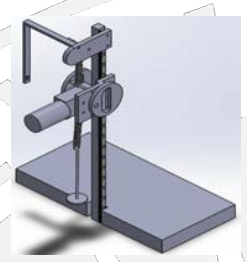

Figure 3. Solidworks creation of the final design

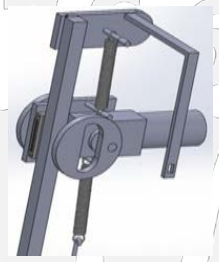

Figure 4. Closeup of the primary system including dc motor and the 2 eccentric masses

Fundamental Formulae

$$F_p = m_p g$$

$$k_p = \frac{F_p}{x_p} \quad k_a = \frac{k_p m_a}{m_p}$$

$$F_0 = m_p e \omega_p^2 \quad \omega = \frac{2\pi N}{60}$$

$$X = \frac{(k_a - m_a \omega^2) F_0}{(k_p + k_a - m_p \omega^2)(k_a - m_p \omega^2 - k_a^2)}$$

$$X_1 = \frac{k_a F_0}{(k_p + k_a - m_p \omega^2)(k_a - m_p \omega^2 - k_a^2)}$$

Project Data

Variable	Item	Value	Units
m_p	Primary Mass	0.6	kg
m_a	Absorber Mass	0.386	kg
m_e	Eccentric Mass (2)	0.18	kg
e	Eccentricity	0.006	m
k_1	Primary Spring Stiffness	105.65	N/m
k_2	Absorber Spring Stiffness	68.04	N/m

Figure 5. Values used while working on the calculations.

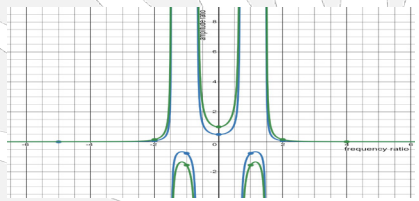

Figure 6. Depicts the excitation frequency ratio vs amplitude ratio, the amplitude of the absorber is green while the primary system is blue. Shows the system being dampened.

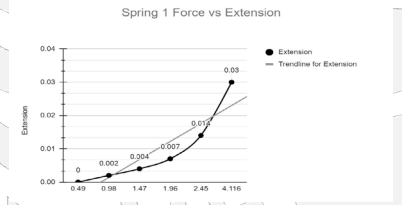

Figure 7. On the left, the Force vs spring constant graph depicts how the initial spring constant (stiffness) was attained.

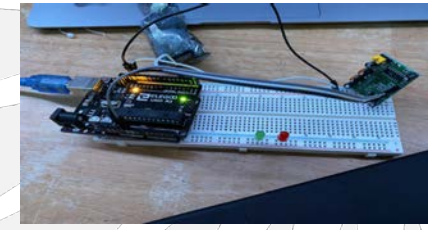

Figure 8. Above is the motion sensor being used in conjunction with the Arduino code

Individual Components

- Uxcell Double Shaft Worm Gear Motor DC 12V 250RPM High Torque Speed Reduction Motor with Metal Gearbox
- High-Cycle Low-Profile Ball Bearing Carriage
- Eisco Labs Stainless steel hanging mass
- 440 Stainless Steel Guide Rails
- Jrk 21v3 USB Motor Controller with Feedback
- Steel Extension Springs with Loop Ends
- HiLetgo 3pcs HC-SR501 PIR Infrared Sensor Human Body Infrared Motion Module for Arduino Raspberry Pi
- BNTECHGO 22 Gauge Silicone wire red and black each 10ft Flexible 22 AWG Stranded Copper Wire

Acknowledgement

We would like to thank Professor Andrew Norris for his guidance and support throughout the creation of our project. Our sincerest gratitude to Professor Basily Basily for all the help, advice and insight we received. We would also like to thank the Rutgers Department of Mechanical and Aerospace Engineering.

N1

RUTGERS
School of Engineering
MAE Design and Manufacturing

RUTGERS FORMULA RACING
BRAKE DYNAMOMETER

Mazen Abdalla, Dahany Choi, Kishan Patel, Gregory Scatko, Asaad Shaikh, Dr. Assimina Pelegri

PROBLEM STATEMENT

The Rutgers Formula Racing team is dedicated to designing, manufacturing, and racing a formula style race car. To be competitive, the team is constantly advancing vehicle systems to increase performance. Our focus for this project is the vehicle's braking system. In an effort to maximize braking capability, the group decided to design a brake dynamometer that would independently validate the manufacturer's specification of their brake pads.

MECHANICAL

A 2 horsepower motor with a freespeed of 1725 rpm is configured with a 10:1 worm gearbox to simulate the torque and rotational speed of a vehicle. A brake rotor is mounted at the end of the output shaft of the gearbox and a fixed brake caliper applies a known braking force to the rotor. This is done through a spring tensioning hydraulic system that can be fine tuned to apply a specific braking force to the rotor.

ELECTRICAL

Our induction motor is powered using a single-phase 120V AC connection. Motor operation can be toggled from our custom data acquisition system. Powered this system is an STM32G4 series mircontroller. The system is able to read the surface temperature of the brake rotor, the input power to the motor, as well as the RPM of the motor to perform power and torque calculations.

OBJECTIVE

The objective of this project is to maximize the vehicle performance by optimizing the braking system. Since current methods of validation are quite expensive, we are trying to provide a cheaper alternative to test a variety of brake pads and motors. The main objective is to design a cost-effective method of empirically measuring the coefficient of friction of different brake pad materials so that the team can justify braking parameters with high-precision data.

DESIGN ITERATION

During the design approach, it was determined that in order to extract the coefficient of friction value from the brake pad, the system must rotate the brake rotor with a known applied torque and rotational speed. Then the brake pad must apply a known force to the rotor. This would ultimately establish the design requirements:

- Motor and transmission system to provide rotation and necessary torque to the brake rotor.
- Method of accurate applying the brake pad force to the brake rotor.
- Sensors to collect necessary data to perform coefficient of friction calculation.

Through the design iteration process, a number of transmission methods were considered. Ultimately, the final design incorporated the use of a worm gearbox. This would provide the motor reduction necessary and also provide a structure to mount other components. In addition, a spring tensioning hydraulic system was designed to accurately apply the brake pad force.

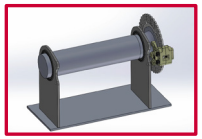

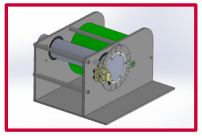

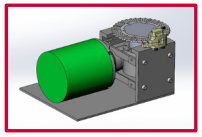

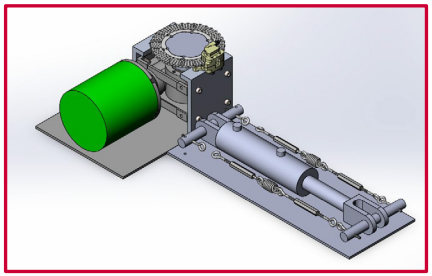

IMAGES

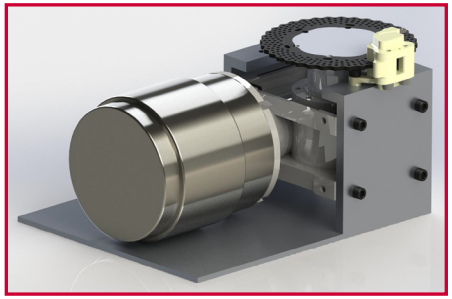

Fig 1. Final CAD Prototype

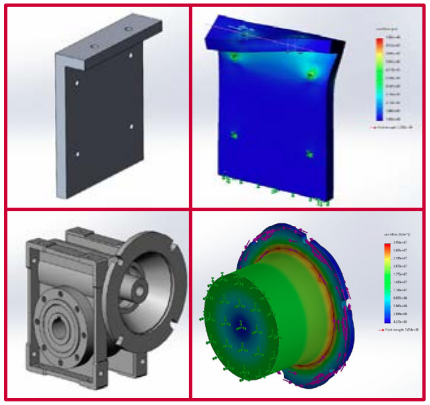

Fig 2.
(a) Worm Gearbox Plate (b) FEA Analysis of Worm Gearbox Plate
(c) Worm Gearbox (d) FEA Analysis of Worm Gearbox

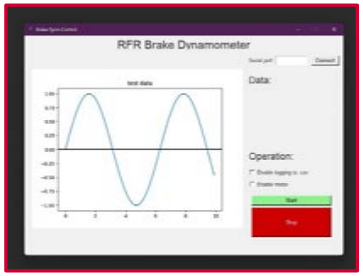

Fig 3. Data Acquisition Software

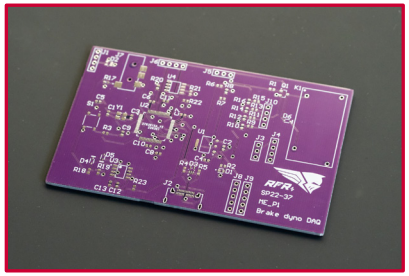

Fig 4. Custom Brake Dynamometer PCB

MANUFACTURING

The brake dynamometer has multiple parts that need to be custom machined and pieced together with fasteners. The fasteners are used to bolt together the pieces of 6061 T6 plates to the alloy steel base plate as well as the worm gearbox to be held in place. The fastener method is better than welding as we are able to easily take apart the system and customize the assembly easily unlike if the system was welded. This also allows for cheaper material to be used for materials that are less stressed than others that don't have to be limited to the entire system to be the same material. The majority of the system has to withstand relatively low amounts of load where aluminum can be used in place of steel to increase rigidity with the effect of not being able to handle high amounts of stress, however this was planned. To manufacture some of the parts such as the keyed shaft and the connector that connects the keyed shaft to the rotor, we need to use CAM software to program the profile we need to have cut from a CNC mill.

Requirements

In order for the final product to be deemed successful, it must meet the following requirements:

- The test bench should be able to withstand any loads, stress, and vibrations experienced from the brake dynamometer system.
- The motor should be able to apply a fixed amount of torque
- A data acquisition system should be able to acquire rotational speed of the rotor
- The system should be able to apply a fixed and known amount of force

RUTGERS School of Engineering

MAE Design and Manufacturing

Vacuum Tube Solar Steam Generator

Kevin Szymborski, Peter Bui, Sushrut Awasarmol, Thomas Chen, Sammy Breslau, Xingqi Che

Advisor: Professor Todd Rossi

Problem Statement

As the price of fossil fuels increase worldwide, the desire of having alternative energy for daily usage grows; but the price of solar green energy is affordable for most people and requires sometimes extensive knowledge of the system. Along with this, there are generally limitations upon certain alternative energy sources and thus leads to issues of under performing when not under their ideal conditions.

Purpose

The answer to this problem is a Vacuum Tube Solar Steam Generator. This system is mean to take the water and is heated rays of the sun. Steam is produced and can be used in order to provide heating for the houses that it is attached to. Along with this, it can provide after heating the homes is to provide distilled water and provide reusability.

Future

We would like to look into:

- Using the produced steam to generate electricity by adding additional components after checking if the pressure is high enough to power such an object
- Seeing if this can act as a permanent renewable alternative for heating in homes
- Expanding the scale of operation by adding more solar tubes and/or expanding the general setup to accommodate for more steam generation.
- Changing the design of the system so that it can better retain its heat throughout the transfer to the manifold

Principle of Vacuum Tube Solar Steam Generator

The purpose of this project is to manufacture steam at 15 PSI from water that has been fed into the vacuum tube. These vacuum tubes can reach up to 400 °F with just air while our goal is to reach 213 °F with water.

Background

The sun is a renewable resource that we can use to heat up steam. Steam itself is a valuable method of heat transfer to which has many applications. The goal is to make direct use of the sun's rays for steam production and to measure the energy output of said steam.

Design and Components

1. Dewar Vacuum Tube
2. Insertion Tubes
3. Intake Manifold
4. Frame
5. Pressure Relief Valves
6. Heat Exchanger
7. Insulated Tank

Final System form

The design of the system overwent several iterations to get to the form that it is now:

- Originally, the insertion device did not have a hose pipe around it
  - Before the design of the insertion device was simply a socket for the glass tube to entered however there was a slight difference of the size; allowing the steam to escape and render the project unable to perform its function
- The system previously had two pipes leading to the bucket however this lead to loss of heat rapidly and was taken out.

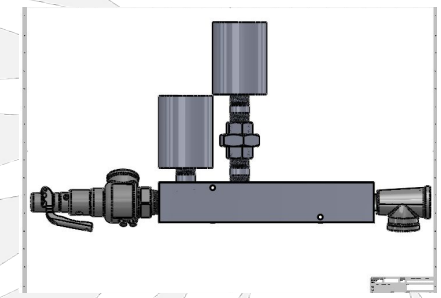

How it works

Water is added to the vacuum tubes. These tubes absorb the sun's rays and boils the water into steam.

The steam flows into the manifold where a pressure relief valve and pressure sensor is connected to ensure safety and keep steam within certain pressure limits.

Also connected to the manifold is a series of copper pipes that will lead the steam to a heat exchanger in order to release heat and turn back into water. This is meant to simulate a house pipe system; meaning that the house will act as a condenser if the project is used as a heating unit.

The result is the water was in the Dewar Vacuum tube in a storage space. With this, the water can either reused back into the system and be used multiple of times. Another choice is to use the distilled water and fitler it in order to provide clean drinking water for the people that use the system.

References

- Aluminum Anodizers Council. (2020). What is Anodizing? Retrieved December 11, 2020, from https://www.anodizing.org/page/what-is-anodizing.
- Bhatia, S. C. (2014). Solar thermal energy. Advanced Renewable Energy Systems, 94-143. doi:10.1016/b978-1-78242-269-3.50004-8
- Lowenstein, A. (2020). Steam-Generating Solar Collector. Retrieved December 12, 2020, from http://ailr.com/our-technology/steam-generating-solar-collector/
- Union of Concerned Scientists. (2018, May 24). Global Warming FAQ. Retrieved December 09, 2020, from https://www.ucsusa.org/resources/global-warming-faq.

R1

Mechanical Skin Stretching Device for Transdermal Drug & Gene Delivery

RUTGERS School of Engineering
MAE Design and Manufacturing

Sean O'Reardon, Jackson Nguyen, Rudolph Masia, Christopher Malty, Brian Nodine, Mitchell Ortega, Professor Jerry Shan

Problem Statement

Recent research has found that applying strain to an injection site after administering a vaccine increases DNA uptake, enhancing the efficacy of the vaccine. In order to further investigate this phenomenon, we have been tasked with creating a device that can accurately measure the stress and strain being applied to the skin of a test subject.

Solution (cont.)

used to find the force applied to the skin by measuring the torque of the motor. Further testing will establish the relationship between the motor's torque and the force it applies. This will ultimately allow us to go from measured current to torque to force, enabling calculation of stress applied to the skin.

Current to Torque Calibration

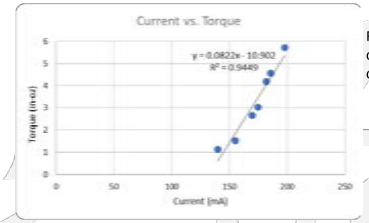

Fig. 5. The current-to-torque calibration curve.

Future Work

Further tests of fluorescent protein injections with lab rats will ideally lead to an optimal strain, strain rate, and stress to maximize DNA uptake. In the far future, assuming the research continues successfully, a similar device would be applied to every individual's skin following an injection.

Proposed Solution

Basic Assumptions: Skin will be treated as an isotropic, homogeneous material to enable easier analysis at the cost of some accuracy.

Lateral Stretching Device: This device utilizes contact pads that attach to the subject using an adhesive. Servo motors pull the contacts away from each other in x and y directions, resulting in 2D skin stretching.

Strain Measurement: In order to measure the strain, a grid pattern is stamped at the injection site of the vaccine. An Arduino board and a microcamera are mounted above the stretching device and are used to photograph the stretched and unstretched grid. These photographs are uploaded to a laptop and processed using the Resemble.js Javascript library. The Resemble.js library outputs a percentage describing quantitatively how different two images are. Given that the only difference between our two images is the grid displacement, this serves as our strain measurement. This can be checked by manually comparing the length of the gridlines (in pixels) of the undistorted and distorted images using an application such as MATLAB.

Force Measurement: The servo motors are first used to raise various weights using pulleys and strings. As the servo motors perform this, their torque is measured to find an equation relating the torque of the motor and the actual force output by of the motor. This equation is then

Design

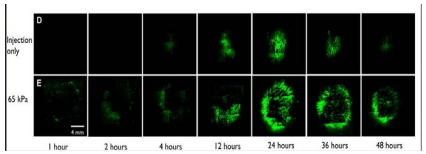

Fig 1. Photos illustrating a rat's response to injection with a fluorescent protein with and without skin stress applied to the area post-injection.[1]

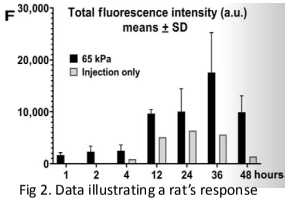

Fig 2. Data illustrating a rat's response to injection with a fluorescent protein with and without skin stress applied to the area post-injection.[1]

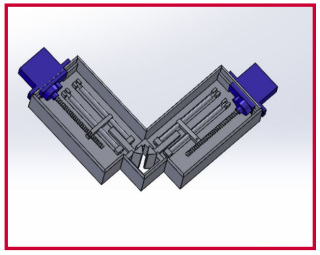

Fig 3. CAD design for the device.

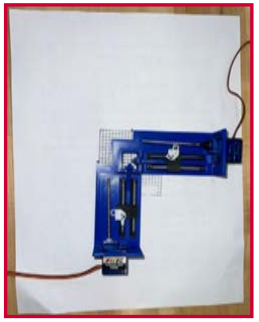

Fig 4. The device itself. The skin goes in the center square. It is shown against a piece of A4 paper for scale.

Strain Analysis

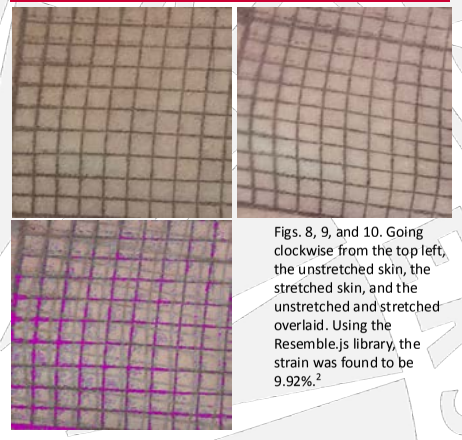

Figs. 8, 9, and 10. Going clockwise from the top left, the unstretched skin, the stretched skin, and the unstretched and stretched overlaid. Using the Resemble.js library, the strain was found to be 9.92%.[2]

References

1. Lallow, E. O., Jhumur, N. C., Ahmed, I., Kudchodkar, S. B., Roberts, C. C., Jeong, M., Melnik, J. M., Park, S. H., Muthumani, K., Shan, J. W., Zahn, J. D., Shreiber, D. I., Singer, J. P., Park, Y. K., Maslow, J. N., & Lin, H. (2021). Novel suction-based in vivo cutaneous DNA transfection platform. Science Advances, 7(45). https://doi.org/10.1126/sciadv.abj0611
2. Cryer, James, Huddle Development Team (2022) Resemble.js,Image Analysis and Comparison, https://github.com/rsmbl/Resemble.js

Gecko-Inspired Robot

RUTGERS School of Engineering
MAE Design and Manufacturing

Animesh Chakraverty, Luke Eidle, Aadil Mahmood, Agam Modasiya, William Rice,
Prof. Jonathan Singer

Problem Overview

One of the many goals of engineering is the automation of tasks that are either too dangerous, too costly, or too repetitive for human workers. Inspection and exploration are two of these tasks that our senior design group has chosen to tackle. Infrastructure like bridges, tall factory towers, and space stations are often inaccessible or require expensive machinery to put a worker in position for inspection. Similarly, exploration in unknown areas, such as natural disaster sites for search and rescue, is risky and difficult for humans. Current solutions of flying drones are very energy intensive and walking robots are not able to traverse tall obstacles. To solve these issues, a new class of robots, climbing robots are being developed.



Proposed Solution

Our solution is a gecko-like robot that is capable of climbing vertical surfaces using energy efficient adhesive footpads developed by team ME_S5. This quadruped robot will be capable of walking on surfaces at various angles to move into dangerous positions and perform inspections without endangering an employee. The robot can be equipped with sensors necessary for inspection and search-and-rescue.

Design Considerations

To ensure our robot could effectively and efficiently climb on walls we had several design considerations:

Mechanical:
- Low Center of Mass
- Low Weight

Maneuverability:
- Ability to travel in any direction and large range

Electrical:
- Low Power Consumption

Manufacturing:
- Modular and easy to prototype

Mechanical and Electrical Design Choices

Ultrasonic Sensor

Autonomy is an essential aspect for many robots especially when humans are not available. Our gecko adjusts the direction of movement, even when it is being physically controlled to move away from obstacles in front of it. For future improvements, we could use more capable sensors, such as Lidar, to avoid obstacles in other directions, like the image below.

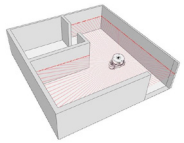

Double Servo Shoulder

The use of two independent servo motors gives us a walking motion with two degrees of freedom. This allows us to have total control over the position of our gecko feet with our control software.

Additionally, having two servos near the body provides 2 key improvements over traditional robotic arm designs:
- halves applied torques on each shoulder servo
- reduces moment arm and torque on wing servo

High Torque Micro Servo

High-torque micro servos are essential to the success of this project. They are small, relatively strong, and easy to work with. The choice to use 16 of the same type was a deliberate one; using identical servos for every aspect of the design means that we only needed a few backup motors in the event of a malfunction. With short deadlines and long wait times for part orders, we couldn't count on reordering specific motors if one burnt out.

Spring-Loaded Tail

Our tail mechanism applies a countertorque that reduces the normal adhesive forces on the top pair of feet. A passive spring is used as opposed to an active servo system to reduce the weight and complexity.

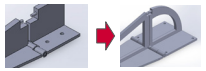

Design Iterations:
Our original design had issues while 3D-printing, so we moved the hinge to be flush with the bottom of the mechanism. We also moved the spring higher and closer to apply a greater torque.

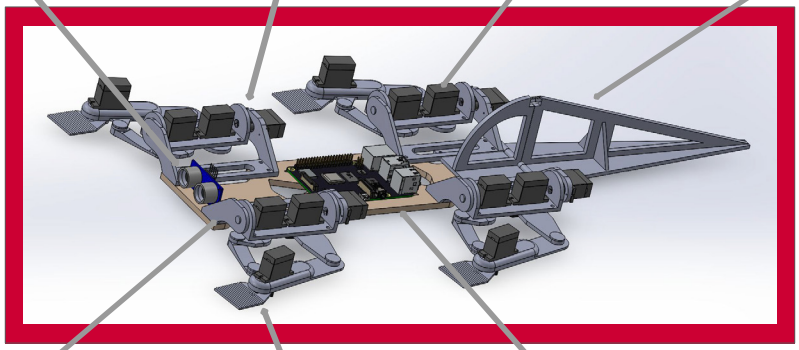

Drop-through Wing

The wing that holds the whole leg mechanism was designed such that the bottom of the body and the foot pads exist on nearly the same plane. This minimizes the distance between the center of mass of the robot, and the walking surface.

Design Iterations:
Throughout the semester we began moving material to high stress points and changing the height of the bracket to get the leg as low to the ground as possible.

Peelable Foot

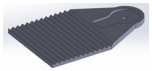

The foot is arguably the most important part of the robot. It must hold up the entire weight of the bot through passive adhesion, but also be able to release from the wall when needed. Our design utilizes a notched surface that adds flexibility to create a peeling action much like what happens when tape is pulled at one end. This concentrates all the lifting force on one point of the foot, overcoming the adhesive forces in the pad.

Skeleton Frame Body

We designed one leg mechanism that could be replicated 4 times and attached to a simple base.

Design Iterations:
Originally, we planned to use a rectangular balsa wood board for the material's light weight. However, when put into practice, the balsa wood proved weak and flexible. We decided to design and 3D print a trussed base to connect the 4 legs and tail instead. The PLA material proved sturdy enough for our needs and the trussing ensured it remained lightweight.

External Power Supply

Our robot is powered by an external power supply. Our original plan was to power everything with on-board lithium Ion batteries, but this would have drastically increased the weight of our design. We decided that for an initial prototype, using an external power supply with a power harness/tether would give us a higher chance of success.

Optimization and Control

To aid in both optimization and control we calculated the inverse kinematics by decomposing the design into two independent parts, simplifying the computational cost.

$$q_2 = \cos^{-1}\left(\frac{x^2+y^2-a_1^2-a_2^2}{2a_1a_2}\right)$$

$$q_1 = \tan^{-1}\frac{y}{x} - \tan^{-1}\frac{a_2\sin(q_2)}{a_1+a_2\cos(q_2)}$$

The design was parameterized and an optimization program was created to both visualize the range of motion and the joint positions. The cost function for optimization was the largest radius of motion while the constraints were the torque limits and joint intersections.

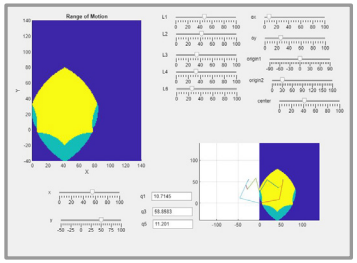

After a suitable design was chosen, its range was used to calculate the points needed to follow a walking gait. This was calculated as a linear path and sinusoidal arc based on angle inputs from the programmed joystick controller. The joystick also allows control of the speed of the gait.

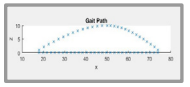
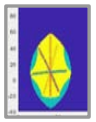


Conclusion

We designed and built a proof-of-concept robot that can crawl and be controlled remotely. Our project proves that a relatively cheap crawling robot can be designed and constructed, and theoretically, will be capable of scaling vertical surfaces. With more time:

- We would like to improve the maneuverability by adding body flexing control.
- We would like to optimize the current structure of our robot to reduce weight even further.
- We would like to design a way for sensors to be attached in a modular fashion allowing for higher functionality with one robot

S2

Gecko-like Foot Pad

RUTGERS School of Engineering
MAE Design and Manufacturing

Gaurav Aggarwal, Darrel D'Souza, Alex Liu, Sydney Jenkins, Catherine Nachtigal, Dr. Jonathan Singer

NSF Award: 2019849

Abstract

People have often looked to nature for inspiration for engineering phenomena in order to mimic its capabilities. In this research study, a gecko's foot is used as the tool of inspiration. These feet are capable of strong adhesion to a multitude of surfaces in order to allow a gecko to climb up smooth surfaces, due to the combination of a complex macro- and microstructure on the gecko's foot. The macrostructure consists of a series of setae on the millimeter scale, which are then covered in a microstructure consisting of thousands of structures called spatula on each setae. These structures will be mimicked through using a combination of a PDMS base created from a resin mold to create the setae pillars, and an electrospray deposition coating used to create the complex spatula structure on the setae pillars. The efficiency of the foot will be tested through adhesion tests on a custom-made table to compare its adhesion on different surfaces in comparison to other materials. Once properly manufactured, this foot will be employed on a gecko-like robot to make it capable of climbing up walls.

Gecko Feet

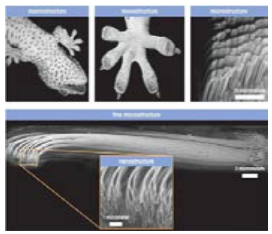

Diagram of Gecko Feet [1]

- With the help of its setae, just one foot of the gecko can hold up to 20 times the animal's weight!
- Gecko feet can adhere to any surface except Teflon
- Feet are covered in microscopic hairs (setae) covered in tiny nano-scale spatulae located on the gecko's foot
- Interactions between the gecko's feet and climbing surface are dictated by Van der Waals forces

Electrospray Deposition

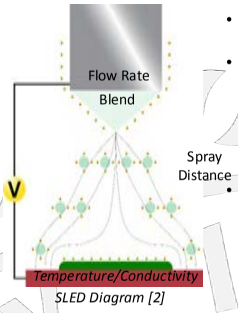

SLED Diagram [2]

- Electrospray deposition is a nanocoating process
- It utilizes an electric field to charge a solution, causing it to disperse into a spray and follow the electric field lines to be deposited on a grounded substrate
- This process can be thickness self-limiting (SLED) as the film builds up a charge over time, causing further droplets to be deflected to uncoated areas of the target

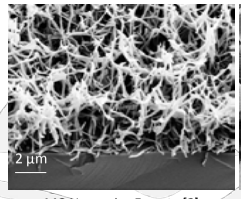

MC Nanowire Forests [3]

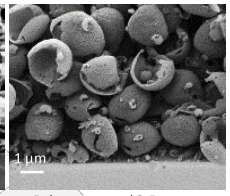

Polystyrene and 2-Butanone Electrospray Shells [2]

- These coatings can also result in films with a variety of complex nanostructures and nanotextures
- This can be used to mimic the nanostructures on a gecko's foot

Methods

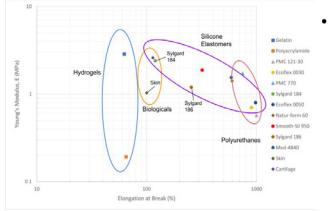

Young's Modulus and Elongation of Various Materials

- Silicone and other artificial plastics exist whose material properties mimic that of skin, and can be used as a base to apply the electrospray coatings to
- Different materials for the foot pad were tested based on this chart, as well as based on what materials would be conducive to ESD, including gelatin and Sylgard 527
- These materials were poured into silicone molds consisting of pillars of multiple sizes to test the best pillar size for adhesion

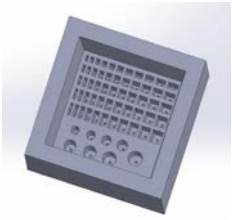

Foot Pad Mold CAD Model

- The foot pads were sprayed with blends of polystyrene (PS) and Kraton or epoxy oils and PVP to improve adhesion
- These foot pads were then tested on a custom-built adhesion testing device and compared to other adhesive materials like glue

Adhesion Testing Apparatus Schematic

- (1) Table, (2) Breadboard, (3) Tilting Table, (4) Sample, (5) Spring Scale, (6) Pulley String, (7) Pulley, (8) Cup.

Results

Normal and Shear Test Results Using the Pulley-based Testing System

Shear Test Results for Aged Gelatin + Glycerol Pads

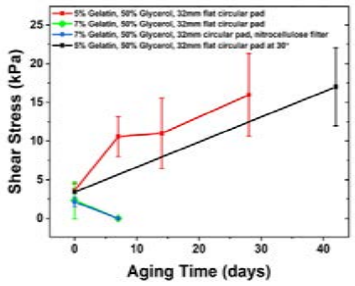

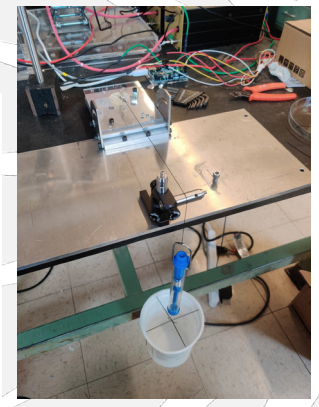

Adhesion Testing Apparatus Setup

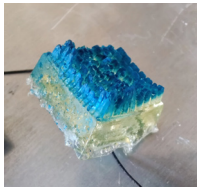

Textured and Electrosprayed Gelatin Sample

Three Prepared Untextured Gelatin Samples

Conclusion

- For the foot pad material, 7% gelatin blended with 50% glycerin was found to provide the most optimal pillar resolution and strength
- A custom, pulley-based adhesive testing system was designed and successfully constructed. Adhesive strength at various loading angles was measured
  - Unsprayed, 5 and 7% gelatin flat pads displayed the highest adhesive strength out of all the foot pads tested
- Foot pads were successfully coated with self-limiting ESD
  - PS + Kraton sprays successfully coated gelatin pads
  - Epoxy oils + PVP sprays were successful on PEGDA pads
  - PS + Kraton sprays significantly reduced gelatin pad adhesive strength
    - Spray may have applications in environments where low friction is needed
- Future work will attempt to fine-tune our dry adhesive spray formulation to prepare a foot pad for eventual applications in a gecko-like robot that can scale vertical surfaces

References

[1] Autumn, K. (2006). "How gecko toes stick". American Scientist. 94 (2): 124–132.
[2] Lei, L., Kovacevich, D. A., Nitzsche, M. P., Ryu, J., Al-Marzoki, K., Rodriguez, G., Klein, L. C., Jitianu, A., and Singer, J. P. (2018). Obtaining Thickness-Limited Electrospray Deposition for 3D Coating. ACS Applied Materials & Interfaces. 10 (13): 11175-11188.
[3] Lei, L., Chen, S., Nachtigal, C. J., Moy, T. F., Yong, X., Singer, J. P. (2020). Homogeneous gelation leads to nanowire forests in the transition between electrospray and electrospinning. Materials Horizons. 7: 2643-2650.

S5

Automatic Shifting CVT Bicycle System

RUTGERS School of Engineering
MAE Design and Manufacturing

Dimitri Duma, Dylan Fallows, Ralph Ricciardi, Yash Sanghvi, Xiaohan Xu
Professor Stephen Tse

PRIORITY BICYCLES

Introduction

The goal of the project is to design a system which can shift gears on a bicycle without input from the rider. The optimal cadence for a human pedaling on a bicycle is between 60-90 RPM, and staying within that range allows for the most efficient way to transport oneself. The automatic shifter will monitor rider cadence and continuously shift to ensure the rider is at their desired cadence. To increase efficiency, a CVT rear hub is used to allow infinite adjustability within the CVT's range.

Background

The increasing awareness of global emissions and healthy lifestyles has created a rise in the demand of biking as a transportation method. Currently some of the main deterrents to biking are the complexity newcomers face with learning to shift gears and the sense of serenity that is loss due to the constant attention a rider needs to give to shifting gears. We hope our system will further promote the healthy switch to bicycling.

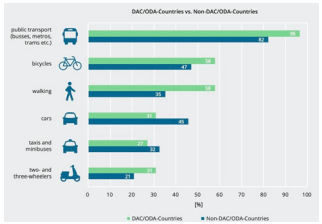

Reid, C. (2020, October 10). *Bicycles and buses will be future's dominant modes of urban mobility, predict 316 transport experts*. Forbes. Retrieved December 10, 2021, from https://www.forbes.com/sites/carltonreid/2020/10/09/bikes-and-buses-will-be-futures-dominant-modes-of-urban-mobility-predicts-346-transport-experts/.

Design

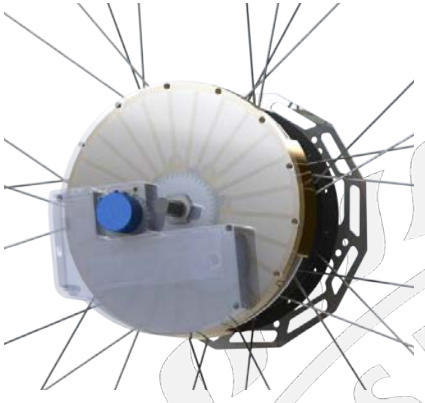

- Shifting mechanism uses a worm gearbox and a 12V DC motor connected the CVT Input with gears.
- A potentiometer reads angular position, used to determine current CVT ratio.
- Shifting mechanism fits onto the rear wheel of the bike. Universal fit for any bicycle with axle mounting standard.
- Casing holds a hall effect sensor to read a ring with magnets to get the wheel angular speed correlating to bike velocity.
- Gears and Casing are 3D printed with nylon.

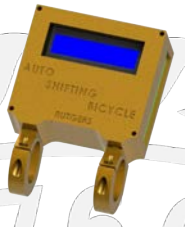

- Control unit houses an Arduino and Display LCD
- Control unit is user programmable to adjust cadence setpoint and switch to manual mode
- Code runs two PID loops, two interrupt functions for hall effect sensor reading, and display logic.
- Whole system is run of 14.8V battery system.

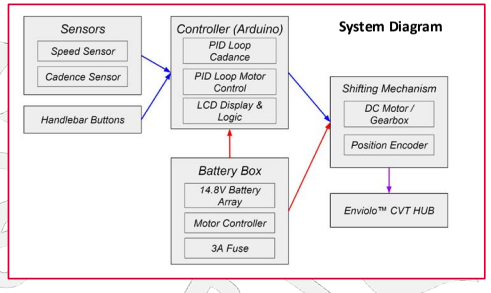

- Optimal rider cadence is between 60-90 RPM.
- PID control loop continuously uses the rider cadence and bike velocity to actuate the shifter mechanism to continuously adjust the riders cadence.
  - As a rider goes up a hill, their cadance drops due to increased force required - the system will shift down to increase cadence pace.
    - As a rider increases speed or goes down a hill, their cadence will increase to an efficient cadence range - the system will shift up to decrease cadence pace.
      - When the rider is coming to a stop, the bike will engage the shifter to the lowest gear for the easiest start.

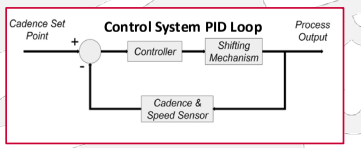

Integration and Testing

- Initial tests are performed on a specialized testing rig. These test the basic functionality of the electronic components.
- Rider testing is performed riding the bike on Busch Campus. Manual control was implemented first and reliability of the system was tested through repeated shifting under load.
- Sensor data was compared to a aftermarket system to calibrate sensor reading accuracy
- Final rider testing and data acquisition was performed by riding the bike on a route with a combination of inclines and sustained flat areas.

Analysis

- Data acquisition system used to analyze performance and optimize control loop.
- Collected data on time within acceptable cadence range and rider energy use.
- Results compared to similar data collected from a standard manual shifting bicycle.
- System deemed successful if shifting took place within time response of Hall effect sensor.

Future Developments

- Further testing for the purpose of better optimization.
- Inclusion of other parameters, like applied torque, hill gradient, or power.
- Redesign components for universal use, as opposed to a specialized design for our model.
- Create a design for a more traditional chain drive gear hub.
- Make the casings waterproof and airtight to protect the instruments from the elements.

T1

RUTGERS
School of Engineering
MAE Design and Manufacturing

Fishing Equipment with Sensory Feedback

Aaron Malixi, Darien Sajewski, Gerard Wietecha, John Juco, Sean Doran
Dr. Stephen Tse and Mr. Frank Iatarelli

Overview

A haptic fishing system allowing people with physical disabilities to have a fulfilling and satisfying endeavor by developing a mechanism to lower the physical requirements while also providing sensory feedback to the user.

Casting

The casting system is primed by an electric drill motor. The rod is flung forward by a torsion spring. The rod is permitted to be flung forward when the shear pin of a solenoid is released.

Reeling

The reeling system is actuated by an electric motor from a drill. This design would include a solenoid that presses the push button on the spincast reel which controls the release of the line, as well as a drill that is bolted to the aluminum sheet that will serve as the housing.

Feedback/Controls

The feedback/controls system is centered an Arduino microcontroller which allows the user to interface with the other subsystems with buttons and analog inputs. With enough time, haptic feedback and a handheld controller could be implemented.

Detailed Design

The casting subsystem sets to launch a spring-loaded fishing hook which is clamped and axially mounted with a torsion spring in the casting direction. The design utilizes an arm to prime the spring-loaded system and a solenoid shear pin that contracts the rod length during priming. A motor serves to drive the arm at high torque, low speed to equip the casting distance more precise and accurate. Calculations concerning rotational kinematics were conducted in an experiment to test optimal casting distance for a 6'6" fishing rod.

$$\theta(t) = \theta_0 + \omega_0 t + \frac{1}{2}\alpha t^2$$

The reeling subsystem consists of a spincast reel and a gear motor. Using the geared motor, consistent torque can be implemented to electronically "reel" in the fish. The spincast reel acts in association with the solenoid to simulate casting and reeling using the push of a button. Experimentation with "reel torque" provided insight on torque measurements needed using drag settings and given force assumptions.

$$\mathbf{r} \times \mathbf{f} = \mathbf{T}$$

Feedback relies on some simple digital inputs using buttons and analog inputs using a potentiometer. The Arduino Mega serves as the primary source for programming the system's functions. Combined with a motor controller, a geared motor and drill motor are used to drive the vital components of our system.

Prototype

USER-CONTROLLED ELECTRONIC FISHING SYSTEM WITH ACCESSIBLE FEEDBACK AND OPERATION FOR DISABLED PEOPLE

PICTURE 1: CASTING SUBSYSTEM: CONSISTS OF A GEARED MOTOR TO PRIME THE FISHING ROD ON A TORSION SPRING, RELEASED BY A SOLENOID

PICTURE 2: REELING SUBSYSTEM: CONSISTS OF A DRILL MOTOR DRIVING A SPINCAST REEL PRESSED BY A SOLENOID

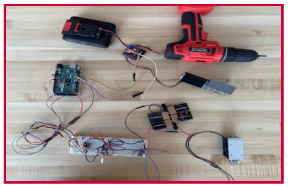

PICTURE 3: CONTROL SUBSYSTEM: CONSISTS OF AN ARDUINO MEGA THAT CONTROLS A SOLENOID POWERED BY 9V BATTERIES AND TWO MOTORS VIA A MOTOR CONTROLLER POWERED BY THE DRILL BATTERY

PICTURE 4: OVERALL DESIGN

The overall design combines all three subsystems to function as one. Using the feedback subsystem, the user can activate the casting subsystem and control the reeling subsystem with minimal physical exertion and dexterity. This enables the user to experience the joys of fishing without being limited by any physical disabilities.

Progression/Timeline

September 2021 - Project Conception
October 2021 - Project Definition and Planning
November 2021 - Project Development
December 2021 - 1st Round of Parts Ordering
January 2022 - 2nd Round of Parts Ordering
February 2022 - Prototype Assembly
March 2022 - Prototype Testing and Revision
April 2022 - Presentation and Poster Preparation
May 2022 - Project EXPO

Standards Used

- ASTM D882-00
- SAE AMS QQ-A-200/8
- Machined Surface and Edge Requirements Per ASME B46.1 and Tolerance Fits per ANSI B4.1
- IEC 62841-3-13:2017
- IEEE/ANSI 315

References/Acknowledgements

- Professor Tse - As our advisor, Professor Tse gave us vital guidance and made sure we met the goals necessary for the project.
- Frank Iatarelli - The project's IP owner and mentor, Frank was very helpful coming up with ideas and tests to further the project.
- Dr. Basily - Guiding our parts selection and machining, Dr. Basily was an excellent resource to have for the project.

T2

High Strength,Light Weight Spherical Pressure Vessel with Fiber-Reinforced Composites

RUTGERS School of Engineering
MAE Design and Manufacturing

Usmaan Chaudry, Hao Wu, Kinza Iqbal, Zhuocheng Han, Lihao Feng, Keming Yan
Dr. George Weng

Introduction

Pressure vessels are specially designed containers that can withstand certain pressure loads of a stored gas or liquid. The concept of pressure vessels was not clear until the industrial revolution in the 1800s. With the invention of steam engines which assisted in the development of pressure vessels. The primary use of pressure vessels is for industrial purpose as storage vessels, heat exchangers, fraction distillation and pressure reactors. Our project is to build a lightweight high strength spherical pressure vessel. We mainly follow the ASME Section VIII code for engineering standards, which is applicable to the pressure vessel. The Vessel will have a maximum pressure of around 200 psi and when a factor of safety of 6 is applied the maximum operating pressure drops to 32psi. Carbon fiber filament, epoxy resin, hardener, styrofoam as the mold, and a valve is used to construct our pressure vessel. Simply, we will firstly get the epoxy and hardener mixture with ratio 5:1 and brush it uniformly on the mold. Then carbon fiber yarn will be wrapped on by sections. After each subsequent layer is wrapped on epoxy resin will also be brushed on. We applied three layers of carbon fiber and it took 4 days to fully cure. A hydrostatic tesi will be used because a pneumatic test would be too dangerous.

Objective

- The high strength, lightweight spherical pressure vessel is made of carbon fiber epoxy resin material with an inner mold and a valve placed on the top.
- The sphere is 12'' in diameter, ⅛" in wall thickness and can hold 3.9 gallons in volume.
- Performing hydrostatic testing is a safe and effective way to test for any leakage.

Prototype

Initial Prototypes

Tiny Basketball

- A polyester ribbon was wrapped around a basketball
- Practice the wrapping method and epoxy resin mixture

Frozen Ice Balloon

- Water was poured into a plastic balloon and frozen
- Polyether ribbon was wrapped around the vessel
- Ice mold was too heavy and defrosted while working

Air Filled Balloon

- Yarn was wrapped around a spherical balloon filled with air
- Allowed members to gain experience with wrapping method
- Balloon would deform under the compressive wrapping stress

Final Prototype

Spherical Styrofoam

- A plastic balloon was glued inside a styrofoam sphere with the valve protruding from it
- Two layers of polyester ribbon was wrapped around the sphere
- Epoxy was applied on the sphere but cured too quickly, so epoxy was then directly applied to the ribbon as it was feed onto the sphere

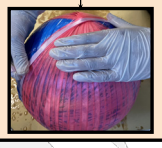

Manufacturing

- Final Spherical Presuure Vessel
- 12" Styrofoam Spherical Mold
- Valve Inserted into Mold before Wrapping Carbon Fiber
- 5:1 Resin to Hardner Ratio
- 3 Layers of Carbon Fiber Filaments
- No Leaks From Hydrostatic Test
- 4 Days to Fully Harden
- Resists Temperatures up to 250℉

Design

We are designing a thin wall spherical vessel. We analyzed the fluid pressure exerting force and tensile stress in the wall. The final equation gives us the relationship between the thickness, radius and pressure.

$$p = \frac{2\sigma t}{r}$$

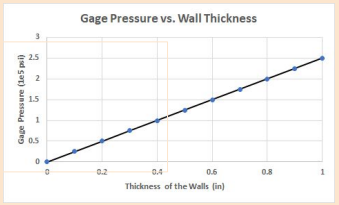

Figure D1: Gage Pressure vs Wall Thickness

Table 3 lists viable polymer composites that could be used to construct our spherical pressure vessel. We decided to use carbon fiber because it has better physical properties compared to Kevlar and Fiberglass, despite its higher cost.

Characterization	Carbon Fiber	Kevlar	Fiberglass
Cost	1	3	10
Tensile Strength	10	8	7
Strenth to Weight	10	9	5
Compressive Strength	10	3	6
Ragidity	10	6	6
Fatigue Resistance	6	10	8

Table 3: Material Comparison

Citation

McLaughlin, Pat B., et al. "Composite Overwrapped Pressure Vessels, a Primer." *Ntrs.nasa.gov*, 1 Mar. 2011, ntrs.nasa.gov/citations/20110008406. Accessed 15 Apr. 2022.

Zu, Lei, et al. "Design of Filament-Wound Spherical Pressure Vessels Based on Non-Geodesic Trajectories." *Composite Structures*, vol. 218, 15 June 2019, pp. 71–78, www.sciencedirect.com/science/article/pii/S0263822319303848, 10.1016/j.compstruct.2019.03.045. Accessed 15 Apr. 2022.

AE W1

A Smart Fertilizer Machine for Urban Organic Waste Recycling

Leonardo Stefanelli, Wilson Pratts, Derek Schmidt, Yutian Xu, Zachary Yammer, Manuel Espinoza, Dr. Qingze Zou, Dr. Basily

Mechanical and Aerospace Engineering, Rutgers, The State University of New Jersey

RUTGERS School of Engineering

MAE Design and Manufacturing

What's The Problem?

Food waste has become an enormous issue in recent years but has always been a lingering problem. In today's day and age, 30-40% of the food meant to be eaten ends up being wasted every year. To put this in greater perspective, it amounts to about 219 lbs. of food waste per person, in the United States alone. Moreover, this rotting food waste also contributes to greenhouses gases which release chemicals into our atmosphere that are not ideal at all for our environment, or ourselves.

Background Information

Organic waste has become an increasingly severe environmental concern in the United States in more recent years. The United States specifically discards more food than any other country in the world: nearly 40 million tons, or 80 billion pounds, each year. This again is estimated to account for 30-40% of the total food supply. Food is the most significant single component that occupies landfill space in the United States, accounting for 22% of municipal solid waste. And, this is just one nation's contribution out of many.

The solution we are providing is a compost producer that will harvest as much energy as possible from the food waste. It can not only convert the food waste into fertilizer to be used at home, on a farm, in a garden, etc., but it can also produce biogas as a byproduct. The biogas energy can then be used as an alternative power solution and be sold to restaurants, businesses, and even homeowners. Due to limited resources, our prototype aims to produce biogas on a small scale to test a possible largescale operation of a large group of these units.

Objective/Solution

Our project not only aims to create a smart machine to convert urban organic waste into usable energy in the form of biogas and fertilizer, but to also automate the process as much as possible. The goal to reduce user interaction and shorten the expected time to compost food waste was another top priority, as simplicity for users is always key for products. The automation will allow the user to complete this process with minimal moderation and await completion much quicker than traditional composter.

Observation/Calculations

We noticed many inconveniences when trying to build upon the previous group's work on this project, so we used the concepts and ideas from their work to essentially redesign the physical build and formulate new ideas to be implemented of our own, as well. One of the main issues we found was the time it would take for fermentation and subsequently collecting the gas from an inefficient production method. With the original workings, we noticed making fertilizer out of the organic waste was the only viable outcome of the two as producing biogas wasn't feasible. Our design shift allowed biogas production to not only occur but made storing the gas possible as well, instead of just venting it off as the old designs called for. We also decided to go ahead with calculations for mixing purposes to determine the best type of combination between water and organic food waste to ferment faster.

Anaerobic Process: $C_6H_{12}O_6 \rightarrow 3CO_2 + 3CH_4$

$$\tau = F \cdot d = 26.8N \cdot 7.62 \cdot 10^{-2}m = 2.042Nm = 18.073in \cdot lbf$$

$$HP = \frac{\tau \cdot RPM}{63{,}025} = \frac{(18.073in \cdot lbf) \cdot 1750RPM}{63{,}025} = .5028HP$$

Project Management

Here is an overview of our group's progress this whole school year from start to end, above. It is shown in the form of a Gantt Chart. The above tasks were divided equally among all group members. For some tasks, sub teams were utilized to split work and optimize progress.

Design/Schematics/Prototype

Here we have included pictures of our design, schematics, and prototype at its current build during the creation of our poster:

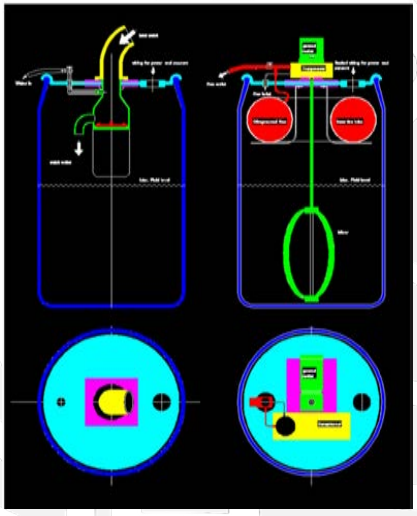

Pictured on left hand side (top to bottom): Design schematic of final build, External (normal) view of build at the deadline of poster's completion. *Final part arriving soon. First phase shredder testing competed at this point.

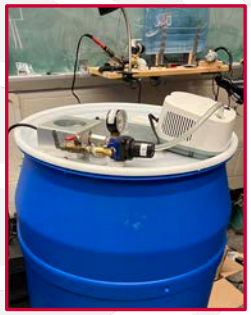

Pictured on right hand side (top/left to bottom/right): Top view of shredder, Bottom view of shredder, top view of mixer/compressor, Side view of mixer/compressor. *Motor part not delivered yet but to be on top of mixer/compressor

Prototype/Standards

In our prototype, we were able to incorporate the biogas storage component within the inside of our barrel. After our critical design report of the fall semester, there were some minor changes to the design provided, but the main scope of the project is still the same. For example, there is still a chute function for organic waste inlet, but a smaller radius than the one provided in that report. This acts as a safety standard, so people cannot fit their hand in the inlet. There is also a water feed connected to the shredder as it is needed not only for mechanical needs of the shredder but for the waste to ferment better too. When turned on for food waste to travel through the shredder, the water will automatically be pumped in simultaneously with no user interaction needed.

Now onto the mixing machine. When the barrel reaches the limitation for food storage, the cover can be switched, and we transition to the mixing stage. In this part, the fermentation process happens over time and produces biogas. Using a compressor, these gases will be collected and stored in a tire tube. Once the tire is full, the excess gas will be vented off through the safety valve. This is another safety standard we implemented. And to note: the alert of the bin reaching capacity and venting off excess gas alike are both automated through our use of computing tools and pneumatic circuit/solenoid valves.

Acknowledgements

A great appreciation and thank you to:

- Dr. Basily for assisting us greatly with design, machining, and manufacturing while joining many team meetings
- Mr. Scott Schipper and ASCO Valve for assisting in sponsored project parts (2 ASCO 24/DC Solenoid Valves)
- Dr. Zou for providing us with exceptional guidance, a personal lab to work in, and assisting us the whole way
- Prof.'s Gu and Pelegri for conducting a great course for all

Z3

Mechanical & Aerospace Engineering at Rutgers

The Department of Mechanical Engineering at Rutgers was founded in 1908 with a focus on driving the country's industrial growth. Aerospace Engineering was added in 1965 as a certificate program with a full degree program established in 2015. It is now the only Aerospace Engineering degree offered among New Jersey's public universities. The Department is a vibrant academic community offering three undergraduate degrees in Mechanical Engineering, Aerospace Engineering, and Applied Science (Packaging Engineering concentration). The Department has state of the art laboratories used for research leading to M.S., M.Eng., and Ph.D. degrees. Undergraduate and graduate students participate in cutting edge research funded by federal and state agencies, and industrial partners. With more than 35 full-time faculty members, the Mechanical and Aerospace Engineering Department educates more than 750 undergraduate students and more than 160 graduate students. Excellence in both research and teaching is the top priority for our faculty.

RUTGERS MECHANICAL AND AEROSPACE ENGINEERING WOULD LIKE TO EXPRESS ITS APPRECIATION FOR THE SUPPORT OF THE FOLLOWING SPONSORS

GENERAL DYNAMICS
Mission Systems

EMERSON | ASCO Distributor

LOCKHEED MARTIN

PRIORITY BICYCLES

NSF

NASA

RFR

RUTGERS
School of Engineering

Mechanical and Aerospace Engineering
Rutgers, The State University of New Jersey
98 Brett Road
Piscataway, NJ 08854-8058
(848) 445-2248
mae.rutgers.edu